Addis Ababa University

Addis Ababa Institute of Technology

School of Mechanical and Industrial Engineering

Design and Manufacturing of Solar Injera Dryer

A Thesis

Submitted to the School of Graduate Studies

Addis Ababa University in Partial Fulfilment of the

Requirements for the Degree of Masters of

Science in Mechanical Engineering

(Thermal)

BY

Senay Teshome Sileshi

(B.Sc.2014)

Supervised By

Dr. Abdulkadir A. Hassen and

Dr. Kamil Dino Adem

October 2020

Addis Ababa, Ethiopia

Declaration

I, the undersigned, declare that this MSc thesis is my original work, has not been presented for fulfilment of degree for this or other university, and all sources and materials used for the thesis work is acknowledged.

Senay Teshome Sileshi	_____	_____
Name	Signature	Date

This thesis has been submitted for examination with approval as a university advisor.

Dr. Abdulkadir A. Hassen	_____	_____
Advisor	Signature	Date

Addis Ababa University

Addis Ababa Institute of Technology

School of Mechanical and Industrial Engineering

School of Graduates Students

Design and Manufacturing of Solar Injera Dryer

This is to certify that the thesis presented by Senay Teshome Sileshi, titled as "Design and Manufacturing of Solar Injera Dryer" and submitted to the School of Mechanical and Industrial Engineering in the partial fulfilment of the requirements for the award of the degree of masters of science in Thermal Engineering with the regulations of the university, and meet accepted standards with respect to originality and quality.

Approved by Board of Examiners

Dr. Abdulkadir A. Hassen	_____	_____
Advisor	Signature	Date
Dr. Abdulkadir A. Hassen	_____	_____
Thermal Engineering chair	Signature	Date
Dr. Yilma Taddese	_____	_____
Internal Examiner	Signature	Date
Dr. Wondwossen Bogale	_____	_____
External Examiner	Signature	Date
Dr. Yilma Taddese	_____	_____
Dean of SMiE	Signature	Date
Dr. Ermias Tesfaye	_____	_____
Director of Post Graduate Program	Signature	Date

Acknowledgment

It is my pleasure to take this opportunity to thank those people who provided their unreserved support for the successful completion of this thesis during the course of this research.

First, I would like to express my deepest and heartfelt thanks to my advisors Dr. Abdulkadir A. Hassen and Dr. Kamil Dino Adem (Addis Ababa university institute of technology) for their continuous assistance, guidance, suggestions, critical comments and encouragement. This thesis would not have come to completion without their unreserved support.

My special thanks also go to all members of Addis Ababa University, AAiT, SMiE staffs and members of SMiE workshop staffs who helped me, without their comments, support and suggestion; I would not have been able to accomplish this research.

Last but not least, I would like to thank my almighty God and friends and families for their positive reinforcement, advice and appreciation.

Abstract

About two-third of Ethiopian diet consists of injera, which has a strong cultural significance and high nutritional value, as it is rich in fibre, amino acids, calcium, iron and most importantly it is gluten-free. Injera is dried and prepared in times of food scarcity or for commercial and household usage. The objective of this thesis was to design and evaluate a mixed-mode natural convection solar injera dryer with unique vertical air distribution unite with 20 injera drying capacity.

Three dimensional simulation of unloaded solar dryer was developed to simulate the performance of the modified mixed mode solar dryer using the computational fluid dynamics (CFD) software ANSYS FLUENT for month of July and April by solving the governing equations describing the unsteady fluid flow. Dual-band discrete ordinates (DO) radiation model, Species transport model and shear stress transport (SST) k-omega (k-ω) turbulence models were employed. The dimensions of the dryer were: 2 m, 2 m^2, 1.4 m, 2.2 m, 1.5 m and 1 m for collector length, collector area, height of the vertical air distributer channel, the height of the drying chamber, length and width of the drying chamber respectively.

The simulation result indicated the collector outlet temperature was 10^oC above the ambient throughout the drying period. The overall temperature distribution through the drying trays shows a uniform temperature distribution. The average velocity and mass flow rate through the drying trays were found to be 0.1 m/s and 0.061 kg/s respectively and both were uniformly distributed through the drying trays. There was a pressure gradient through the drying tray, which helps to maintain the airflow through the dryer.

From the experimental result, it was clear that the modified mixed mode drier performance was higher by 19% when compared with other similar mixed mode drier. In addition, the temperatures of the drying air inside the drier was found to be more than 5^oC from the ambient temperatures. A uniform temperatures distribution was noticed through the drier, this is the result of the vertical air distributer channel, which was newly developed and integrated through the drying chamber, and the collector and drying efficiency of the drier were found to be 30% and 15.25% respectively. The drying rate of the drier was $2.634*10^{-5}$ kg/s and the Verma thin layer-drying model fits best for injera drying based on the X^2, RMSE and R^2. The experimental result was compared with the simulation result and the simulated temperature result showed an average overestimation on drying chamber by -1.5% and underestimation on collector outlet by 1.6 %.

***Keywords*:** Solar drier, Mixed mode drier, Injera, Simulation, Vertical air distributer channel.

Table of Contents

List of Table

List of Figure

List of Symbols / Acronyms

a	Constant velocity per unit pressure gradient, (m^3s/kg)
h_a	Enthalpy of dry air, (J/ kg)
C_a	Specific heat of dry air at constant pressure, (kJ/kg K)
C_P	Specific heat capacity of injera, (kJ/kg K)
Q_a	Heat gained by the heated air, (kJ/s)
$\dot{m}$	Mass flow rate of drying air, (kg/s)
m_{in}	Mass of single injera, (g)
m_i	Initial mass of the injera to be dried per batch, (kg/batch)
t_{in}	Average thickness of injera, (mm)
D_{in}	Diameter of injera, (cm)
m_{w}	Mass of water evaporated, (kg)
M_i	Initial moisture content on wet basis, (%)
M_f	Final moisture content on wet basis, (%)
$\mathrm{M_{cw}}$	Wet basis moisture content, (%)
$\mathrm{M_{cd}}$	Dry basis moisture content, (%)
$\mathrm{M_w}$	Mass of wet sample, (kg)
$\mathrm{M_d}$	Mass of dry matter in the sample, (kg)
M_{dr}	Average drying rate, (kg/hour)
E	Useful heat energy required to evaporate moisture, (kJ)
A_T	Total energy collection surface area, (m^2)
v_c	Average velocity of the drying air, (m/s)
u	Air velocity, (m/s)
h_L	Drying bed thickness, (m)
H	Minimum height of exit above the collector inlet, (m)

L_c Solar collector length, (m)

L_{dc} Drying chamber length, (m)

W_c Solar collector width, (m)

W_{dc} Drying chamber width, (m)

d_c Depth of the collector, (m)

A_{cv} Air vent area of the collector, (m^2)

A_{dv} Air vent area of the drying chamber, (m^2)

L_v Latent heat of evaporation, (J/kg)

t_d Drying time, (hrs)

I_T Incident solar radiation on the tilt surface, (w/m^2)

I_o Solar constant, (W/m^2)

I Hourly average solar radiation on the aperture surface, (kWh)

v_a Wind speed, (m/s)

$\dot{V}_a$ Volume flow rate of drying air, (m^3/s)

η_d Drying efficiency, (%)

d Vertical distance between two adjacent trays, (cm)

A_d Drying chambers floor area, (m^2)

A_c Collector surface area, (m^2)

V_a Volume of air required, (m^3)

P_a Atmospheric pressure, (N/m^2)

R_a Specific gas constant, (J/kg K)

T_a Ambient air temperature, (K)

T_0 Temperature of air at the collector outlet, (K)

T_f Temperature of air leaving the drying bed, (K)

T_b Boiling point of water, (K)

T_c	Critical temperature of water, (K)
$\dot{m}_a$	Mass flow rate of air, (kg/s)
$T_{d,max}$	Maximum allowable drying air temperature, (^{o}C)
ΔP_T	Gross pressure drop in the dryer, (Pa)
ΔP_B	Pressure drop across the drying bed, (Pa)
∇p	Static pressure gradient, (Pa)
$\vec{v}$	Fluid velocity vector, (m/s)
D_h	Hydraulic diameter, (m)
$\vec{F}$	Momentum source term, (kg/ m^{2}s^2)
E	Total energy transfer, (J/kg)
h_j	Enthalpy of species j, (J/kg)
$\vec{J}_j$	Diffusion flux of species j, (kg/m^{2}s)
S_h	Volumetric heat sources, (W/m^3)
$\bar{\bar{\tau}}_{eff}$	Viscous stress tensor, (N/m^2)
Y_j	Mass fraction of species j, (Kg water/kg dry air)
T_{ref}	Reference temperature, (K)
h	Sensible enthalpy, (J/kg)
$\vec{q}$	Heat flux, (W/m^2)
κ	Turbulent kinetic energy, (m^2/s^2)
S_i	i^{th} Species source term
$D_{i,m}$	Mass diffusion coefficient for species i, (m^2/s)
$D_{T,i}$	Thermal diffusion coefficient, (m^2/s)
Sc_t	Schmidt number for turbulent flow
I_λ	Intensity of radiation of wavelength λ, (W/m^2)

$I_{b\lambda}$ Black body radiation intensity, (W/m^2)

g Gravitational acceleration, (m/s^2)

n Refractive index

$\vec{r}$ Position vector

$\vec{s}$ Direction vector

Greek symbols

β_{opt} Optimum collector tilt angle (^{0})

β Dimensionless parameter

ρ_{in} Bulk density of injera, (kg/m^3)

ρ_a Density of ambient air, (kg/m^3)

φ Phase function

ω Specific dissipation rate, (m^2/s^3)

ρ^* Average air density in the air-heater, (kg/m^3)

ρ Density of air (kg/m^3)

α_λ Absorption coefficient for wavelength λ, (m^{-1})

σ_s Scattering coefficient, (m^{-1})

Ω' Solid angle, (degrees)

μ_t Turbulent viscosity, ($N\ s/m^2$)

$\bar{\bar{\tau}}$ Stress tensor, (N/m^2)

ω Humidity ratio of air, (kg of water/kg of dry air)

IR Infrared radiation

IESR Internal emissivity for solar radiation

IEIR Internal emissivity for infrared radiation

Subscripts

j specie

Chapter One : Introduction

1.1 Background

The staple Ethiopian fermented bread injera is made from teff (Eragrostis tef) [1] and it is difficult to overstate the importance of teff in Ethiopia. Teff is cereal crop, which is produced in the Ethiopian highlands for thousands of years and it is Ethiopia's indigenous grain. But other cereals may also be used in combination with teff for making injera [2]. Injera is a flatbread with a unique taste; it is a circular pancake that is sour and tasty and has a soft-spongy like structure with a thickness of 2–4 mm and a diameter of around 58 cm [2]. About two-third of Ethiopian diet consists of injera and it accounts for about two-thirds of the daily protein intake of the Ethiopian population. Injera together with 'wot' (sauce) is the major staple food eaten by Ethiopians and Eritreans both living in their country and abroad as well as people from some areas of Somalia and Sudan [2], [3]. Injera has a strong cultural significance and high nutritional value, as it is rich in fibre, amino acids, calcium, iron and most importantly it is gluten-free [4].

Solar radiation use for drying is one of the oldest applications of solar energy, it was used since the dawn of mankind [5]. Solar heat was the only available energy source to mankind until the discovery and use of wood and biomass. As pointed out in [6],the first installation for drying by solar energy was found in South France and is dated at about 8000 BC. Until today people take advantage of solar radiation for drying and preservation. Sun drying mainly used for food preservation but also for drying other useful materials as cloths and construction materials.

Drying is defined as a removal of moisture due to simultaneous heat and mass transfer [7]–[9]. Drying process (or de-watering) is a simple process of excess water (moisture) removal from a natural or industrial products like, sea foods, meat, food crops, cash crops, fruits, vegetables and wood in order to reach the standard specific moisture content or total removal of moisture until it has no moisture at all [6], [10].

Traditionally, in times of food scarcity, mouldy injera is dried and prepared for household consumption by using open air sun drying and it is called *Dirkosh* [4].However, open air sun drying of injera is not only used for mouldy injera but also before mould spoilage by simply spreading injera out on apparel mat they preserve and store injera for a longer period by avoiding mould development but this technique suffers from many drawbacks such as it is labour intensive, demands large area, no control over drying rate, over drying, poor quality, attack of insects and fungi, consequently leading to contamination [25]. In addition, some commercial enterprises like

Dirkosh prepares dried injera and called it “Dirkosh Crunch” with higher operation cost using electric oven and provide for their customer.

The importance of injera has resulted in increased research, which can be categorized into three main areas. Most of researches in Ethiopia and abroad have made attempts to improve the efficiency of injera baking stoves to save energy, reduce indoor air pollution and CO_2 emission [2].

1. Study on nutritional status of injera and human health effect [1], [11]–[13]
2. Study on injera consumption [14], [15]
3. Study on the injera preparation and improvement on efficiency of injera baking system
    a. Fuel energy used and Energy consumption [3], [16]–[20]
    b. Cooking system design [17], [21]–[24] and
    c. Improvement of injera shelf life [4]

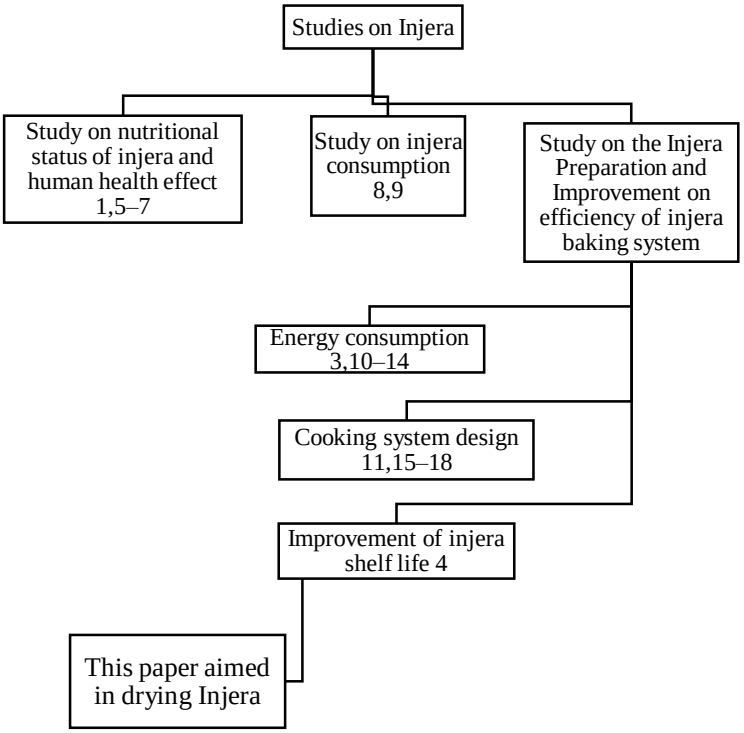

Figure 1.1:Summary of work reported concerning injera

Figure 1.1 is a summary of different areas of work reported concerning injera. The figure shows that the studies of injera were divided into three divisions and the third one can be further divided into three groups, which refer to the fuel energy used and energy consumption, cooking system design and improvement of injera shelf life. Studies on fuel energy used and energy consumption focus on different types of source of energy used and the consumption of this energy source in baking injera with comparison with respect to its environmental effect and efficiency.

Studies on cooking system design focus on different arrangement of the cooking system and its heating capacity also on improving health and general welfare of the users. Studies on improvement of injera shelf life focus on preserving injera for longer time by adding different chemicals with different concentration immediately before baking. Nevertheless, none of the above researches focused on drying injera for preservation and maintaining the quality of dried injera or dirkosh.

This prompted the study towards the design and evaluation of solar injera dryer designed specifically for Addis Ababa Ethiopia. By using this method, we can achieve a low cost drier which is affordable by local communities of Ethiopia with improved quality of dried injera and reduce risk of spoilage and drying area.

1.2 Statement of Problem

Food losses are major problem of the world especially for developing nations where 25% of food is lost by mishandling, spoilage and pest infestation [26] and in Ethiopia post-harvest losses of 15% was recorded and approximately 20.5% of households are estimated to be food insecure in 2016 [27]. Unfortunately, injera storage period does not usually exceed three days at ambient temperature (temperature in the highlands of Ethiopia is between 17 and 25^{o}C) under the traditional storage conditions essentially due to mould spoilage and it is a common practice to discard mouldy injera[4].

Open sun drying has been used till now predominantly to dry injera by simply spreading the injera out on apparel mat and this method is used widely as food preservation mechanism for several thousand years because of its simplicity and its low-cost and the dried injera is used in household for consumption and commercial enterprises supplied it to the local customers and even export it abroad, but this technique suffer from many drawbacks such as it is labour intensive and demands large area also no control over drying rate, over drying, discoloration by ultraviolet radiation (UV) and susceptible to attack by insects and fungi, consequently leading to contamination[26], [28], [29].

On the other hand, in electric oven drying which requires substantial quantity of conventional fuel or electricity to operate and to use this method in household requires financial capacity to procure electric oven dryer and additional payment for electric bill. These scenario leaves dirkosh producers with poor quality of dried injera which propagate to significant food losses and makes production of dried injera uneconomical.

As indicated in [30] one business group whom working in ways to position dried injera in international markets. Nevertheless, none of the studies focused on the design of injera drier using renewable solar energy in economically feasible way and for a better quality of dried injera.

This instigated the study towards the design and fabrication of solar injera dryer and by using this method, we can achieve faster drying rate, reduced risk of spoilage and higher throughput with reduced drying area. This method requires low initial investment and almost zero running cost, it is affordable by local communities of Ethiopia, which also contributes for new job creation and can help the existing firms in improving their income with improved quality of dried injera. Since the Ethiopian government has emphasized its mission for small agribusinesses because the contribution of agriculture to value added fell from 56.4 percent in 2000/01 to 36.7 percent in 2015/16 [27] and the contribution from dried injera export will play significant role to the value added export commodity of the country in many ways.

1.3 Objectives

1.3.1 Main Objectives

The objective of this project is to design, simulate, manufacture and test the solar injera dryer.

1.3.2 Specific Objectives

The specific objectives of the project are:

- To design an optimum layout for solar injera dryer.
- To simulate the performance of the designed solar injera drier
- To manufacture a prototype of the solar injera drier.
- To experimentally investigate the performance of the solar injera drier.
- To compare the simulation result with the experimental result.

1.4 Scope of the Present Work

The study focused on the design and fabrication of a solar injera dryer, suitable for small-scale production for weather condition of Addis Ababa, Ethiopia. The study tries to find appropriate type of solar drier. Simulation of the airflow through the drier was carried out to evaluate the drier performance without including the product. Teff injera was used for the experimental test. The experimental result was compared with the simulation result. Finally, selected thin layer drying models were tested to find out the best drying model equation, which represent the injera drying using the experimental result of drying.

1.5 Limitations of the Study

In this study, the simulated results were used only to compare the results of unloaded solar dryer and the effect due to the presence of injera on different flow parameter was note simulated. The drying model, which was selected, can only represent the current experimental results. Time and cost limits the scope of the project.

1.6 Significance of the Study

Traditionally Ethiopians practiced open sun drying to preserve and store injera for a longer period but this technique suffers from many drawbacks such as it is labour intensive, demands large area, no control over drying rate, poor quality and exposed for attack by insects and fungi, consequently leading to contamination. In addition, some commercial enterprises prepare dried injera or dirkosh using electric oven that contributed to higher operation cost. This prompted the study towards the design and fabrication of solar injera dryer. By using this method, we can achieve faster drying rate, reduced risk of spoilage and higher throughput with reduced drying area. Since it requires low initial investment and almost zero running cost, it is affordable by local communities of Ethiopia, which also contributes for new job creation and can help the existing firms in improving their income with improved quality of dried injera and helps by creating good export opportunity.

Chapter Two : Literature Review

This chapter aims to give background knowledge regarding solar drying and the need for drying with different types of solar driers which are previously designed are reviewed starting from 1986 up to 2018. Simulation of solar driers with drying fundamentals and mathematical modelling of thin layer drying were reviewed. Finally, factors that influence the dryer performance were explained.

2.1 Introduction

The principle objective of drying is to preserve food products for longer period with good quality by supply the required thermal energy in an optimum manner. The heat from the sun coupled with the wind has been used to dry and preserve foods for several thousand years. Use of solar energy technologies in recent years are rapidly gaining acceptance as an energy saving measure in different application area where thermal energy is required, because it is abundant, inexhaustible, and non-polluting [9], [31].

2.2 Solar Drying

Solar radiation use for drying is one of the oldest applications of solar energy, it was used since the dawn of mankind [5]. Solar heat was the only available energy source to mankind until the discovery and use of wood and biomass and as pointed out in [6],the first installation for drying by solar energy was found in South France and is dated at about 8000 BC. Until today people take advantage of solar radiation for drying and preservation. Sun drying mainly used for food preservation but also for drying other useful materials as cloths, construction materials. Favourable weather condition of Ethiopia with great diversity of climate, diverse topography and 13 months of sunshine with relatively longer sunshine hours per day will have a positive impact on using solar energy for drying purpose.

Drying is defined as a process of moisture removal due to simultaneous heat and mass transfer [7]–[9]. Drying (or de-watering) is a simple process of excess water (moisture) removal from a natural or industrial products in order to reach the standard specific moisture content or total removal of moisture until food has no moisture at all [6]. These products include foods, sea foods, meat, food crops, cash crops, fruits, vegetables and wood [10].

Drying may be required for several reasons, for preservation, quality improvement and processing purposes, moisture must often be removed from both organic and inorganic materials [32], [33]. The removal of moisture prevents the growth and reproduction of microorganisms like bacteria, yeasts and moulds and minimizes many of the moisture-mediated deteriorative reactions

[34]. Solar drying can also be used to retain the quality of product by reducing its mass and volume which helps in good packaging of these products for their better mobility and smaller space for storage [10], [35].

In drying process the most common technologies used are, open sun drying and solar drying which uses sun as source of energy and mechanical dehydration uses fossil fuels as source of energy [32]. Sun drying is a low-cost drying method but the final quality is variable and poor. Solar driers are simple devices, which are employed in many applications requiring low to moderate temperature (below 80°C) such as food drying and space heating and this method is more efficient than sun drying [36].

Mechanical dehydration or conventional dehydrator is an energy intensive process and contributes substantially amount of greenhouse gas emission [8], [10], [32]. Concerning energy use, In most of industrialized countries, about 7 to 15% of energy is spent for drying process [32], [37]. Mechanical dehydration according to [6], [32], uses its large portion of energy during transforming liquid water into vapour, which is 2258 kJ/kg at 101.3 kPa or it requires approximately 2.4 MJ of energy to evaporate one litter of water. This can be described in terms of oil usage as, to dry one metric ton of fruit it requires approximately 100 litters of oil and in terms of greenhouse gas emissions, one metric ton of fruit in a conventional dehydrator produces approximately 300 kg of carbon dioxide.

The importance of food drying using solar energy is likely to increase time to time [38] and Concern over global warming and cost of electricity forces us to focus our attention in using renewable and non-polluting sources of energy on energy intensive processes like drying [32], [38]. Even though, the use of solar food drying is proven to be practical, economical and environmentally a responsible approach [34],the lack of information through traditional media in developing countries like Ethiopia impedes the dissemination of valuable and even essential techniques like solar drying and others ; due to this, solar drying technology is not significantly introduced [10].

2.2.1 Open Sun Drying

Open sun drying as shown in Figure 2.1, has been used as long as humans have inhabited the planet and it is one of traditional drying methods. It involves draping or spreading the food on the ground, mat, cement floor, rooftops or placing on either horizontal or vertical shelves exposed in open to solar radiation and natural air currents. The food is usually stirred occasionally in order to expose different parts of it to the sun [9].

Open sun drying have a positive features like small capital cost, low running cost and its independence on fossil fuel but it have inherent limitations which leads to high food losses due to inadequate drying, fungal and insect infestation, birds and rodent encroachment, and weathering effects [9], [10], [39]. Also during the wet season, sun drying poses serious practical problems because, the food has to be removed to storage or protected from rain and to do so, continues follow up is mandatory which makes it a labour intensive process. Since the temperature of the product is raised by the direct absorption of solar radiation and this usually results in poor final quality due to product discoloration caused by enzymic and non-enzymic browning [40], [41] and since the temperature attained during drying is usually lower it results longer drying time.

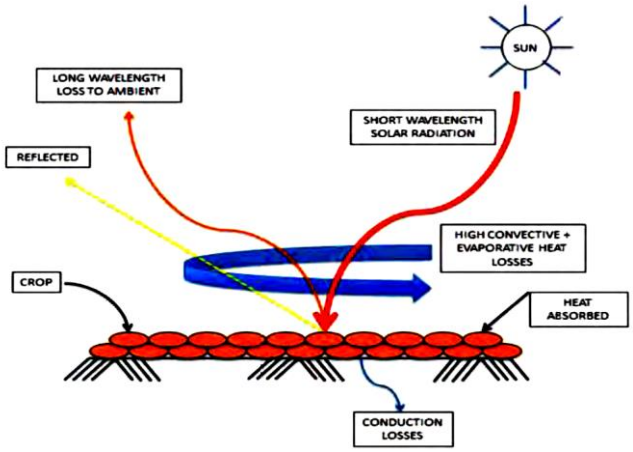

Figure 2.1: Open Sun Drying [9]

Due to this factures and other related problems the output of open sun drying is low and can be of very poor quality and often degraded seriously, sometimes beyond edibility [9].

To overcome this in inherent inefficiency of open sun drying, it is recommended to use solar driers. In a solar dryer the temperature of the air surrounding the product is raised above the ambient air temperature and depending on the type of solar dryer, the temperature of the product may also be raised by direct absorption of solar radiation. As a result, the temperatures of drying air in a solar drier is higher than in open sun drying and this reduces the drying time and usually improves the final product quality. In solar drying, the product is protected within the solar drier because it is an enclosed spaces drying method and as a result it prevents the product losses and spoilage [10], [32]. One of the major disadvantage of both methods of drying is the variation in the amount of solar radiation during daytime and its unavailability during night.

2.3 Types of Solar Driers

Different types of solar driers have been designed, developed and tested in the different areas. Different authors classified solar driers in different manner. Depending on the source of flow through the dryer, solar driers were classified in to two main divisions and this are passive or natural convection and active or forced convection solar driers. In addition, this can further be divided in to three modes depending on mode of heat transfer from the sun to the product, which are direct, indirect and mixed modes.

Not common, but solar driers can further sub divided depending on the type of heat transfer fluid, the direction of flow through the drier, and the inclusion of thermal storage and supplementary energy system. In practice, however, some types of solar dryer have proven to be more feasible than others [9], [32], [42]. Figure 2.2 below, shows classification of solar driers and summarizes six different possible combinations showing both the airflow and solar radiation directions [9].

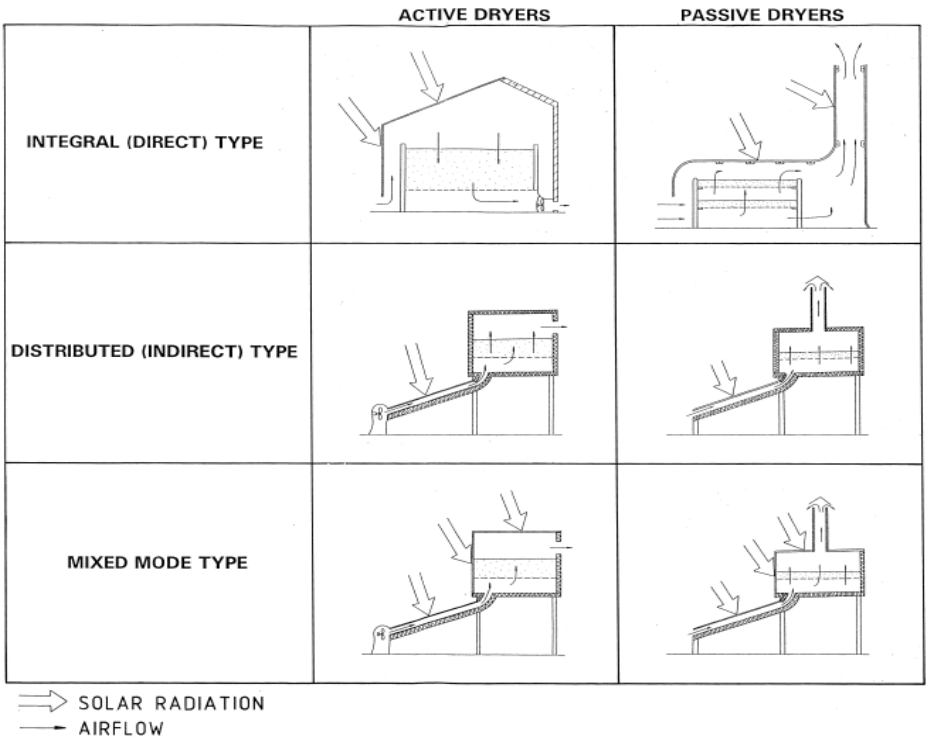

Figure 2.2: Classification of Solar Driers [32]

2.3.1 Natural Convection Solar Driers

In a natural convection or passive solar dryer, the air moves through the system because of the difference in density between the ambient air and the air inside the dryer which is resulted due to the rise in temperature of the air inside the natural convection drier. The less dense air rises

up through the dryer and creates a small negative pressure that in turn induces fresh ambient air into the system. As indicated by [32], [43] ,the air velocity in natural convection solar drier is in the range between 0.1 and 0.5 m/s. In addition, since the air temperature in solar drier is dependent on solar radiation, the airflow in a natural convection solar drier is also variable.

As cited in [44], the airflow rate may be increased marginally using solar chimney at the outlet of the dryer which in return increase the density difference. However, its relatively low and variable airflow is its main limitation. As a result, its performance is usually inferior to a forced convection system. On the other hand, natural convection solar drier are more attractive to the user because it requires lower capital and running cost and since there is no need of electricity to run it, a natural convection solar driers are sometimes the only choice in locations that do not have access to electricity.

2.3.2 Forced Convection

In a forced convection or active solar drier external devices are used to create the airflow through the drier like fans. This helps to control the airflow rate and airflow rate can be varied depending on the stage of drying. In addition, the quantity of food in the dryer can also be increased because the fan can overcome any additional resistance to airflow. The disadvantages of a forced convection system are its higher capital and running costs and the requirement for electricity [32], [45].

2.3.3 Direct Mode

In a direct mode solar dryer, the product is directly exposed to solar radiation. For this to occur, the structure containing the product must be covered with a transparent material as shown in Figure 2.3. The solar radiation passes through the glazing and absorbed by the product and its immediate surroundings. Since most of solar radiation is converted into heat, the temperature of the product and its surroundings air is higher than the ambient air temperature [46]. Its simplicity and relatively lower cost, makes it attractive for both small and large scale producers.

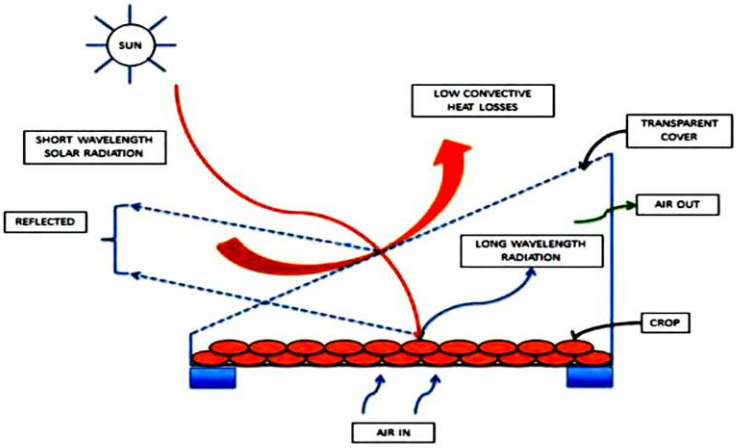

Figure 2.3: Direct Mode Solar Dryer [9]

A natural convection, direct solar cabinet dryer or tray type dryer was presented by [47],and the author stated that this type of dryer is one of the simplest among different type of driers as shown in Figure 2.4. It was constructed by covering the tray with clear polyethylene to allow solar radiation to reach the wet product. The tray can be permanently built on the ground using pressed bricks or concrete blocks, or it can be made portable by constructing it out of wood or metal sheets. The principle operation of this dryer is simple; the solar radiation enters through the top transparent cover and is absorbed by the collector that then heats the air inside the chamber. A continuous flow of air through the dryer was established by density and pressure variation between the ambient air and the air inside the cabinet. The air escapes from the chamber through the outlet holes on the sides of the cabinet and the ambient air was drawn into the chamber through inlet holes along the lower side of the cabinet just below the tray.

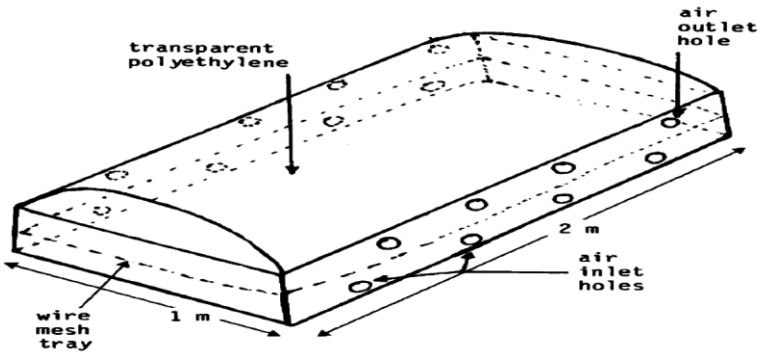

Figure 2.4: Direct Solar Cabinet Dryer [47]

It was observed experimentally that, the role of the air passing through the wet product is not for heating the product but it is to pick up the moisture, which is removed from the product through direct heating from solar flux and this is because the air temperature is less than the

temperature of the product. As described by the author, the performance of this dryer is low due to very low airflow through the product. Even though the ventilation, the air above the tray is usually saturated which causes condensation on the cover and results a reduction of solar radiation transmitted into the chamber.

[36] developed a mathematical model for a natural convection solar cabinet dryer and studied its performance experimental to verify the mathematical model. The dryer was essentially constructed from a wooden rectangular box divided lengthwise into parallel channels of equal width. The dryer was covered with a glass, which provides a substantial screening effect against ultraviolet light, thus reducing photo degradation of the drying product. Inside the rectangular box there is a perforated wire mesh on which the material to be dried is spread and the heated air passes through this perforated wire mesh and for proper and uniform ventilation, the ventilation holes were fitted with short lengths of plastic Figure 2.5.

The predicted plate temperature for no load reaches a maximum of 80-85°C during the noon hours, while with a load of 20 kg of wheat, the maximum temperature is about 45-50°C. It was also observed that the equilibrium moisture content is reached very rapidly for small loads, whereas it is much slower and takes a much longer time for higher load values. Also the products dried in the solar cabinet dryer were superior in quality compared to the open air dried products. But the design has also few drawbacks the first is that the solar energy intercepts on a horizontal surface and results low solar energy input during winter at the higher latitudes and the second is that the air goes out only passes through a single layer of product as a result its utilizable drying capacity could be waste. Further, in some products, direct exposure to sunlight leads to unacceptable local temperature rise in the top thin layer of the product and results an even drying and also the direct exposure might cause discoloration and vitamin loss.

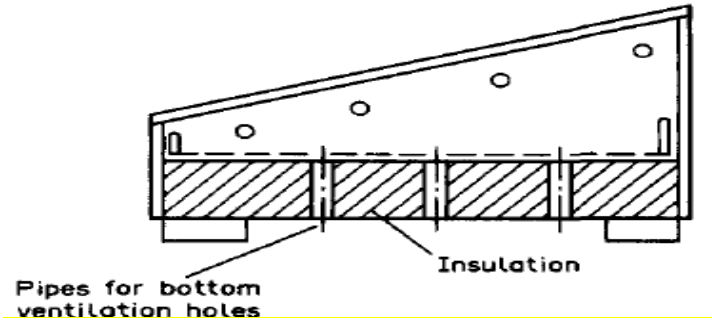

Figure 2.5: Solar Cabinet Dryer with Direct Heating [36]

[48] developed a natural convection direct mode modified cabinet solar dryer. This design is easy to use and simple to construct as shown in Figure 2.6. It has the shape of metal staircase with its base and sides covered with double-walled galvanized metal sheets with cavity filled with

non-degradable thermal insulation. The upper surface was covered with a transparent polycarbonate sheet to allow the sun to pass through and be trapped. Polycarbonate was used instead of glass because it is non-breakable. The dimensions of the dryer are moderate, large enough to allow its three shelves for loading 20 kg of fruit and vegetables. It is 2 m in length, 1m in width and 0.4 m in thickness, with a total glazed surface area of 1.30 m^2. This upper polycarbonate surface is divided into three equal parts which can swing open, to provide access to the three compartments inside the dryer. A chimney of 0.10 m diameter and 0.4 m length is located at the upper end of the dryer to ease the flow of air. The whole setup is placed in a North-south alignment at 30^0 to the horizontal. The base of the dryer has four air entry points, each of 8 cm diameter. The partition walls between the compartments also have four port holes for easy air flow. The samples tested lost over two-thirds of their weight to reach their required moisture contents, which is 1ess than 20% of their initial mass in around 2.5 to 3.5 days. The average drying period for same samples using sun drying is around 12 to 15 days.

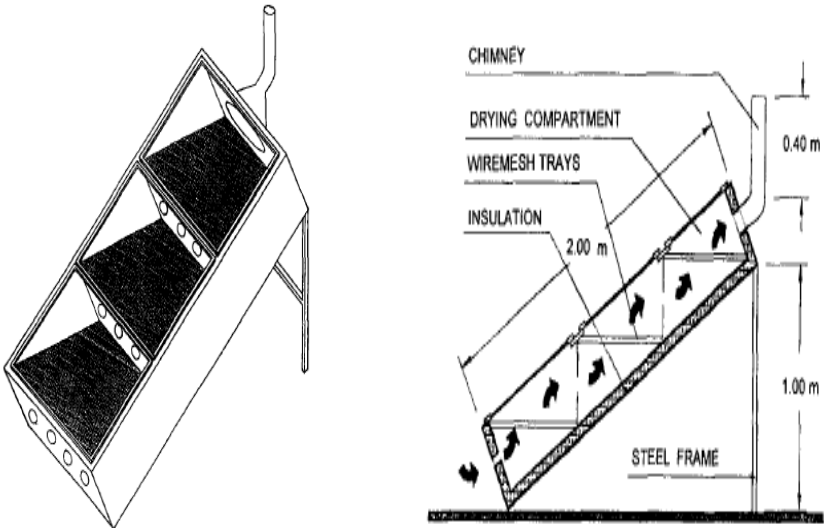

Figure 2.6: Staircase type Solar Dryer [48]

[49] developed a model and analysed reverse flat plate collector used as a heating medium of air for the drying of agricultural products in a cabinet dryer and the whole unit is termed a reverse absorber cabinet dryer (RACD) and is shown in Figure 2.7. The absorber plate is horizontal and downward facing. A cylindrical reflector is placed under it to introduce solar radiation from below. The area of the aperture is the same as that of the absorber plate. The cabinet dryer is mounted on top of the absorber maintaining a gap of 0.03 m for air to flow above the absorber which becomes heated and enters the dryer from the bottom. Unlike a conventional dryer it is not insulated from the bottom. The bottom area of the dryer is equal to that of the absorber plate area.

Thermal analysis was carried out and a mathematical expression was proposed for RACD. Results were compared with those for a normal cabinet dryer. The author stated that none of previous reported studies have considered the effect of vent area and performed optimization of vent area for further improvement of the thermal performance of the system.

Based on numerical computation the author concluded that, the crop and chamber temperatures are less than the plate and fluid temperatures during sunshine hours and the crop temperature remains a little higher than the other temperatures during periods of no sun. The comparison result shows that the variation of the crop temperature with vent area is higher in normal cabinet driers compared to RACD and seems to be insignificant in RACD. The optimum vent width of RACD was found to be about 0.14 m. In addition, the instantaneous thermal loss efficiency factor for RACD was found higher than a normal cabinet dryer. This causes the fast removal of moist air, which, in turn, helps in quick drying, and therefore the crop temperature in RACD is higher than for normal cabinet driers. [50] studied the performance of a RACD with packed bed, which was used for energy storage unit for drying onions. The result shows that the crop temperature depends on the width of the air channel and height of packed bed and the author found that the thermal energy storage affects drying during the non-sunshine hours and helped to reduce the fluctuation of temperature in the drying process.

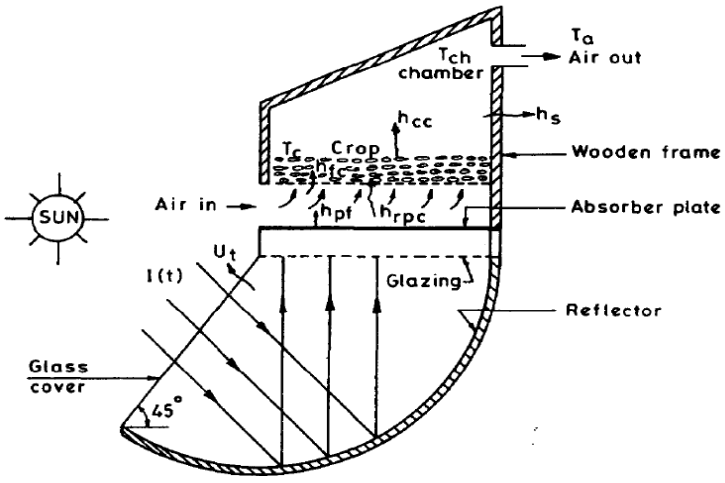

Figure 2.7: Reverse Flat Plate Absorber Cabinet Dryer [49]

[51] proposed modified cabinet dryer with natural convection system. This solar dryer unit consist of drying chamber of 120 cm long, 80 cm wide and 40 cm height, the walls were made from black painted plywood. The drier was insulated with sawdust on its sidewalls. The top of the drier was glazed with a single plastic cover tilted at 45^0 and at 28.28 cm height, which helped to reduce the reflective losses of solar radiation entering the unit. Ambient air enters the cabinet through twelve holes with 1 in pipe at the bottom, distance between each hole is 20 cm, and 5 cm

of charcoal spread among the holes Figure 2.8. Heated air escaped through the hole of bamboo stick, which placed below the cover. The painted black interior surfaces were used to absorb the solar radiation transmitted through the cover and thin layer of charcoal act as collector as well as insulation.

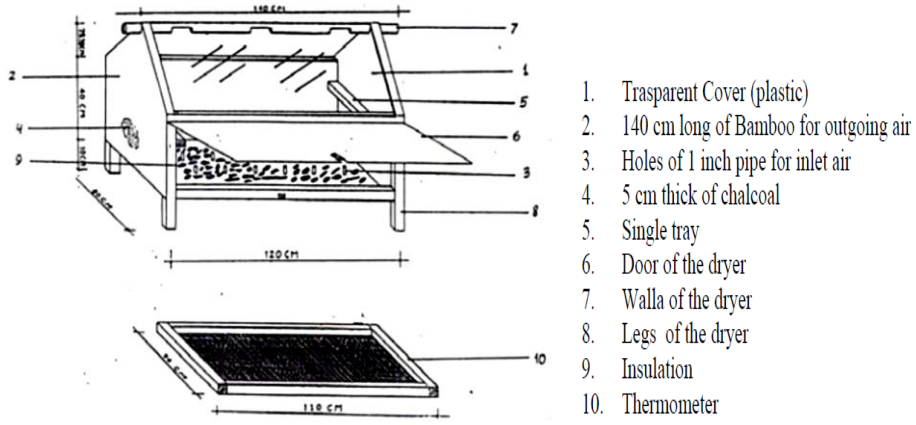

Figure 2.8: Modified Cabinet Dryer [51]

This solar dryer is used to dry Cashew Nut in Shells (CNS) and compared with open-air sun drying of the same product. The results showed that solar dryer unit could heat dry air up to 78.7 ^{0}C maximum on ambient temperature of average 27.2^{o}C. Drying rate of 0.59 % mc/hr, efficient of 64 % with a good quality grade product was achieved. The tested performance showed, the solar dryer had a better overall results compared to open-air sun drying. This design has also drawbacks like most cabinet driers. Since the air, after passing through a single thin layer of the product goes out, its utilizable drying capacity goes to waste. The layer of product cannot be made thicker because the solar radiation heats only the top thin layer and unable to reaches the absorber at the bottom. Further, in some products, direct exposure to sunlight leads to discoloration and vitamin loss and causes an unacceptable local temperature rise in the top thin layer of the product. The charcoal temperature, which was used as insulation, should be controlled due to its potential fire hazards property.

A direct type natural convection solar dryer is designed and tested experimentally for drying cassava and bananas by [52]. It was constructed in local materials (wood, blades of glass, metals). Consists of a drying chamber topped by a chimney, a box and a tray Figure 2.9. The drying chamber dimension are 1.34*0.936*0.45 m. Its structure constitutes the collecting area of the dryer. Onto framework of the drying chamber at the top 4 mm, thick glass cover was used with a tilt angle of 7^{0} with respect to the horizontal. From the experimental result, it was observed that, the drying process allows reducing the moisture content of cassava and sweet banana approximately to 80% in 19 and 22 h, respectively to reach the safety threshold value of 13%. The

advantage of this dryer was its solar chimney assembled on the cover of the drying chamber and it contains a separate absorber, which helps to regulate the velocity of natural convective flow. This design also shares same drawbacks of direct type solar driers.

[53] designed and fabricated a direct solar dryer of cabinet type. It was used to dry a batch of 20 kg of fresh vegetables such as tomato, potato, chilly and bitter guard in two days and the dryer was constructed in India. Experimental drying tests were carried out with a prototype of the dryer having 1.03 m^2 of solar collector area as shown in Figure 2.10. This dryer has a dimension of 100*103*76 cm^3 and its sides were constructed from galvanized steel and the bottom from wood. A glass was used as a cover and a hole of 5 cm in diameter was made for air circulation.

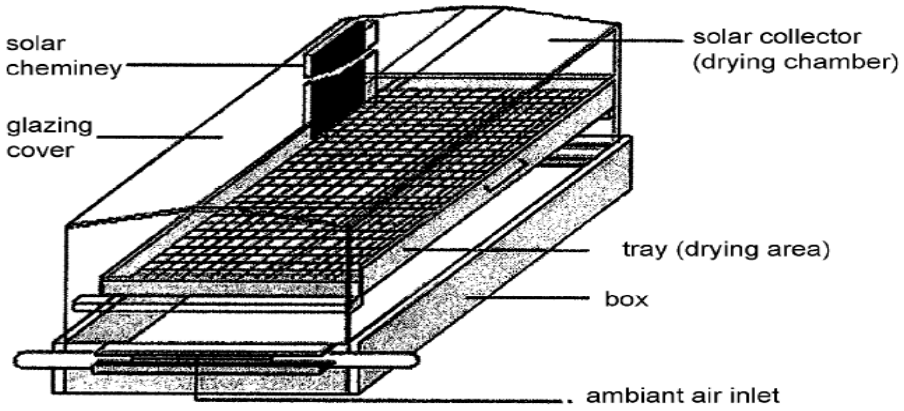

Figure 2.9: Direct type Natural Convection Solar Dryer [52]

Optimum temperature of the solar dryer was found to be 60^oC with inlet air temperature of 30^oC. The author tested the design by comparing it with open sun drying and using same amount of 3 kg of potato for both testes and found that, at the end of the first day of drying, the weight of the potato was reduced to 1.18 and 1.55 kg when dried with direct dryer and open sun drying respectively. In second day, final weight of the potato was reduced to 0.55 and 0.92 kg using the direct and open sun drying respectively and same type of change in weight of the product is observed for chilly and bitter guard but the author did not report the weight reduction and drying time of the tomato. In addition, the average air temperature at the exit was found 46^0C for all tests on direct solar drier.

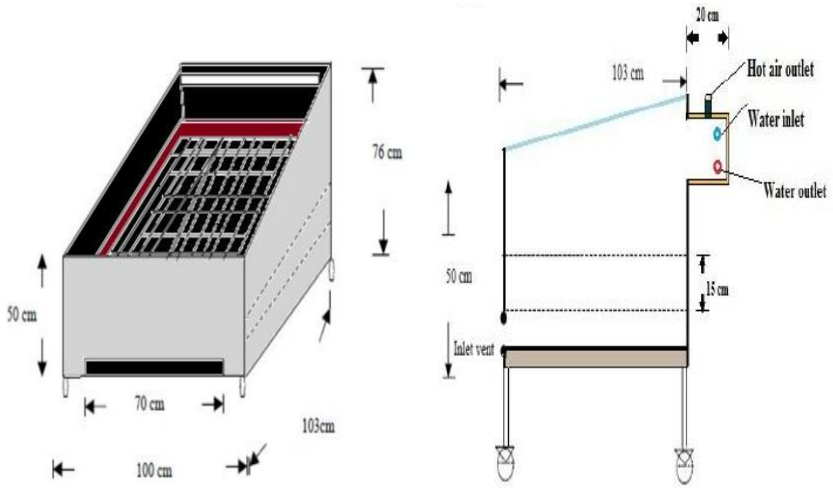

Figure 2.10: Direct Solar Dryer of Cabinet type [53]

The design also included a mechanism of waste heat recover, which uses the heat coming out of the dryer for water heating system and found the average temperature rise of 5^{o}C with inlet temperature of 30 ^{o}C. The authors did not mention the particular application of the heated water, and the advantage of including this system should be compared with the increase in cost that it will incur so that small farmers can afford it.

[54] Presented referring to (Medugu 2010) the performance of a forced convection direct mode solar dryer. In addition to the basic components of a solar dryer, this design consisted of a chimney and a 40 W photovoltaic module used to power and run a DC fan. Drying 50 kg of tomato with an initial moisture content of 90% using this type of solar dryer was completed within 129 h which is about 55% of the time required to dry using natural sun drying. The author also evaluated the performance of the solar chimney dryer in comparison with solar cabinet dryer without a chimney, which took about 138 h to dry the same quantities of tomato also higher quality dried product in terms of its colour and flavour was obtained when using the solar chimney drier.

A drying period of 200 h for drying tomato, which is about more than 5 days, and no justification was given for the long drying periods but it could be due to the fact that the experimental tests were carried out during the wet season, when most of the days were cloudy. In addition, the presence of photovoltaic module as a power source to operate a DC fan makes the fabrication of the dryer expensive.

As described in [37],direct solar driers are the most commonly used devices for drying agricultural and food products. The average drying efficiency of these driers is varying from 20% to 40% depending on the product type, air mass flow rate, and the location of drying. As stated in [32] ,direct mode solar driers can range in capacity from a few kilograms to several metric tons but [37] argued that direct solar driers are limited in drying capacity and stated that since the crop

itself directly absorbs solar radiation controlling the drying rate and crop temperatures became challenging which results undesirable product quality and product overheating. The direct absorption of solar radiation by the product is the most effective way of converting solar radiation into useful heat for drying in direct mode solar driers. But some products final quality deteriorates by losing vitamins and nutrients when dried in direct exposure to ultraviolet solar radiation but some foods may not be affected as stated in [34], [40].

2.3.4 Indirect Mode Solar Drier

Indirect solar drying systems have a separate drying unit and a solar collector. It usually consists of various components; solar collector, drying unit, a fan if the system is active, and ducting for air circulation through these components [37], [55]. In an indirect mode solar dryer Figure 2.12, the product is not directly exposed to solar radiation instead it utilize pre-heated air from a heat source to dry the product which is located in a separate drying chamber [46]. A solar collector absorbs the incident solar radiation where it is converted into heat. The air flows over this absorber and gets heated then this heated air is used to transfer the heat to the product located within an opaque drying chamber [32], [56].

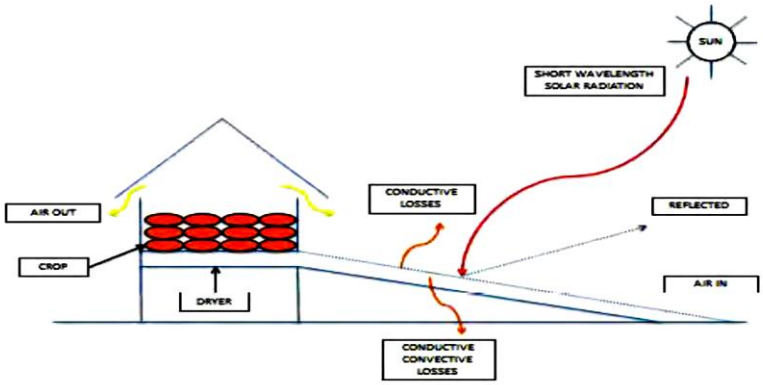

Figure 2.11: Indirect Solar Drying [9]

[40] developed Brace-type passive indirect solar drier made of plywood as shown in Figure 2.12. It is 1.12m long, 1.30m wide, and 0.67 m high, and its collector area is about $1m^2$. The absorber was made of galvanized sheet metal painted black and the air flow at the dryer inlet is regulated by two screened slots. The drying chamber has a volume of 0.13 m^3 and can dry 10 to 15 kg of product in 3 days. The moist air exits through two chimneys, each having 1.5 m high. Drying tests were conducted on salt fish and okra and reported drying time 4 days. The author recommended that, to promote user acceptance of solar driers, drying time must also be reduced and the loading capacities must increase. The drawback of this design is the problem of

waterproofing arose due to the wooden frames since this result in reduction of the useful life of the drier, which is for this design, 4 year of useful life, as reported.

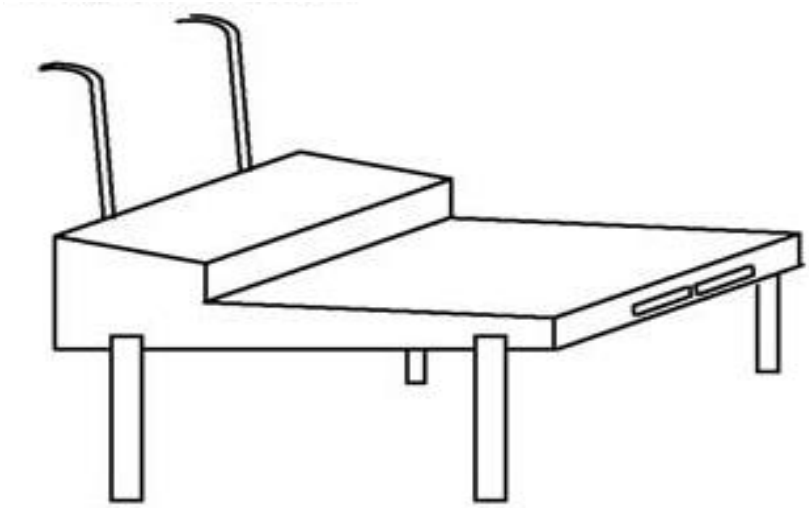

Figure 2.12: Brace-type Passive Indirect Solar Dryer [40]

[57] presented natural convection indirect type driers and it was constructed by combining solar air collector with the drying chamber into a single cubic wooden box. The box was divided into two halves. The first half is a single glazed solar air collector, whereas the drying unit is in the second half. As shown in Figure 2.13, a glazed solar air heater located at the base of the drying chamber provides supplementary heat and preheated air in the solar collector rises through the second half of the system. An additional chimney was provided at the top of the drying unit and the hot air dehydrates the product and gets exhausted through this chimney. The product to be dried were placed on the moveable trays which are constructed from metallic frames attached to the drying unit. The flow rate can be varied by making use of the adjustable inlet opening provided at the inlet section of the solar air heater. The author compared the result from the natural convection cabinet drier with forced convection and multi stacked natural convection indirect type solar driers. From the experimental result, the author concluded that drying was much faster in the case of the indirect forced convection solar drying and this is especially true on partially cloudy days. On clear sunny days, however, the total drying times to complete drying operation in all three different driers were more or less the same and there was no significant difference in the quality of the dried product.

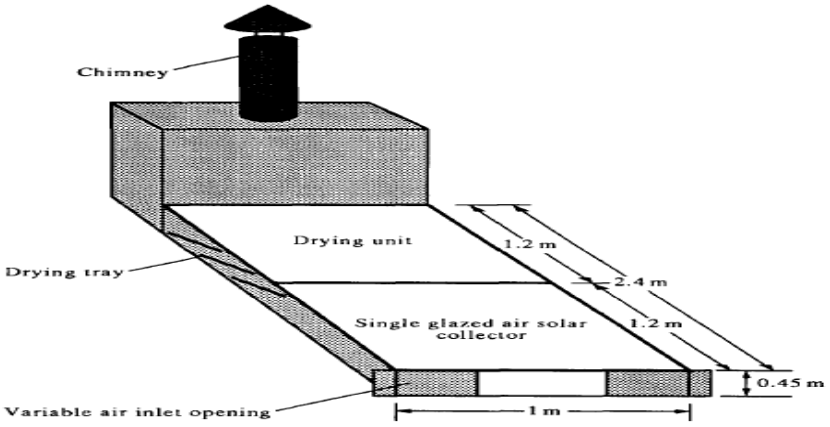

Figure 2.13: Natural Convection Indirect type Driers [57]

[58] developed an indirect passive solar dryer with composite absorber system solar air heater and evaluated its performance by drying fresh samples of mango Figure 2.14. Both the collector and the drying chamber frames were constructed from wooden sheets, and painted pink on the exterior faces to protect the wood from deterioration. The pink colour also absorbs solar radiation and thereby reduces the temperature gradient between the inside and outside surfaces. The interior faces of the collector frame were painted black to enhance absorption of solar radiation. Consequently, the interior faces acted as a fixed absorber system for low temperature drying. The other absorber system was made of a mild steel mesh fitted on a removable wooden frame and painted black. A door with a plastic gauze was fitted on the collector inlet to provide access for interchanging the wire absorber system and to prevent insects and rodents from entering the air heater. The top of the solar collector was covered with a single glass layer and the whole collector was tilted at 16° to the horizontal plane. All faces of the drying chamber were constructed from opaque materials to prevent direct sunlight from reaching the drying bed. Additionally, these faces were painted white to enhance reflection of radiation. The chamber accommodated three plastic-mesh trays that were constructed by fitting a plastic mesh on wooden frames (porous trays allow passage of heated air through the matrix of the food pieces but prevent the food pieces from dropping down). A chimney was fitted on top of the drying chamber. The chimney was constructed from a galvanized steel sheet and painted black to increase, the solar absorption, thermo-siphoning of air, and the overall efficiency of the dryer.

The maximum observed collector outlet temperatures were 45.9 °C and 42.9 °C with and without a wire screen absorber, respectively. The outlet air temperature was higher than ambient air temperature during sunshine hours with a maximum value around solar noon. In contrast, the relative humidity in the air generally decreased to a minimum value of about 51% around midday. The mean flow rate of air was 0.0083 kg s^{-1}which yielded thermal efficiency values of 21.3% and 17.0% for the wire mesh absorber and wooden absorber plate, respectively. The author stated that,

this efficient difference is due to metals are good radiation absorber and conductor of heat. However, the author stated that, use of a wooden absorber is more attractive than a metallic absorber because wood is readily available and affordable in developing countries.

The author compared his efficiency result with results obtained by other authors and found out his efficiency values agree very well with their result. But small variations of efficiency when compared with other authors whom designed with the same parameter are expected because the thermal efficiency of a solar collector does not only depend on the design and construction parameters but also weather and other conditions.

The advantages of this dryer is its integrated flat plate collector which had composite absorber systems which can be used interchangeably with different materials in one collector frame to achieve the desired temperature and to improve its efficiency and the collector can still perform without the removable absorber plates.

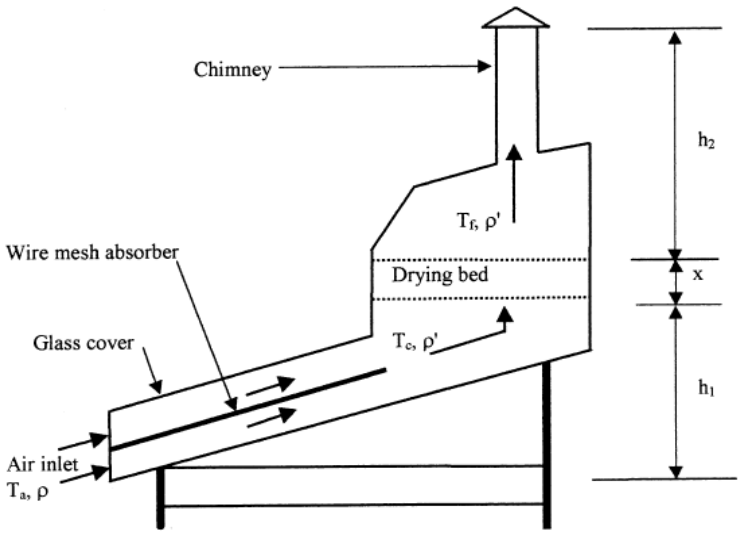

Figure 2.14: Passive Indirect Solar Dryer with Composite Absorber [58]

[59]designed and tested the performance of a new natural convection solar dryer, which consists of an absorber with fins painted matte black, glass cover, flexible connector, reducer with plenum chamber and chimney at the top of drying chamber as shown in Figure 2.15. The drying chamber and solar collector were both insulated with glass wool. At the air inlet, shutter plates were provided to stop the air flowing during the night and to prevent insects from entering the dryer, wire mesh was fixed at the inlet side of the collector. The drier was constructed using galvanized iron sheet.

The author reported the developed natural convection solar dryer is capable of generating an average temperature between 50 to 55°C and an adequate flow of hot air. The drying airflow

rate increases with increase in ambient temperature and this is due to thermal buoyancy in the collector as reported. The reported collector efficiency ranges between 26% for 0.0126 kg/s and 65% for 0.0246 kg/s and the drying time was reduced by 43% when compared with the open sun drying of grapes.

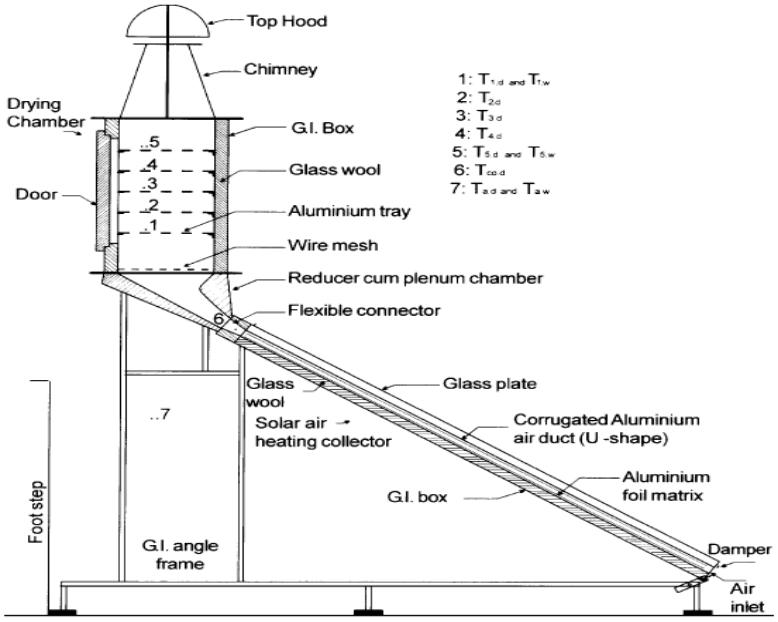

Figure 2.15: New type Natural Convection Solar Dryer [59]

[60] developed and evaluated an indirect passive solar dryer using a box type absorber collector used for drying crop. The dryer as shown in Figure 2.16, consists of an air heater, an opaque crop bin, and a chimney. The black painted box-type absorber collector was covered with glass and inclined at angle of 17.5^0 from the horizontal. The collector of this dryer has an effective area of 0.415 m^2 with an insulation lining and covered with transparent glass of thickness 4 mm with air inlet vent area of 0.084 m^2. The drying chamber contains two rack with each having area of 0.168 m^2. At the top of the drying chamber, there is a chimney with 0.01 m^2 area and 0.35 m height. The author compared the result with flat plate absorber and fin-type absorber and reported the maximum efficiency obtained in box-type absorber was 60.5% while those of flat plate and fin-type absorber were 21% and 36%, respectively and the maximum average temperature inside the collector and drying chamber were 64 and 57.3^{o}C, respectively, while the maximum ambient temperature was 33.5^{o}C. From the test result the author absorbed, the maximum temperature obtained in the dryer is a function of solar radiation, ambient temperature and wind speed. In addition, as the mass flow rate increases, the pressure drop and the collector efficiency increases and this is associated to the increase in the convective heat transfer coefficient and the decrease in collector heat losses as indicated in the report.

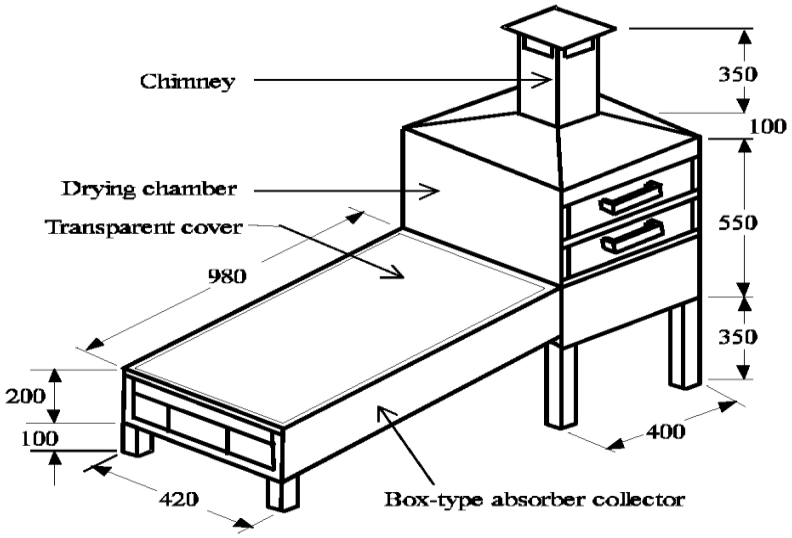

Figure 2.16: Indirect Solar Dryer using a Box-type collector [60]

[61] Designed and experimentally tested the performance of indirect type solar dryer for banana drying as shown in Figure 2.17 and it consists of flat plate collector having V-corrugated absorber plate painted black with the total area of 2 m^2 and covered with glass. Both the drying chamber and collector were insulated and drying chamber was provided with a chimney for exhaust air and four aluminium wire mesh trays.

From the experimental result, the mass of banana is reduced from 2 kg to 0.5628 kg and the moisture content of banana was reduced from average initial value of 356% (db) to final value of 16.3292%, 19.4736%, 21.1592%, 31.1582%, and 42.3748% (db) for Tray 1, Tray 2, Tray 3, Tray 4, and open sun drying respectively. The average thermal efficiency of the collector and drying efficiency were reported to be 31.50% and 22.38% respectively. Finally, the author concluded that the temperature, humidity and air velocity of drying air are the most important factor during drying to improve the drying rate and concluded that indirect type of solar drying is more effective than open sun drying as it reduced the drying time and improves the quality of dried product. The major shortcoming of multiple trays cabinet dryer is uneven drying of the products being dried on different trays and the extent of the variation of the drying product moisture content on different trays is an indication for this drier.

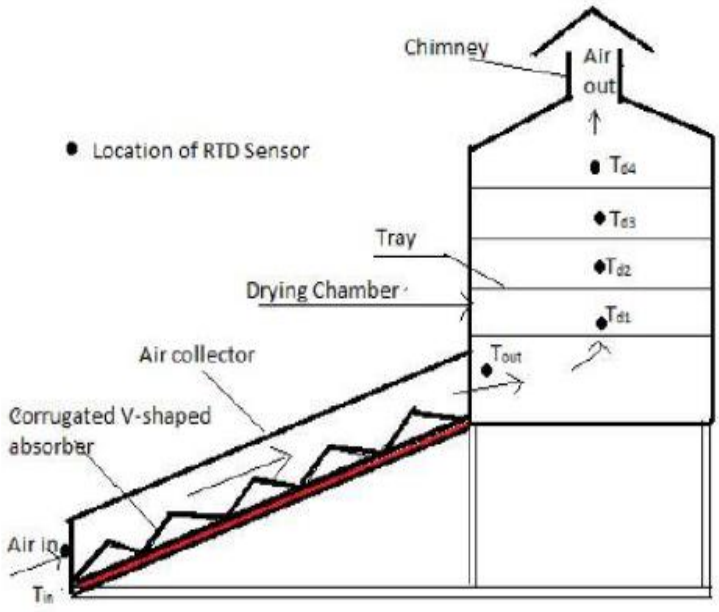

Figure 2.17: Indirect type Solar Dryer with V type Absorber [61]

Indirect solar drying technique has advantages when compared with direct solar dryer [62]. For some crops, particularly herbs and some spices, the final quality is reduced if the product is exposed directly to solar radiation and an indirect mode solar dryer is therefore more suitable for this kind of product [32].

2.3.5 Mixed Mode

In some cases, a solar drier design combines the direct and indirect modes and known as a mixed mode solar dryer [9]. In this type of solar dryer the product temperature is raised by both direct absorption of solar radiation and heat transferred from the air coming from solar absorber [54].

[47] reported mixed type natural convection solar dryer, which is an improvement made on direct tray type cabinet drier. The modification helped the drier to be used as an indirect type drier for products affected by direct exposure to solar radiation as shown in Figure 2.18. Clear polyethylene plastic was placed over the heating chamber to allow solar radiation to heat the air and black polyethylene was placed under the chamber to absorb solar radiation and to keep out moisture from the ground. An opening in front of the unit was provided to allow ambient air to enter the heating chamber and another opening at the rear of the drying chamber, which allows moist air to escape from the unit. The result indicated the airflow was very low and the improvements did not significantly improved the performance of the dryer.

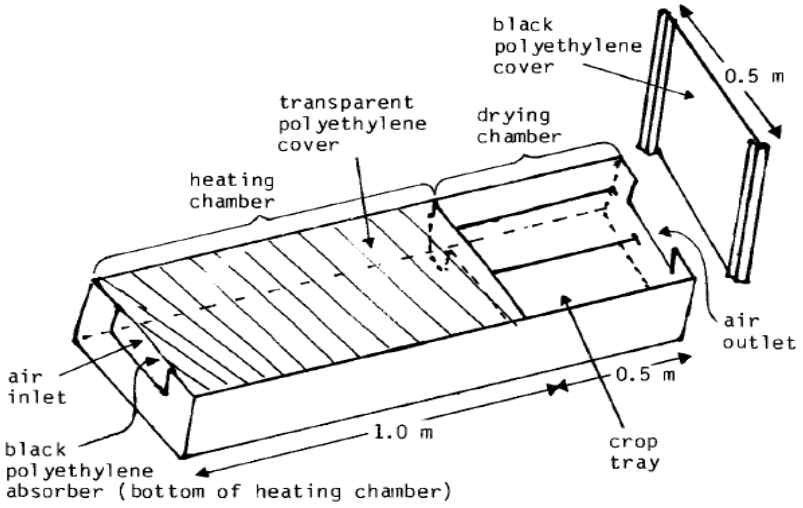

Figure 2.18: Mixed type Natural Convection Solar Dryer [47]

[63] Presented an optimized mixed mode drier, which can also be used as an indirect mode natural convection solar drier used for drying maize. The drying chamber for a mixed-mode was covered with transparent cover whereas for the indirect mode it was covered with an opaque material. Drying chamber width was equal to the collector width. Airflow in the dryer is driven by buoyancy pressure, which is created in the single covered collector and the space inside the drying chamber.

The result of the optimization of the mixed mode and indirect mode natural convection solar driers was presented with a performance comparison of the two modes by the author. The result indicated that to dry same amount of 90 kg grain, the collector length was found to be 1.8 m and 3.34 m for mixed mode and indirect mode drying respectively. The drying cost, annual cost and initial cost of the mixed mode were lower than that of the indirect mode. The quantity of dry grain obtained for the whole year from the mixed mode was less than the indirect mode however the drying cost for mixed mode was less than the indirect mode.

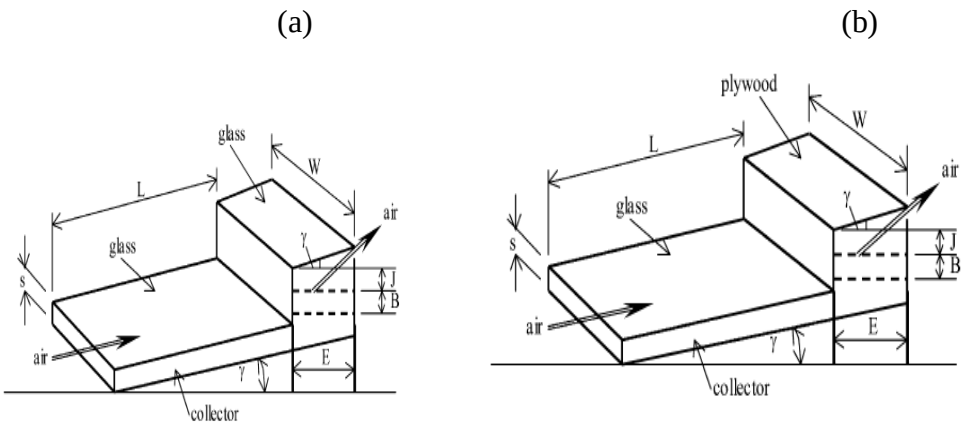

Figure 2.19: (a) Mixed mode and (b) Indirect mode Passive Solar Driers [63]

[64] designed a mixed-mode natural convection solar dryer as shown in Figure 2.20. The dryer consists an air-heater (primary collector), a drying chamber, and a chimney. The primary collector is a single pass air-heater with double duct and a non-porous absorber plate suspended between the top glass cover and the base plate providing two channels through which air flows on both sides of the absorber plate which helps the system to provide twice as much surface area for heat transfer. The drying chamber houses three drying racks with each drying rack consisting of two drying beds arranged vertically. The roof of the drying chamber or called the secondary collector and sidewalls were transparent and the top of the drying chamber was provided with a chimney, through which the moist air flows and escapes into the surrounding. Back doors were provided for access to the chamber.

The authors proposed a methodology combining concepts and rules of thumb that enable the design of mixed mode natural convection solar crop dryer and the resulting empirical model requires as input the crop physical properties, location and ambient condition also the author indicated that using the overall efficiency as an indicator of performance of a dryer is misleading for a dryer not loaded to its design capacity and instead the normalised drying efficiency (%/kg) is a better indicator of performance for a dryer not loaded to its design capacity.

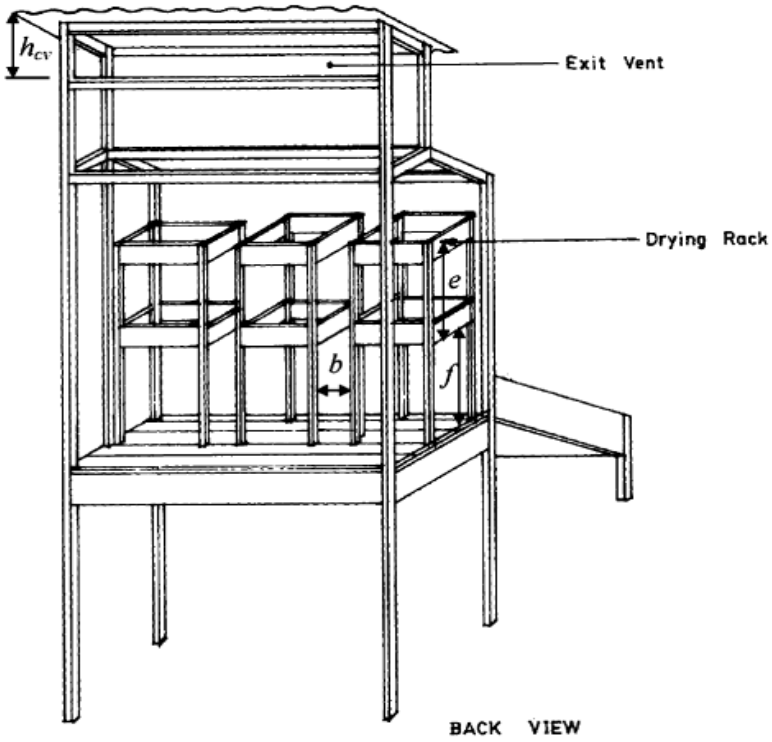

Figure 2.20: Mixed mode Passive Dryer with double Duct Absorber [64]

[65] designed and constructed a mixed mode solar dryer and tested its performance Figure 2.21. The dryer, contains double duct solar collector and drying chamber. The drier absorbs solar energy directly through the collector and the transparent walls and roof of the drying chamber. The results obtained during the test period revealed that the temperatures inside the dryer and solar collector were much higher than the ambient temperature during most hours of the day. The temperature rise inside the drying cabinet was up to 74% for about three hours immediately after 12.00h (noon). The drying rate and system efficiency were 0.62 kg/h and 57.5% respectively. The rapid rate of drying in the dryer reveals its ability to dry food items reasonably to a safe moisture level. The disadvantage of this dryer was for some products the direct exposure to sunlight leads to discoloration and vitamin loss and causes over drying on the product placed at the top of the drying tray.

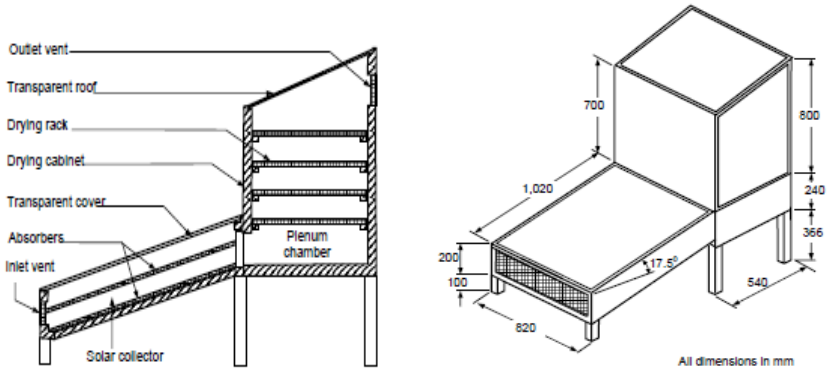

Figure 2.21: Mixed mode Solar Dryer with Transparent Drying Chamber walls [65]

[66] Developed and tested the performance of multi chimney mixed mode solar crop dyers with and without thermal storage materials. The system consists of a solar collector, which was constructed using galvanized iron sheet painted matt black, the top of the collector and drying chamber were covered with 4mm clear transparent glass and heat storage material was rock, which is used in one of the collectors as shown in Figure 2.22. Fiberglass was used to insulate both the air heaters and the remaining two sides of the drying chambers and the drying chamber was divided into three each with an independent chimney at the back and a galvanized iron wire mesh tray. To connect the drying chamber with the collector, insulated connecting duct was constructed and at the back of the drying chamber, an access door was provided. The dimensions of the collector length, collector area, height of the drying chamber, chimney height, the drying chamber length and width were, 0.65 m, 0.30 m^2, 0.9 m, 0.7 m, 1.64 m and 0.43 m respectively.

The performance of the mixed mode solar driers was evaluation under the same meteorological conditions of Zaria, Nigeria with and without thermal storage materials. From the result, it was observed that the average drying rate, collector and drying efficiency with and without thermal storage was 2.71 and 2.35 * 10^{-5} kg/s, 67.25% and 40.10%, 28.75% and 24.20% respectively. Maximum collector outlet air temperature with and without thermal storage materials for no-load test was found to be 66^0 C and 53^0 C respectively at maximum solar insolation of 872 W/m^2. The drying rate variation on different trays was also investigated and it was shown that, there was no significant difference between the drying rates of the yam slices on different positions of the trays.

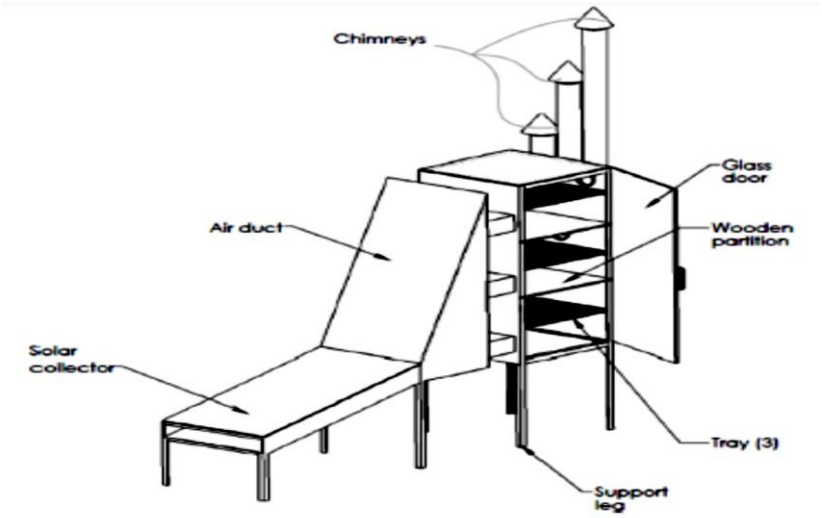

Figure 2.22: Mixed mode Solar Dryer with Multiple Chimney [66]

2.4 CFD Simulation of Drying Process

Simulation is the imitation of a real world process or system over time. It is the act of putting models to work [67]. Simulation soft wares come in different forms and in this work ANSYS software is selected due to different reasons. The main reason for this decision is based upon knowledge and the experience about ANSYS software already exists in the university study and also different authors [67]–[72] reported that their simulation results of solar dryer using ANSYS was in good agreement with the experimental results.

ANSYS software is a general purpose finite element modelling package which numerically solve a wide range of problems in areas such as heat transfer, fluid mechanics, static and dynamic structural analysis. It allows construction of computer models of a structure and it gives a detailed insight to the flow distribution, heat and mass transfer, separation of particles that is much more expensive, difficult and even impossible to study in real experiments and it permits an evaluation of a design without having multiple prototypes in testing[67], [73].

[68] airflow inside the hybrid solar dryer was simulated using the ANSYS-CFX 11 software package. The computational domain includes the dryer without the trays and drying products. The author compared the numerically result with the experiment and concluded that the numerically results were in agreement with experimental result.[71] used ANSYS software to examine the temperature and velocity distribution inside indirect solar dryer. The simulation implemented discrete ordinates (DO) radiation model with direct solar irradiation of 1423W/m^2. The author verified the result with an experiment and the numerical result matches well with the experiment. In addition, the author concluded that not very long exposure to sun rays is required

to achieve temperatures high enough for preservation and indirect solar driers could be applicable in regions of the world with fewer hours of sunshine.

[74] used ANSYS FLUENT software to analyse air velocity, temperature and static pressure, distribution in the direct cabin type multipurpose dryer. The airflow in the drier was parallel with the product and fan was used to force the air. The simulation was carried to investigate the air velocity, temperature and static pressure, distribution in the cabin at various air inlet temperature between 40, 50 and 60 ℃ and with constant air velocity of 26 m/s. From the numerical result, the average temperature distribution in the system was in a range between 33.2 and 52.7 ℃ while the average air velocity was 1.965 m/s and the maximum pressure in the system was found to be 6453.32 Pa. The author concluded that, the result from the CFD showed even and adequate air distribution, which also translated to an even and adequate temperature distribution within the system and the increase in the air temperature highly reduced the energy required and enhance the dryer efficiency.

[72]developed CFD model using ANSYS FLUENT software by implementing Discrete Ordinates (DO) method for solar radiation model with dual-band spectrum and demonstrated the important physical phenomena in the solar drying process such as the greenhouse effect and the direct absorption of radiation by crop. As stated in this work, the model helped visualizing the airflow within the natural convection solar dryer and its result revealed air stagnation within the dryer, which was reported as a factor, which limit the drying capacity. The predicted temperature and humidity distribution was found comparable to the experimental observation, however there was an over prediction of both temperature (8.5%) and humidity (21.4%). The author observed that eliminating stagnation and improving natural convection would increase the rate of moisture removal and the dryer efficiency and the author stated the model could be used to study the effect of design change on the dryer performance.

2.5 Drying Fundamentals

Drying involves removal of moisture and, in thermal drying this is achieved through the application of heat to the product. The heat increases the vapour pressure of moisture in the product above that of the surrounding air and the pressure and thermal gradients cause the moisture, both liquid and vapour, to move to the surface of the product and from there evaporation takes place and water vapour is transferred to the surrounding air. This air may become saturated but the process of drying continues if this moist air is replaced by less saturated air [9], [32], [75].

Water may be contained in various forms. Free or loose held moisture is regarded as unbound and bound moisture is trapped in closed capillaries of the material. In most of products, there is a combination of free or unbound and bound moisture. Free moisture is water that can move through the product in an unrestricted way. Its movement is not dependent on the internal structure of the product. The vaporization-evaporation process is at a maximum when there is sufficient free water in the product to replace that evaporated at its surface. As this moisture evaporate, the moisture content of the product falls and the product temperature is close to the wet bulb temperature of the drying air. This period in drying process is usually known as the constant rate drying period and shown in Figure 2.23. The factors that determine the drying rate in this period are mainly external parameters such as air temperature, velocity and the surface area of the product [32], [37].

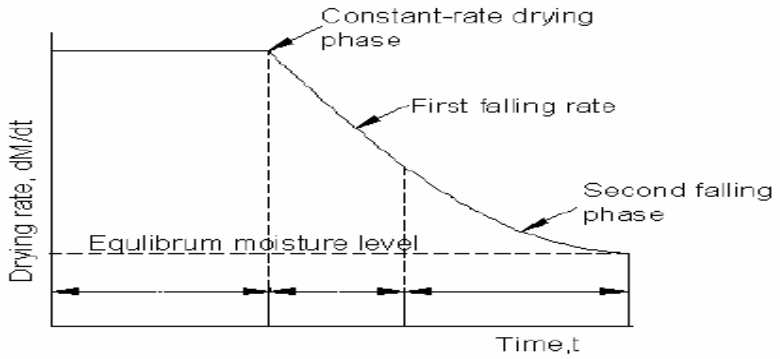

Figure 2.23 Drying Curve [32]

At a certain point known as the critical moisture content, there is insufficient free moisture to maintain the maximum drying rate. The remaining moisture in the product is bound moisture and is held within its cell structure. This means that the moisture cannot move freely through the product to its surface. The rate of moisture movement to the surface of the product falls progressively and consequently the drying rate declines. This stage of the drying process is known as the falling rate period. Now the factors determining the drying rate are mainly internal

parameters specific to the product. These internal parameters are often conveniently grouped together and expressed as a diffusion coefficient or alternatively a drying constant [34].

The moisture content of a product can be expressed in two different ways, either as a percentage wet basis (% wb) or as percentage dry basis (% db). The moisture content of a product expressed as a percentage dry basis is the ratio of the amount of water in the product at any time compared to the amount of dry matter in the product and the wet basis moisture is the ratio of mass of water in a sample to wet mass of the sample. Commercial producers mostly use the wet basis moisture content while researchers and academic professionals use the dry basis moisture content. It is necessary when results are reported to define the moisture content basis that is used [32]. Whichever basis is used, there are two moisture content levels, which are of interest. These are the initial moisture content, which is the moisture content of the sample before drying, and final moisture content, which is the moisture content of the product that must be achieved by drying and sometimes known as the safe moisture content. These two moisture content levels vary between products and locations [34], [55].

2.5.1 Mathematical Modelling of Thin Layer Drying

Thin layer drying in general means to dry slices of a product as one thin layer and because of its thin structure, the temperature distribution through the product can easily assumed uniform. These models fall into three categories, namely, theoretical, semi-theoretical and empirical as described in[76], [77]. [78]Stated that for the purpose of design and analysis, it is often sufficient to use semi empirical expression because it can adequately describe the drying kinetics when the external resistance to heat and mass transfer is eliminated or minimized. A common way to achieve this is to carry out drying experiment using a thin often a single layer of material.

A. Theoretical models

The most widely used theoretical models were derived from Fick's second law of diffusion, which describe the rate of change in moisture transfer within the solid. During drying, diffusion is a complex process that may involve, molecular diffusion, capillary flow, Knudsen flow, hydrodynamic flow, or surface diffusion and if one combine these process in to one the effective diffusion (D_{eff}) can be defined from Fick's second law [79] as given below,

$$\frac{\partial M}{\partial t} = D_{\text{eff}} \nabla^2 M \qquad \text{Equation 2.1}$$

Where, M is moisture content (kg water/kg dry matter)

The effective moisture diffusivity was estimated by using analytical solution of Fick's second law for unsteady state diffusion. The falling rate period of biological materials is best described by Fick's second law of diffusion .The analytical solution of above equation is solved by considering a slice of food as an infinite slab geometry, assuming uniform initial moisture distribution, constant temperature and diffusivity coefficient, and negligible external mass transfer resistance [79], [80].[81] The solution for the above equation is of form:

$$MR = \frac{M_t - M_e}{M_0 - M_e} = \frac{8}{\pi^2}\sum_{n=1}^{\infty}\frac{1}{(2n-1)^2}e^{\left(-\frac{(2n-1)^2\pi^2 D_{eff}}{4L^2}t\right)} \qquad \text{Equation 2.2}$$

For long drying time the first term of the series dominates and the equation is simplified to following equation [81].

$$MR = \frac{M_t - M_e}{M_0 - M_e} = \frac{8}{\pi^2}e^{\left(-\frac{\pi^2 D_{eff}}{4L^2}t\right)} \qquad \text{Equation 2.3}$$

Where, $D_{eff}$is effective moisture diffusivity (m^2/s), t is drying time (s) and L is half the thickness of the sample slice (m).

B. Semi-theoretical models

Similarly, semi-theoretical models are generally derived from Fick's second law and modifications of its simplified forms and other semi-theoretical models are derived by analogues with Newton's law of cooling[76]. They depend mostly on experimental data and are less complex, require small time compared to theoretical thin layer models with fewer assumptions[82]. Table 2.1 shows among some of widely used semi-theoretical thin layer drying models which are stated in literatures [33], [67], [76], [82]–[85].

Table 2.1:Thin Layer Drying Models

S.no	Thin-layer drying model	Equation
1	Two-Term Exponential Model	$MR = a * exp(-k * t) + (1 - a) * exp(-k * a * t)$
2	Henderson and Pabis Model	$MR = a * exp(-k * t)$
3	Lewis (Newton) model	$MR = exp(-k * t)$
4	Page Model	$MR = exp(-k * t \text{ ^}n)$
5	Modified Page-I Model	$MR = exp(-k * t)\text{^}n$
6	(Yagcioglu et al.) Logarithmic (Asymptotic) Model	$MR = a * exp(-k * t) + c$
7	Verma et al. Model	$MR = a * exp(-k * t) + (1 - a) * exp(-b * t)$
8	Midilli et al.	$MR = a * exp(-k * t \text{ ^}n) + b * t$
9	Demir et al. Model	$MR = a * exp(-k * t)^n + b$
10	Modified Henderson and Pabis Model	$MR = a * exp(-k * t) + b * exp(-g * t) + c * exp(-h * t)$

2.6 Effect of Various Factors on Dryer Performance

[86] stated that the temperature, flow rate and relative humidity of the air are one of the key drying variables. Drying capacity of air can be increased by heating the air above the ambient temperature which as a result reduces the relative humidity of the air [87]. Similarly in solar driers better product quality and optimum system efficiency can be obtained from optimum air mass flow rate [75] and not only the flow rate but the uniformity of the drying air with uniform temperature distribution inside the drier [88].

2.6.1 Effect of Air Temperature

The temperature of the air used in the drying process is one of the major factors influencing the rate of drying. increasing the energy input to a dryer by raising the temperature of the air will increase the rate of drying [67], [89], [90].

It is important to limit the drying temperatures of most food products and this may be 40 to 60^{o}C. Even though this is a general case, care should be taken to avoid excessively high

temperatures, which can damage the product, or results case hardening and nutritional degradation [88], [89], [91].

2.6.2 Effect of Relative Humidity of the Air

Relative humidity is an indication of the amount of water vapour contained in a given amount of air divided by the maximum amount of water vapour the air could hold at that temperature and it is expressed as a percentage value [90]. The moisture content of air entering a dryer will have an effect on the water removal capabilities of the air once it is heated [90]. If the ambient air relative humidity is high before it is heated, then the moisture content of the air will be high. This means that when heated, the ability of the air to remove water will not be as great as if the air had a lower initial moisture content [88].

2.6.3 Effect of Air Velocity

The velocity or speed, at which the air is travelling, is also an important factor in drying. [88] stated that when there is no movement of air across the surface, air at the surface becomes saturated with water, as a result, water on the surface cannot be removed and result a layer of air clings to the surface of a material and prevents efficient moisture removal and this phenomenon is called a stagnant boundary layer. In addition, the author stated based on test result that, an air speed of 0.25 m/s allows the peppers to dry reasonably well. However, when the speed increased from 0.25 m/s to 0.50 m/s, there is a noticeable improvement in how fast the drying occurs and air velocities higher than 0.5 m/s were found to have very little additional impact. However, in [45] work, for industrial dryer constricted for fruits and vegetable drying the result showed that an air velocity greater than 1.2 m/s did not result significant increase in the drying rate.

[32], [43] reported, air velocities in the range of 0.1 to 0.8 m/s was found acceptable for natural convection dryer. [43] observed in his test the effect of solar radiation on air velocity and observed that, less radiation pinged on the collector causes lower air temperatures and as a result lower velocity.

2.6.4 Drying Air Distribution

The flow patterns and uniformity of air flow in the drying chamber have important impact on the drying process as stated in [88]. [45], [92] identified that, uniformity of the moisture content inside the final product could be obtained through a proper distribution and guidance of the drying air inside the drying unit. [45] stated that, Non-uniform drying of product could be avoided by designing the drying chamber for air to pass only one tray per pass so that uniform drying of all trays would be obtained, due to the similar temperature and relative humidity of the air.

2.6.5 Selection of a Dryer

The selection of a dryer plays an important role in drying process and one should consider the economically and technically feasible before selecting a drier. Therefore, it is vital to develop a simple, practicable and economical dryer.

Different authors recommended the selection parameters of solar drier and their suggestion includes manufacture cost, final product quality, safety considerations, lifetime, durability, thermal performance, environment condition, maintenance and ease of installation [90], [93].

2.7 Summary of Literature Review

A comprehensive literature review of solar drying systems including different solar dryers, applications of software in solar drying, mathematical modelling of thin layer drying and effects of various parameters on drying process have been performed. These studies were showed the importance of solar driers and drying by solar energy. Software applications have been used widely with a drying application such as ANSYS and CFD techniques. Comparison between simulated and measured results showed that there was a good degree of similarity between measured and predicted value. Many research studies have been done about mathematical modelling of food drying, thin layer drying have gain acceptance in modelling drying process and results of experiment from solar drying were compared with different thin layer drying models. Different solar driers designs have been indicated with selection criteria and the effects of various parameters on drying process were studied. In designing solar driers, the design of proper air distribution system plays important role to improve the performance of solar drying systems.

From the literature review it is clear that the majority of solar dryer designs, which are available, were used mainly for drying various crops and other products, and No paper were found that explicitly considering solar injera dryer. So this research work is selected to work on this very important issue.

Chapter Three : Materials and Methods

This chapter deals with the methodology applied in this study. First, the design procedure is described after which research site and design concept comparison and selection procedure is described. Then it is followed by fundamental design conditions, constraints and sizing of the solar dryer with its materials selection and fabrications is addressed. Finally, performance evaluation technique is presented.

3.1 Design procedure (Methods)

The following procedures will be followed throughout the course of the project:

1 After design concept comparison and selecting the most efficient and adequate solar dryer for the purpose, detail thermal and mechanical design will follow. At this phase of the project, detail part design of the solar drier, drying chamber, drying racks and others, material selection and layout design was carried out. Since the quality of dried injera depends on the uniform distribution of the drying air velocity and temperature inside the drying chamber, the uniform distribution of the drying air velocity and temperature inside the drying chamber will be achieved using proper arrangement of the drying racks.

2 Simulation/mock-up: This phase is where different parts of the solar dryer was simulated. Partial testing of solar drier with appropriate layout and other significant parameters was performed using ANSYS. Also the governing continuity, momentum and energy equation were solved using finite element design tool ANSYS and also thermal analysis on different parts of the dryer subjected to thermal load (solar load) was done with appropriate inputs.

3 Manufacturing and fabrication: This stage is where different mechanical parts were manufactured or ordered for fabrication and assembling of the parts were completed at the end of this stage.

4 Testing: The machine was tested for proper functionality weather it fulfils the specific objectives set and compare its result with simulation result. Finally, the drying rate and moisture ratio of the drying process was evaluated.

3.2 Study Area

Addis Ababa, is located in Ethiopia and situated in 9.020 latitude, 38.420 longitude. For empirical calculation the total incident radiation data on horizontal and inclined surface for the representative month and day also average daily temperature and relative humidity was referred from [94], [95].

3.3 Design Concept Comparison and Selection Procedure

Five different types of solar driers were proposed and the evaluation criteria's were set. The list of the proposed design concept is listed below and these alternatives were compared and selected using decision matrix. The decision matrix contains the design parameters, weighting factors and rank. The weighting factors were set on a scale from one to three and three being more important criteria than the other and one being the contrary. Each design concept was then ranked on a scale from one to five and five being given for design concept, which satisfy the criteria more than the other and one being the opposite. The rank for each design concept was multiplied with the weighting factor. Finally, the results from the multiplication were added for each design concept and the highest value was selected. The complete discretion of the proposed design concepts and the result of the decision matrix are shown in **APENDEX A-C**. From the decision matrix, a mixed mode natural convection solar dryer was found to fit the purpose of this paper.

A. Direct cabinet type solar dryer.

B. Mixed type solar dryer.

C. Mixed type solar dryer with three collectors.

D. Mixed type solar dryer with a collector connected to the drying chamber with a hose.

E. Cabinet type solar dryer with downward facing absorber and parabolic solar reflector.

3.4 Fundamental Design Constraints, Conditions and Sizing

3.4.1 Solar Dryer Design Constraints

According to different authors, the design constraints, which applies to mixed mode natural convection dryer includes the following:

1. For natural convection airflow, the average velocity of the drying air, v_c at the exit (or outlet) of the collector is expected to be between 0.20 and 0.40 m/s [64].

2. The optimum collector tilt (β_{opt}) for maximum collection of incident solar radiation for all year round operation of a collector is to be taken as the latitude of the site [64]. But to avoid the accumulation of rain water on the collector during rainy period collector tilt of 13^o was used and this value is recommended for the latitude of the location by [91].

3. Drying bed thickness (h_L) for natural air circulation through a drier was recommended to have $h_L \leq 0.2$ m [64] and the optimum value of 0.2m was used for this study.

4. The length to width ratio of solar collector ($\frac{L_c}{W_c}$) for optimum performance is recommended in the range 1– 2 [54], [64].
5. The maximum height of the hot air column, H, is recommended to be between 2 and 6 m for corresponding total pressure across the drier between 0.8 and 2.5 Pa [64].
6. The drying temperature was established as a function of the maximum limit of temperature the food might support. The maximum allowable drying temperature of foods and grains without compromising its quality was maintained and recommended between 50 to 60 ^{0}C [54].
7. It has been recommended that the depth of the air channel should be 1/15 to 1/20 of the length of collector [54].
8. It has been suggested to account for the heat lose through the roof and wall of the solar drier to the surrounding and 8 to 12% of the heat required to be lost as heat losses[96].
9. Since bound water is to be evaporated from the product to be dried, the value of latent heat of evaporation (L_v) is to be increased by a factor of 10–20% [64].
10. The mass flow rate,$\dot{m}$ through the dryer has been found to lie in the range 0.02 to 0.9 kg/s [64].

3.4.2 Design Conditions

To carry out sizing of the solar injera drier, the design conditions applicable to the geographical location of the dryer were considered. Data regarding the loading quantity per batch with the, climatic condition, property of injera and other design parameters, which are used in sizing the solar drier, is listed in the Table 3.1 below.

Table 3.1: Design Conditions and Assumptions

1.	Location	Addis Ababa, Ethiopia at 9.020 latitude and 38.420 longitude
2.	Food	injera
3.	Bulk Density, ρ_{in}[kg/m^3] [97]	1160.55
4.	Specific Heat Capacity, C_P[kj/kg.k] [97]	3.440
5.	Design drying period	July
6.	Mass of single injera m_{in} [g][2], [97]	310
7.	Design initial mass of the injera to be dried per batch, m_i[kg/batch] **	10 ** (20 injera)
8.	Average thickness of injera,t_{in} [mm] [2]	2 to 4
9.	Diameter of injera D_{in} [m] [2]	0.52
10.	Design initial moisture content of injera, M_i[%] w.b [22], [97]	58%
11.	Design final moisture content of injera, M_f[%] w.b*	13%
12.	Ambient air temperature, T_a [^{o}C] [95]	25
13.	Ambient relative humidity, RH_a[%],[95]	72%
14.	Maximum allowable drying air temperature, $T_{d,max}$ [^{o}C] [54]	50
15.	Drying time (sunshine hours 8hr) t_d [hrs]*	16
16.	Incident solar radiation on the tilt surface I_T [w/m^2] [94]	390
17.	Wind speed, v_a [m/s]	0.5
18.	Drying efficiency, η_d [%]*[58], [64]	21
19.	Vertical distance between two adjacent trays, d [m][66]*	0.3
20.	Optimum collector tilt angle, β_{opt}[^{o}] [91]*	13
21.	The ratio of drying chambers floor area to the collector surface area ($\frac{A_d}{A_c}$)* [66]	0.75

* Are assumptions, ** 50% added to account for mass variation from the standard value.

3.4.3 Sizing Solar Dryer

a) Mass of water evaporated or moisture removed

Amount of moisture to be removed from injera to bring it to the desired moisture from its initial moisture content is estimated from the initial moisture content and the final desired moisture content. It can be obtained using Equation[64], [66].

$$m_{\mathrm{w}} = \frac{m_i(M_i - M_f)}{100 - M_f} \qquad \text{Equation 3.1}$$

Where:

m_i = Initial mass of injera, kg

M_f = Final moisture content, percentage wet basis

M_i = Initial moisture content, percentage wet basis

b) Total useful heat energy required to evaporate moisture

The quantity of heat required to evaporate water from injera is calculated from the equation below [66],

$$E = m_w L_v \qquad \text{Equation 3.2}$$

Where:

E = useful heat energy required to evaporate moisture, kJ

m_w = mass of water evaporated or moisture to be removed, kg

L_v = latent heat of vaporization of water at mean temperature [29], [58],kJ/kg

c) Solar aperture area

In mixed-mode driers, solar aperture area is the effective total surface area of the dryer for collecting incident radiation (A_T) [90] and it includes the collector area and the drying chamber floor area which is given by [64], [90],

$$\eta_d I_T A_T t_d = E = m_w L_v \qquad \text{Equation 3.3}$$

Therefore, area of the solar collector A_c is:

$$A_T = \frac{E}{I_T \eta_d t_d} \qquad \text{Equation 3.4}$$

Where

E = useful heat energy required to evaporate moisture, kJ

I_T = total global radiation on an inclined surface during the drying period, W/m^2

η_d = drying efficiency

t_d= drying time, hrs

d) Sizing the drying chamber

The width of the drying chamber, W_{dc} is made equal to the width (W_c) of the collector. Thus, the drying chamber length, L_{dc} is determined from the relation below[64],

$$L_{dc} = \frac{A_d}{W_{dc}} \qquad \text{Equation 3.5}$$

Where

A_d = drying chambers floor area, m^2

W_{dc}= drying chamber width, m

e) The total volume of air required for drying

Total volume of air required (V_a) for removing moisture from injera is evaluated from the equation given by [64], [66],

$$V_a = \frac{m_w L_v R_a T_a}{C_p P_{atm}(T_o - T_f)} \qquad \text{Equation 3.6}$$

Where

V_a= volume of air required, m^3

P_{atm} = atmospheric pressure, N/m^2

m_w = Mass of water evaporated or moisture to be removed, kg

L_v = latent heat of vaporization of water at mean temperature, kJ/kg

T_a = ambient air temperature, K

R_a = specific gas constant, 287 J/kg K[64]

C_p= specific heat capacity of air at constant pressure, J/kg.K

T_o= temperature of air at the collector outlet, K

T_f= temperature of air leaving the drying bed, K

The temperature of air leaving the drying bed (T_f) is calculated from the equation below [66],

$$T_f = T_a + 0.25(\Delta T) \quad \text{Equation 3.7}$$

Where

ΔT = drying air temperature rise over the ambient.

T_f= temperature of air leaving the drying bed (K)

And the drying air temperature rise over the ambient (ΔT) is calculated from the equation below [64],

$$\Delta T = 2\beta(T_b - T_c)(\frac{I_t}{I_o}) \quad \text{Equation 3.8}$$

Where

β= dimensionless parameter whose value is in a range 0.14 to 0.25 and 0.2 was assumed

$T_b - T_c$ = the temperature difference between the boiling and freezing point of water at atmospheric pressure and 100 ^{0}C is taken,

I_t= is the intensity of radiation incident on the plane of the collector, W/m^2

I_o= is solar constant and its value is given as 1367 W/m^2.

The volume flow rate ($\dot{V}_a$) and mass flow rate of drying air ($\dot{m}_a$), were calculated as shown below:

$$\dot{V}_a = \frac{V_a}{t_d} \quad \text{Equation 3.9}$$

$$\dot{m}_a = \rho_a \dot{V}_a \quad \text{Equation 3.10}$$

Where

V_a= volume of air required, m^3

t_d = Total drying time, hr (a batch in two days)

ρ_a = density of ambient air, 1.2kg/m^3

$\dot{V}_a$= volume flow rate of air ($\frac{m^3}{s}$)

f) Average drying rate

Average drying rate, M_{dr} is determined from the mass of moisture to be removed by solar heat and drying time by the following equation[88]:

$$M_{dr} = \frac{m_{\mathrm{w}}}{t_d} \qquad \text{Equation 3.11}$$

Where

M_{dr} = average drying rate, kg/hour;

M_w = is mass of water evaporated which is $M(\,t + dt\,) - M(t)$ and

t_d = Total drying time, hr

g) Height of the hot air column

[64] Stated in his paper, the height of the hot air column (H) is the minimum height of the exit vents above the collector inlet for moist air escape to the ambient under natural convection. At this height, steady state conditions were assumed with additional assumptions those stated below and the height can be calculated by applying Bernoulli's equation between important units of the drier and simplifying its result as shown in equation 3.12,

- The drying depth h_L, is small compared to H,
- The structure is airtight.
- The steady state average temperature and density values of the air inside the dryer are T_o and ρ*, respectively.

$$H = \frac{\Delta P_T}{g*(\rho_a - \rho^*)} = \frac{\Delta P_T * R_a}{g*\left(\frac{1}{T_a} - \frac{1}{T_0}\right)*P_a} \qquad \text{Equation 3.12}$$

Where;

ΔP_T = gross pressure drop in the dryer, Pa

R_a= specific gas constant 287 J/kg K [64]

T_o=Temperature of air at the collector outlet, K

T_a=Temperature of ambient air, k

g = gravitational acceleration, m/s^2

P_a = Atmospheric pressure, Pa

3.5 Solar Dryer Important Part Design

Table 3.2:Results of Part Design

No.	Equation	Description	Applied Design Constraint	Result
1	$m_w = \frac{m_i(M_i - M_f)}{100 - M_f}$	Mass of water evaporated or moisture removed		5.172 kg
2	$E = m_w L_v$	Total useful heat energy required to evaporate moisture	Design constraint 9 with 12% heat losses and design constraint 10 with 15% for bound water evaporation (heating the product)	16,505.954 kJ
3	$A_T = \frac{E}{I_T \eta_d t_d}$	Solar aperture area	Applying design condition 21 $(\frac{A_d}{A_c} = 0.75)$	$A_c = 2\ m^2$ and $A_d = 1.5\ m^2$
4	$L_{dc} = \frac{A_d}{W_{dc}}$	Length of the drying chamber	Design constraints 5 (l_c / w_c) with optimum value of 2	L_{dc} =1.5 m, $W_c = W_{dc}$=1m
5	$V_a = \frac{m_w L_v R_a T_a}{C_p P_{atm}(T_o - T_f)}$	The total volume of air required for drying		$1459.63\ m3$
6	$\dot{V}_a = \frac{V_a}{t_d}$	The volume flow rate		$0.03 \frac{m^3}{s}$
7	$\dot{m}_a = \rho_a \dot{V}_a$	Mass flow rate of drying air		$0.036\ \frac{kg}{s}$
8	$M_{dr} = \frac{m_w}{t_d}$	Average drying rate		$0.323\ kg/hr$
9	$H = \frac{\Delta P_T}{g * (\rho_a - \rho^*)} = \frac{\Delta P_T * R_a}{g * \left(\frac{1}{T_a} - \frac{1}{T_0}\right) * P_a}$	Height of the hot air column	Using design constraint 6 with 2.4m and using design constraint 8 with air duct depth of 1/20 of the length of collector	H=2.4m, total pressure drop across the drier was found to be 1.03 Pa and Collector depth (d_c)=0.1m

From this result we can check whether the collector air vent area able to produce the calculated volume flow rate by multiplying its value with 0.4 m/s velocity (Constraint 1). The A_{cv} results a $0.04\frac{m^3}{s}$ volume flow rate, which is more than the required volume flow rate and this additional $0.01\frac{m^3}{s}$ can be consider as compensate for the volume of air lost from air infiltration by considering 0.001m gap between joints of the drying chamber walls therefore the value of the A_{cv}, is acceptable.

In the construction of the dryer, an allowance of 0.3 m was made for the height of the solar collector inlet above the ground level to allow air to flow naturally through it [64] and above the top drying racks 0.8 m space is provided. At the inlet of the drier, a plenum chamber is provided with a height of 0.3 m from the base of the drying chamber. The position of the first tray (bottom tray) is 0.2 m above the plenum and between each tray, 0.3 m space was provided. From this the height of the drying chamber is 2.2 m and the total height of the hot air is 2.7m which is in the recommended range of between 2 and 6m for corresponding total pressure across the dryer between 0.8 and 2.5 Pa. It is important to point out that because of constructional difficulties some of the dimensions may be changed slightly to allow for ease of assembly within the design constraints.

3.6 Materials selection and fabrications of the solar dryer

The dryer contains two parts, the collector and drying chamber. The collector, with a dimension 1 m *2 m * 0.1 m was tilted at an angle of 13º to the horizontal and its sides and bottom were built using plywood. The top of the collector was covered with 5 mm thick transparent glass. Its absorber was constructed using galvanized steel and painted mat black with its bottom side filled with sawdust as insulation and between the absorber and the sawdust there is an air gap, which can further help to reduce the heat loss. The front and back sides of the collector were open to help circulate the air through the drier. Sliding connection is provided between the collector and the drying chamber, which helps to move the solar dryer easily from place to place.

The drying chamber walls were constructed using plywood with its front partially open and connected to the collector outlet. At the back, there is a door that helps for loading and unloading the drying chamber racks or trays, and 0.1m opening at the top to ventilate the drying chamber humid air and prevents vapour accumulation on the drying chamber internal walls. The drying chamber top was covered with transparent cover with triangular shape and its two side were inclined to the horizontal at 13^0.

Inside of the drying chamber, there are three parts. The first is a plenum chamber with a height of 0.3m from the base of the drying chamber and 1m wide, which helps to stabilize the pressure and velocity of the air coming from the collector. The second part is a vertical air distribution channel, which is constructed from 2 mm galvanized steel. This part helps to regulate and maintains uniform distribution of velocity, temperature and other flow parameters over the racks of drying chamber. The third part of the drying chamber is a set of four injera storage racks, which were evenly placed within the drying chamber, and the dimension of these racks is 1m * 1.1m. The position of the first tray is 0.2 m above the plenum and between each tray 0.3 m space was provided. The trays were made of galvanized wire mesh with rectangular wooden frame. The drier was constructed using locally available materials and shown in Figure 3.1 below. The standard for food processing units were not followed in material selection process due to the scope of the project. The technical drawing of the solar drier was prepared using SolidWorks 2013 and the detail part and assembly drawing of the solar injera drier can be referred from **APENDEX E**.

Figure 3.1: The Prototype Solar Injera Drier

3.7 Performance Evaluation

a) Moisture content

The moisture content, M_c, is a measure of wetness or dryness of material. It can be calculated on either a wet or dry basis. The wet basis moisture $M_{cw}$is the ratio of mass of water in a sample to wet mass of the sample [61] that is,

$$M_{cw} = \frac{M_w - M_d}{M_w} \qquad \text{Equation 3.13}$$

The dry basis moisture M_{cd} is the ratio of the mass of water in a sample to the mass of the dry matter [61], that is:

$$M_{cd} = \frac{M_w - M_d}{M_d} \qquad \text{Equation 3.14}$$

Where:

M_w = mass of wet sample, [kg]

M_d = mass of dry matter in the sample, [kg]

b) Average drying rate

Average drying rate, M_{dr} is determined from the mass of moisture to be removed by solar heat and drying time by the following equation[88]:

$$M_{dr} = \frac{m_w}{t_d} \qquad \text{Equation 3.15}$$

Where

M_{dr} = average drying rate (kg/hr),

M_w = is mass of water evaporated (kg), and

t_d = overall drying time (hr)

c) Drying (or system) efficiency

The system efficiency of a solar dryer is a measure of how effectively the input energy (solar radiation) to the drying system is used in drying the product. [64] suggested to normalize this value by divding it with the intial mass of the product (η_d/m_i), to compare the drying efficiency with othe driers.

For natural convection solar driers, the drying efficiency can be expressed as [66], [90],

$$\eta_d = \frac{m_w L_v}{I A_T} \qquad \text{Equation 3.16}$$

Where

m_w = mass of evaporated water, m_i=intial mass of injera, L_v= Latent heat of vaporisation of water at exit air temperature (J/kg), I = hourly average solar radiation on the aperture surface (W/ m^2), A_T = Aperture area or total energy collection surface area of the dryer (m^2) .

Chapter Four : Mathematical Model

This chapter deals with the mathematical model of solar injera dryer. With numerical simulation procedure with the boundary conditions and assumption which are used in simulation of the solar injera dryer.

4.1 Mathematical Modelling of Injera Drying

For analysis of food drying, mathematical modelling is used widely and effectively in many researches. Out of many mathematical models which described the drying process, the thin-layer drying models have been widely use[76].

4.1.1 Modelling of Semi-Theoretical Thin-Layer Drying

Among semi-theoretical thin-layer drying models, which were considered in this study are listed in Table 4.1 below and the experimental data of moisture ratio (MR) which is computed using Equation 4.2 against drying time were fitted to these semi-theoretical thin-layer drying models to selecting the best model, which describe the thin-layer drying curve of injera. The nonlinear regression analysis was performed using curve-fitting tool in Microsoft office 2016 Excel software.

$$MR = \frac{M_t - M_e}{M_0 - M_e} \qquad \text{Equation 4.1}$$

Where: M_t is the moisture content (kg water/ kg dry matter) at any time t,M_e is the equilibrium moisture content (kg water/kg dry matter), and M_0 is the initial moisture content (kg water/kg dry matter).

The value of $M_e$can be ignored since, during the experiment the relative humidity of the drying air continually changes because it's not controlled, in addition its value is relatively small compared to M_t or M_0[72] and as a result the above moisture ratio equation was simplified as reported [33], [67], [77], [78], [84], [85].

$$MR = \frac{M_t}{M_0} \qquad \text{Equation 4.2}$$

To estimate the goodness of the fit for selected thin layer drying models, three comparison criteria were used. This are, root mean square error ($RMSE$) and reduced chi-square (X^2) based on their lower value and coefficient of determination (R^2) based on its higher value. Several authors used these criteria to select the best thin-layer drying model [77], [82], [84], [98]. The value of $RMSE, X^2$ and R^2 were obtained using Equation 4.3-4.5 below.

$$R^2 = 1 - \frac{\sum_{i-1}^{N} \left(MR_{\exp i} - MR_{Pre\ i}\right)^2}{\sum_{i-1}^{N} \left(MR_{\exp i} - \overline{MR}_{\exp i}\right)^2}$$ Equation 4.3

$$RMSE = \sqrt{\frac{1}{N}\sum_{i-1}^{N}\left(MR_{pre\ i} - MR_{\exp i}\right)^2}$$ Equation 4.4

$$X^2 = \frac{\sum_{i-1}^{N}\left(MR_{exp\ i} - MR_{pre\ i}\right)^2}{N-n}$$ Equation 4.5

Where: $MR_{exp,i}$ is the i^{th} experimental MR, $MR_{pre,i}$ is the i^{th} predicted MR, N is the number of observations and n is the number of model constants.

Table 4.1: Considered Thin-Layer Drying Models [77], [82], [84], [98]

S.no	Thin-layer drying model	Equation
1	Two-Term Exponential Model	$MR = a * exp(-k * t) + (1 - a) * exp(-k * a * t)$
2	Henderson and Pabis Model	$MR = a * exp(-k * t)$
3	Lewis (Newton) model	$MR = exp(-k * t)$
4	Page Model	$MR = exp(-k * t\ \hat{}\ n)$
5	Modified Page-I Model	$MR = exp(-k * t)\hat{}\ n$
6	(Yagcioglu et al.) Logarithmic (Asymptotic) Model	$MR = a * exp(-k * t) + c$
7	Verma Model	$MR = a * exp(-k * t) + (1 - a) * exp(-b * t)$

4.2 Model Development

The governing equations of fluid flow and heat transfer was considered as mathematical formulations of the conservation laws of fluid mechanics. By applying these conservation laws over discrete spatial volumes in a fluid domain, it is possible to describe the changes in mass, momentum and energy as the flow crosses the volume boundaries [72]. In ANSYS fluent the resulting conservation equations of mass, momentum and energy can be written in a general form as shown in Equation 4.6-4.8 below [99]:

$$\frac{\partial \rho}{\partial t} + \nabla \cdot (\rho \vec{v}) = 0 \qquad \text{Equation 4.6}$$

$$\frac{\partial}{\partial t}(\rho \vec{v}) + \nabla . (\rho \vec{v} \vec{v}) = -\nabla p + \nabla . (\bar{\bar{\tau}}) + \rho \vec{g} + \vec{F} \qquad \text{Equation 4.7}$$

$$\frac{\partial}{\partial t}(\rho E) + \nabla . (\vec{v}(\rho E + p)) = \nabla . [-\vec{q} + \sum_j h_j \vec{J}_j + (\bar{\bar{\tau}}_{eff} . \vec{v})] + S_h \qquad \text{Equation 4.8}$$

Where

$\vec{v} =$ is the fluid velocity vector and

$\rho =$ is the density of air

$\bar{\bar{\tau}} =$ stress tensor and

$\vec{F} =$ is the source term for momentum

$E =$ is the total energy

The total energy, which is the sum of internal energy and kinetic energy is given by the Equation 4.9,

$$E = h - \frac{p}{\rho} + \frac{u^2}{2} \qquad \text{Equation 4.9}$$

Where sensible enthalpy h for incompressible flows and h_j is defined as

$$h = \sum_j Y_j h_j + \frac{p}{\rho} \qquad \text{Equation 4.10}$$

$$h_j = \int_{T_{ref}}^{T} C_{p,j} dT \qquad \text{Equation 4.11}$$

Where,

$Y_j =$ is the mass fraction of species j, and

$T_{ref} =$ 298.15 K (for pressure-based solver) [99]

The first three items on the right side of energy equation represents transferred energy due to, conduction and convection fluxes, species diffusion, and viscous dissipation respectively and S_h is heat source term, which includes the heating effects due to radiation.

4.2.1 Turbulent Modelling

ANSYS Fluent can be used to model turbulent airflow [99].Among different turbulent modelling tools in ANSYS, k-omega (K-ω) SST (Shear Stress Transport) turbulence model is recommended by[68], [100], [101],for a flow in a cavity such as solar collectors. As indicated in [101], the K-ω SST turbulence model offer a good compromise between computational cost and accuracy. Furthermore, when compared to other turbulent models, the predictions from this model agreed with the experiment result well for cavity flow. The governing transport equation is defined as,

$$\frac{\partial}{\partial t}(\rho\kappa) + \frac{\partial}{\partial x_i}(\rho\kappa u_i) = \frac{\partial}{\partial x_j}\left(\Gamma_\kappa \frac{\partial \kappa}{\partial x_j}\right) + \tilde{G}_\kappa - Y_\kappa + S_\kappa \qquad \text{Equation 4.12}$$

$$\frac{\partial}{\partial t}(\rho\omega) + \frac{\partial}{\partial x_i}(\rho\omega u_i) = \frac{\partial}{\partial x_j}\left(\Gamma_\omega \frac{\partial \omega}{\partial x_j}\right) + G_\omega - Y_\omega + D_\omega + S_\omega \qquad \text{Equation 4.13}$$

In these equations, $\tilde{G}_\kappa$ represents the generation of turbulence kinetic energy due to mean velocity gradients, G_ω represents the generation of ω. Γ_κ and Γ_ω represent the effective diffusivity of κ and ω, respectively. $Y_\kappa \; and \; Y_\omega$ expresses the dissipation of κ and ω due to turbulence. D_ω describes the cross diffusion term. S_κ and S_ω are the user defined source terms. The detail explanation and formulation of this terms along with default value of model constants which are used can be found in [99].

4.2.2 Species Transport Model

ANSYS Fluent can also be used to model species transport and allow us to include the moisture diffusion. [72] Outlined in what way moisture transport could be accounted in the ANSYS Fluent and indicated that water vapour can be considered as, a scalar property and its presence does not affect the solution of conservation equations for dry air. This assumption is valid because the existence of humidity has little effect on thermodynamic and flow properties of air under the conditions being simulated. The transport of the scalar property was therefore solved independently, with a general conservation equation.

[102] stated, by using species transport model to describing the humid air flow, the system of equation consists with two transport equations, one for the air and the other for water vapour and the equation written as follow,

$$\frac{\partial}{\partial t}(\rho Y_i) + \nabla * (\vec{v}_m \rho Y_i) = -\nabla * \vec{J}_i + S_i \qquad \text{Equation 4.14}$$

Where:

Y_i : is the i^{th}species mass fraction

Diffusion flux of species i due to temperature and concentration gradients ($\vec{J}_i$) is defined for turbulent flows as follow,

$$\vec{J}_i = -\left(\rho D_{i,m} + \frac{\mu_t}{Sc_t}\right)\Delta Y_i - D_{T,i}\frac{\Delta T}{T} \qquad \text{Equation 4.15}$$

Where:

$D_{i,m}$: is mass diffusion coefficient for species i,

$D_{T,i}$: is the thermal diffusion coefficient,

T: is temperature,

μ_t : is turbulent viscosity and

Sc_t is the turbulent Schmidt number and the value used in this work is its default value 0.7 and S_i is user defined source of i^{th} species in our case it is zero [99]. Also at the wall, zero-flux boundary condition for all species was considered.

4.2.3 Radiation Modelling

To account for radiative heat transfer effect on the solar drier Discrete Ordinates (DO) method was been used. To account for heating effects due to radiation, the Discrete Ordinates (DO) method solves the radiative transfer equation (RTE) for a finite number of discrete solid angles and spans the entire range of optical thickness. The result yields a balance of radiative energy over a control volume and accounted in energy equation as a source term. In DO radiation modelling, non-gray radiation with dual band solar spectrum was modelled with fair weather condition assumption. The dual-band solar spectrum represents the incident solar radiation and thermal IR with a band 0.4 to 2.4 μm and 2.5 to 180 μm respectively [72].

For an absorbing, emitting and scattering medium at a position vector $\vec{r}$ and direction vector $\vec{s}$, the radiant energy exchange equation is expressed as [72], [99].

$$\frac{dI_{\lambda\vec{r},\vec{s}}}{ds} + (\alpha_\lambda + \sigma_s)I_{\lambda_{\vec{r},\vec{s}}} = \alpha_\lambda n^2 I_{b\lambda} + \frac{\sigma_s}{4\pi}\int_0^{4\pi} I_{\lambda\vec{r},\vec{s}'}\,\varphi_{\vec{s},\vec{s}'}\,d\Omega' \qquad \text{Equation 4.16}$$

Where λ is the wavelength, α_λ absorption coefficient, Ω′is the solid angle and $I_{b\lambda}$ black body intensity. Scattering coefficient (σ_s), scattering phase functions ($\varphi_{\vec{s},\vec{s}'}$) and the refractive index (n) were assumed independent of the wavelength [99].

In modelling DO radiation in Fluent, absorption coefficient and scattering coefficient of the material are required. Even though the scattering coefficient is important in some industrial processes simulation such as glass making, it has negligible impact to this analysis and therefore it was assumed to be zero[72], [103]. In contrast, absorption coefficient has significant impact. In radiation transfer, the magnitude of radiation intensity can be increased or decrease because of participating medium. This change depends on the intensity of the radiation source, the absorption coefficient, medium temperature and temperature of the surrounding surfaces[103]. Based on this assumption the above equation can be reduced to,

$$\frac{dI_{\lambda\vec{r},\vec{s}}}{ds} + (\alpha_\lambda)I_{\lambda_{\vec{r},\vec{s}}} = \alpha_\lambda n^2 I_{b\lambda} \qquad \text{Equation 4.17}$$

The absorption coefficient defines the rate of exponential attenuation of the radiant energy within the medium. As described in [103], opaque material like metals have higher absorption coefficients and the radiant energy pass through only a few hundred angstroms as a result, high absorption coefficients ensured that the radiation would be attenuated within a very short distance. In this study, for all opaque surfaces an absorption coefficient of 5,000 m^{-1} was set [72].

The presence of water vapour in the air will force as to consider absorption property for moist air because, moist air absorbs or emits radiative energy as described in [103]. Thus the absorption coefficient of the moist air in this study was set to have the same value as the opaque materials as suggested by [72].

Glass is defined to be nearly opaque to the higher wavelength band, whereas it is semi-transparent in the lower wavelength band and from this, the re-radiated energy from the absorber surfaces will be absorbed by the glass [104].The absorption coefficient of glass was calculated using Equation 4.18 [72].

The values for absorptivity of glass was obtained from[105] and for short wave and infrared radiation the absorptivity of glass was given as 0.08 and 0.9 respectively. After substituting this values into Equation 4.18, absorption coefficient of glass were found to be 16.68 m^{-1} and 460.52 m^{-1} for shortwave and infrared bands, respectively.

$$\text{Absorption coefficient } (\alpha_\lambda) = \frac{1}{d} \ln \frac{1}{1-\alpha} \qquad \text{Equation 4.18}$$

Where

α = is absorptivity of glass and

d = is the thickness of glass (m)

The reflected energy from a surface depends on the surface roughness, and can be reflected either specularly (in one direction as a mirror) or diffusely (in all directions) or both of these ways. The specular reflection happens on smooth surfaces while the diffused reflection happens on rough surfaces. Rough surface is a surface that has a roughness height that is much greater than the incident radiation wavelength as described in [104]. The diffuse fraction option in ANSYS Fluent helps as to describe this surface property. For this study all surfaces were taken as purely specular wall.

The solar load was applied to the boundaries of the drier using fluent ray tracing calculator. The calculator uses the geographic location of the drier which in this case is Addis Ababa on latitude 09°02'N and longitude 38°42'E and its orientation (due South) to calculate the sunbeam direction vector. All parameters were computed starting from 09:00 AM on April and July 21. For modelling purposes, average diffuse fraction of solar radiation value of 150 W/m^2 was used [106], and the direct solar irradiation was calculated automatically by the software.

The month of July was used because on this month the solar radiation is comparatively low in the study area [106] and can be used to design the solar drier so that the designed drier can be used throughout the year.

4.3 Simulation result validation

The simulated result was validated by comparing its temperature value against the experimentally measured value. To validate the result, the percent bias (PBIAS) statistics tool was used [72].

$$PBIAS = \frac{\sum_{i-1}^{N} (MR_{exp\,i} - MR_{pre\,i}) * 100}{\sum_{i-1}^{N} MR_{exp\,i}} \qquad \text{Equation 4.19}$$

When the PBIAS is positive the simulation result underestimates and when it is negative it overestimates the experimental result and when it is zero, it indicates an optimum value.

4.4 Numerical Simulation Procedure

After setting the CFD models as described above, the thermo-physical properties and boundary conditions were set as described in Table 4.3-4.4. Then components of the moist air were set to their default values, while the combined mixture properties were defined as follows; incompressible ideal gas for the density and mass weighted mixing law for the thermal conductivity and viscosity were set. Finally, the general solution methods were set and The SIMPLE algorithm were used for pressure-velocity coupling, second order upwind discretization scheme were used for the convection terms of the governing equation, except for the pressure term were the Standards scheme was used. The limits for residuals for all the equations was set to be 1e-03 and for the energy and DO radiation equation as 1e-06 and the under-relaxation factors were set to their default.

4.5 Geometry and Meshing Setup

4.5.1 Geometry

3D geometry of the solar injera dryer was created in ANSYS 19R1 design module. The dryer contains four main parts, the solar collector, the drying chamber, plenum and vertical air distributer channel as shown in Figure 4.2 (left side).

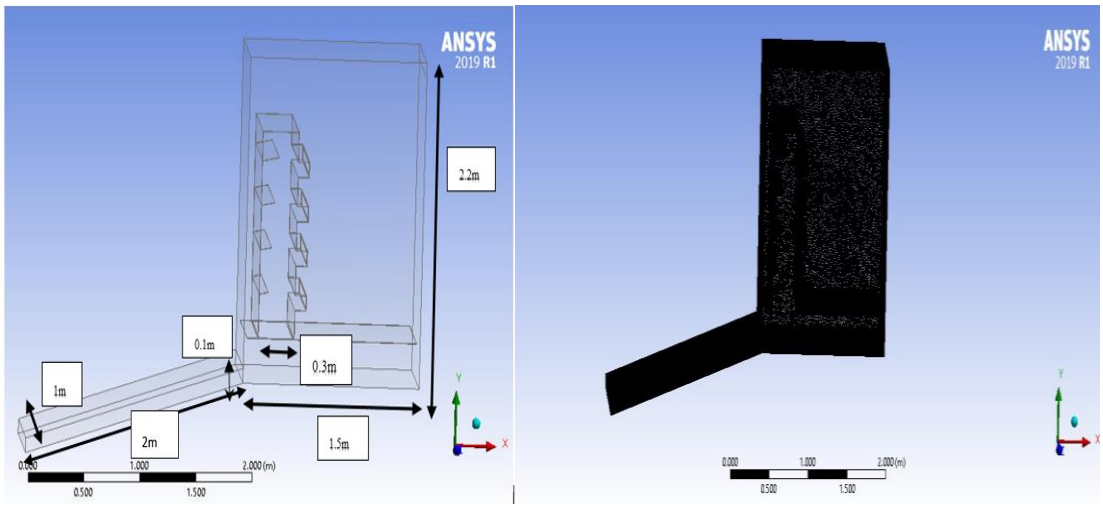

Figure 4.1: 3D Geometry and Mesh of the solar injera dryer

4.5.2 Meshing

The mesh for the geometry were developed in ANSYS-ICEM 19R1 using the recommended unstructured tetrahedral meshing for a model having complex flow domain [107] and it is shown in Figure 4.2 (right side).

4.5.2.1 Mesh Independence Study

The solution of the flow equations depends on the selection of an appropriate mesh. The mesh represents how a computational domain was discretized into a finite number of control volumes. It is obvious that the accuracy of a solution improves with a higher number of mesh size on the other hand, due to limitation in computational speed and memory, a larger number of mesh size is often not possible. At the very least, a fine enough mesh is essential to ensure that the solution is accurate.

The mesh independence of the solution was verified by analysing nine different mesh elements sizes starting from seventy two thousand (72,000) up to four point one million (4,100,000) and all mesh sizes were within acceptable range in there orthogonal quality values [108], [109]. The total heat transfer rate was chosen as the main parameter to study the mesh independence, because it reflects the overall behaviour of moist air inside the modified mixed mode drier. The result of the mesh independence study is shown in Figure 4.2 and Table 4.2 From the result, it can be seen that when the number of mesh element is larger than 2.4 million the difference in total heat transfer rate was less than 0.5% in three consecutive sets of results. Therefore, the mesh having 2,474,510 elements was chosen for this study.

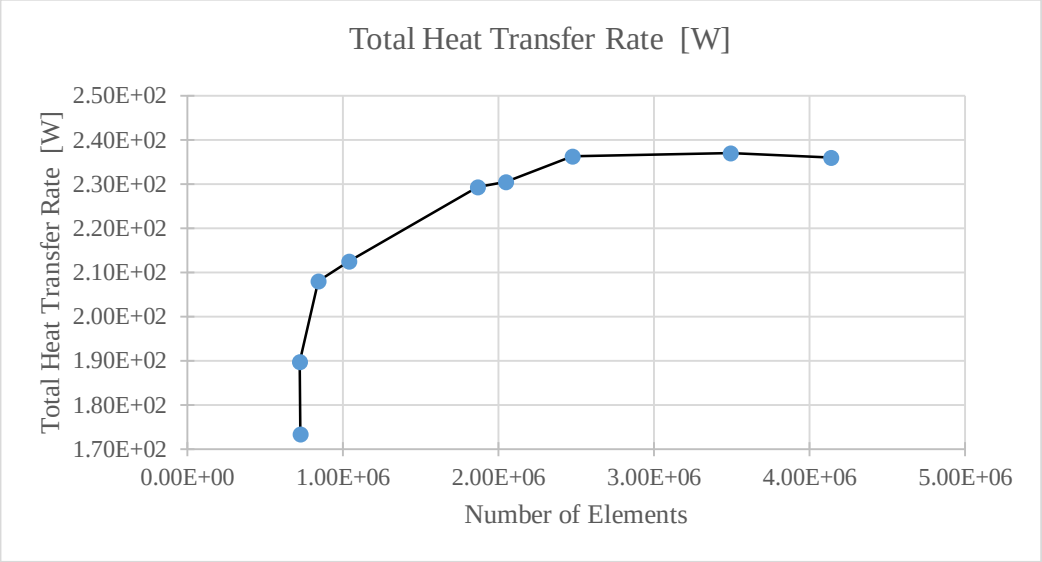

Figure 4.2: Total Heat Transfer Rate Vs Number of Elements

Table 4.2 : Results of Mesh Independence Study

No	P3 - Mesh Element Size [m]	P4 - Mesh Nodes	P5 - Mesh Elements	P6 - Mesh Min	P8 - Total Heat Transfer Rate parameter-2 [W]
1	0.42	135558	724985	0.167369	173.3208
2	0.24	135308	723463	0.174276	189.8013
3	0.04	158134	841529	0.153387	208.1063
4	0.03	196203	1040179	0.1661	212.4954
5	0.02	352518	1867927	0.15744	229.3442
6	0.019	386190	2046749	0.152817	230.5574
7	0.017	467138	2474510	0.15903	236.3622
8	0.014	658699	3490599	0.150121	237.0708
9	0.013	779221	4139393	0.159956	236.0103

4.5.3 Materials and Boundary Condition Setup

4.5.3.1 Material Property Setup

Table 4.3 shows the different materials used for the various parts of the design with their thermo physical property.

Table 4.3:Material property of the Selected Material

Part	Material	thickness	Thermal Conductivity (W/m^*K)	Specific Heat ($J/Kg\ ^*k$)	Density (Kg/m^{-3})	Absorption Coefficient (1/m)	
						IR	Visible
Glazing	Glass	5 mm	1.1	750	2300	16.7	460.5
Glazing 2	Glass	5 mm	1.1	750	2300	16.7	460.5
Absorber	G. Steel	2 mm	Default	Default	Default	5000	5000
Absorber 2	G. Steel	2 mm	Default	Default	Default	5000	5000
Collector side wall	plywood	10 mm	Default	Default	Default	5000	5000
Drying chamber wall	plywood	10 mm	Default	Default	Default	5000	5000
Vertical air distributer channel	G. Steel	2 mm	Default	Default	Default	5000	5000
Fluid	Air		Default	Default	Default	5000	5000

4.5.3.2 Boundary Condition Setup

1) **Inlet and outlet boundary conditions**

The inlet flow was set in normal direction to the collector inlet with 0.5 m/s velocity, zero gauge pressure and 0.014 $\frac{\text{kg water vapour}}{\text{dry air}}$ mass fraction of water vapour. At the outlet boundary zero gauge pressure with default backflow value and zero mass fraction of water vapour were set at normal direction to the boundary.

For both inlet and outlet boundarys the turbulence boundary conditions, turbulence intensity and hydraulic diameter were set and the default value of 5% was used for both turbulent intensity and backflow turbulent intensity and the hydraulic diameter was calculated using Equation 4.20 and the resulting value of 0.1818 was used.

$$D_h = \frac{2*Height*Width}{Height+Width} \qquad \text{Equation 4.20}$$

2) **Wall boundary conditions**

Except for the glass, all walls were considered as an opaque solid walls with no-slip condition but the glass was defined as semi-transparent solid wall with no-slip condition. Convective boundery condition was imposed for the glass wall and all bounders participate in solar ray tracking. Table 4.4 below shows the various boundery conditions used in the modified mixed mode drier simulation.

4.5.4 Assumptions

1) No air leakages.
2) Constant 5 W / (m^2 K) convection heat transfer from the glass to environment was considered.
3) The air flow is assumed to be fully developed turbulent flow.
4) No heat transfer between the air and the injera inside the dryer because the interaction between the injera and the air was not considered in this model.
5) The ambient temperature and relative humidity was assumed to be 25^0C or 298K and 72%.
6) Viscous dissipation was considered insignificant and ignored.

Table 4.4:Summery Boundary Conditions of the Simulation

Boundary	Type	Momentem	Thermal Condition	Radiation	Species
inlet	Velocity inlet	0.5 m/s and turbulent intensity and hydraulic diameter value of 5% & 0.1818	298 K	Boundary temperature	0.014 Kg of water per kg of dry air
Glass 1 and 2	Wall	Stationary wall	Constant convective heat transfer with shell conduction	Semi-Transparent	Default
Absorber 1 and 2	Wall	Stationary wall	Black painted G.Steel with zero heat flux	Opaque with IESR*and IEIR*value of 0.81& 0.92 [110]	Default
Collector side wall	Wall	Stationary wall	Black painted plywood with zero heat flux	Opaque with IESR*and IEIR* value of 0.81& 0.92 [72], [110]	Default
Drying chamber wall	Wall	Stationary wall	Black painted plywood	Opaque with IESR*and IEIR* value of 0.81& 0.92 [72], [110]	Default
Vertical air distributer channel	Wall	Stationary wall	Default	Opaque with IESR*and IEIR* value of 0.81& 0.92 [110]	Default
outlet	Pressure outlet	Turbulent intensity and hydraulic diameter value of 5% & 0.1818	Atmospheric temperature	Boundary temperature	Default

*Internal emissivity for solar radiation (IESR) and Internal emissivity for infrared radiation (IEIR).

Chapter Five : Experimental Methodology

In this chapter experimental testing procedure followed were discussed in detail with instrument used in the experiment.

5.1 Experimental testing procedure

1) In order to compare the performance of the drier to the traditional method of open-air drying, the experiment was carried out in open-air drying and on a partially loaded modified mixed mode drier at the same period and with the same initial mass of injera using only solar energy as heat source.
2) Open-air drying test of injera was carried by spread on a plastic sheet placed on the ground.
3) The experiment was started from morning 09:30am to 14:00pm. However, to achieve the steady state condition inside the drier measurements were started after 1 hr. At 10:30am the product was loaded on both drier with 1.04 kg and each tray were loaded with 260 g of injera.
4) The behaviour of the products from both driers was continuously monitored starting from 11:00 am by measuring the weight of the sample at every 30 min interval until 14:00 pm.
5) The initial moisture content of fresh injera samples were determined by hot air oven method Figure 5.1 at 105ºC for 24 hour, as per ASTM (American society for testing and methods) standard as stated in [61] and followed by [66].
6) After the experiment started samples of about 128 g were taken from both driers. The samples were taken at six locations from open air dryer and from each tray of the chamber. The samples were thoroughly mixed and weighed then placed back in to the

Figure 5.1: Hot Air Oven

dryer in the shortest time possible until no further weight loss of injera was observed and the weight of the injera was not taken during the night.

7) the hourly temperature of the air at the collector inlet (which is equal to the ambient air temperature), collector outlet and above drying trays. This is in agreement with the approach followed by [66], [111] and recommended in [90].
8) After the experiment was conducted, the data collected from both types of drier were taken and graphical represented using Microsoft Excel sheet. Moisture content was determined in terms of both wet basis and dry basis and with product moisture content and time as coordinates drying rate was plotted for both driers on the same graph to have a comparative evaluation of both driers performance.
9) Finally, the moisture ratio of the injera were fitted to thin layer drying model equations to find the best model that describes the injera drying. A similar approach was followed by[111], [112] and recommended in [90].

5.2 Data Analysis

The spreadsheet format shown in **Table D1-D2** at **APENDEX D** was used for the data collection of the temperature distribution in different locations on the solar dryer and instantaneous weight (kg), wet basis moisture content (%) and dry basis moisture content (kg water/kg solid) of injera in the modified mixed mode drier and open sun drier.

5.3 Instruments Used for Data Collection

LabVIEW is a graphical programming language that is used to create programs in block diagram rather than using a text based language. In order to record and control the variable automatically, it was necessary to create a program employing LabVIEW (Laboratory Virtual Instrument Engineering Workbench).

The front panel and block diagram used in this study is shown in Figure 5.2 below. The temperatures at various positions of the dryer were measured with K-type thermocouples (accuracy ±0.2C). Six temperature sensor were used to measure the temperature by fixed them at different locations inside the modified mixed mode dryer and connected to a PC through a Data Acquisition system (DAQ). The thermocouples were place at the inlet and outlet of the collector and the other

four thermocouples were placed above the trays of the dryer to measure the temperature inside the dryer.

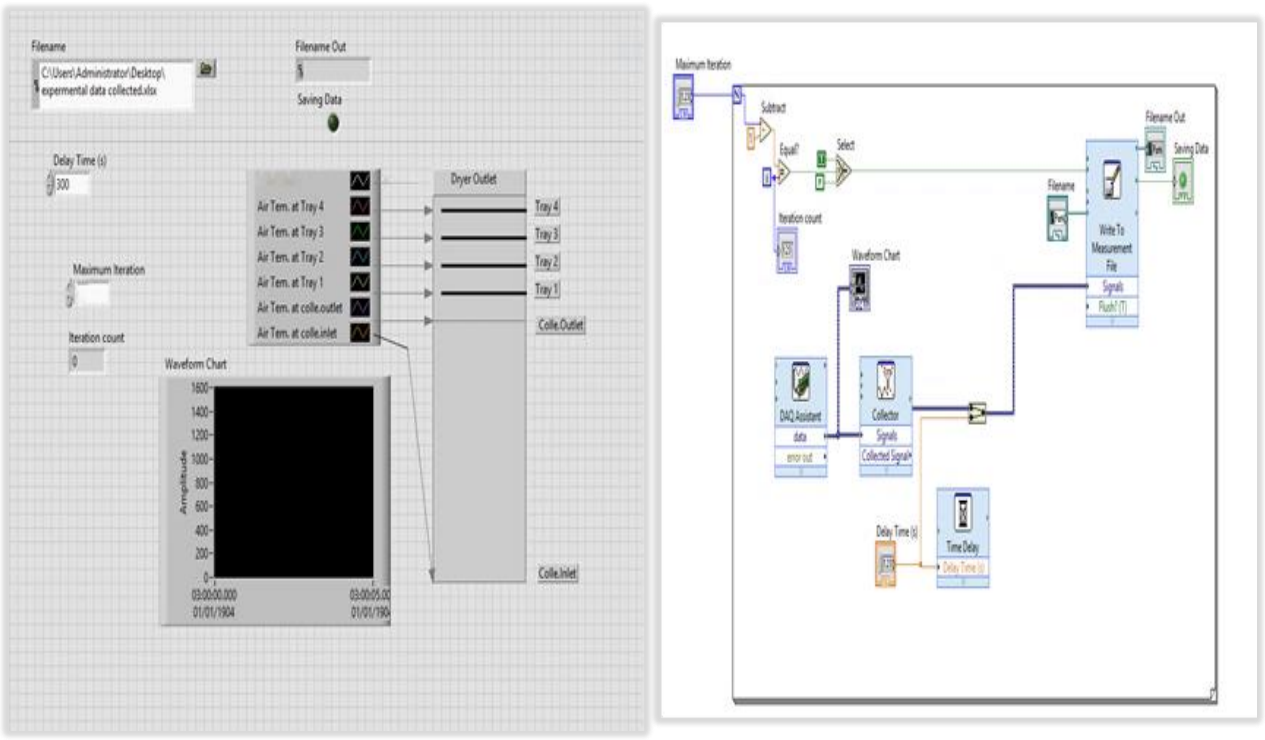

Figure 5.2:Front Panel and Block Diagram used in Labview

The weight of the sample was measured by using Explorer Pre weighing balance with accuracy of ±0.001 g. The air velocity and temperature was measured by using Extech's 4-in-1 Model 45170 4-in-1, which contain an anemometer and thermistor on it with a resolution 0.1 m/s and 0.1 ^{0}C and accuracy ± 0.03 m/s and ± 1.2^{o}C respectively.

Figure 5.3:Weighing Balance and Velocity and Temperature Measuring Device

Chapter Six : Results and Discussion

In this chapter, a discussion of the findings from the Simulation and experiment is provided. Essential points that arise from the results are discussed and comparison between the simulated value and the experimental result are also presented.

6.1 Simulation Results and Discussion

Figure 6:1 shows absorber temperature for simulated month of April and July with respect to the drying time and the temperature profile for both month shows a rapid change from the beginning 9:00 up to 9:16 hours and a maximum temperature of 332 K and 327 K was found for the two months respectively at noon for corresponding ambient temperature of 298 K. There was an increase in the absorber temperature from the beginning 9:00 to 13:30 hours then it starts gently falling till 17 and 16 hours to 313 K and 320 K for both months respectively and this temperature variation coincided with the rise and fall in solar radiation throughout the day. It was also noted the temperature for month of April was always slightly higher than July with a maximum temperature difference of 7 K.

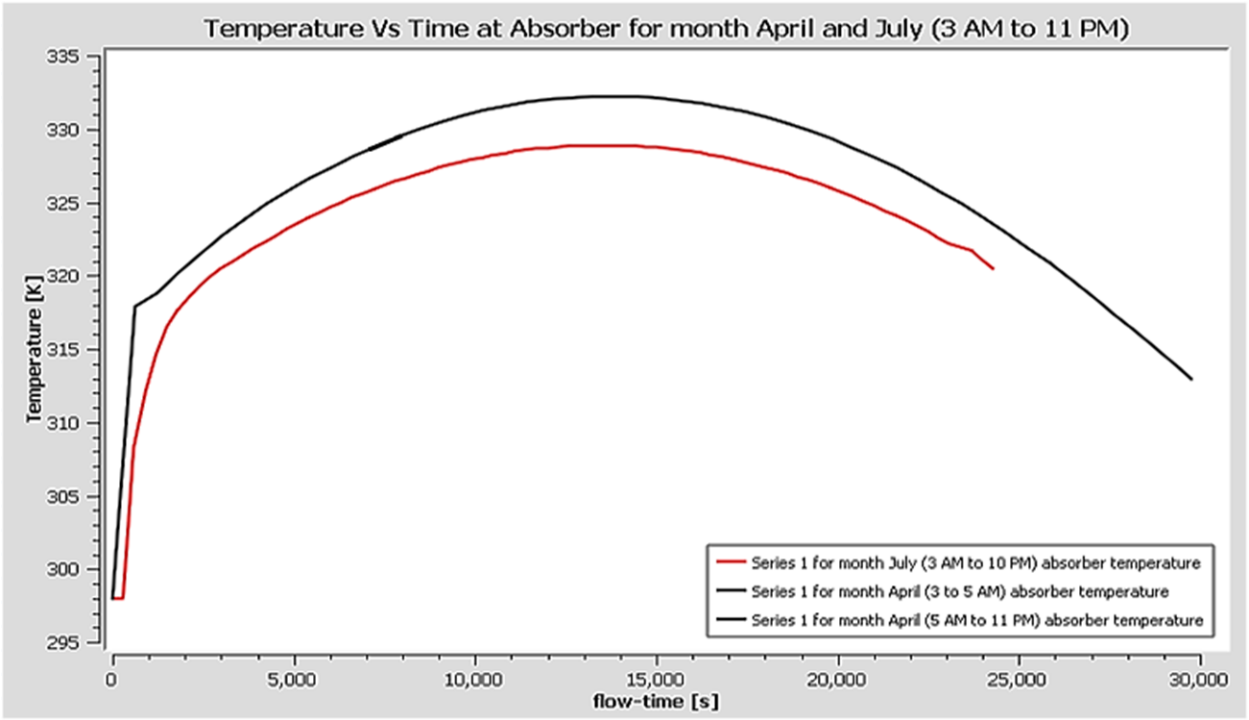

Figure 6.1: Absorber Temperature Vs Time for Month of April and July

Figure 6:2 shows collector exit temperature with respect to the drying time for simulated two months and it was noted a maximum temperature of 318 K and 316 K for month of April and July respectively. This temperature was found to be appropriate, being just below the 323 K, which is recommended maximum drying temperature. It is clear that the collector exit air temperature

was 10 K above the ambient after 20 minutes only from the starting and continues throughout the drying period for about 7 and ¾ hours and this shows the collector design meats the performance

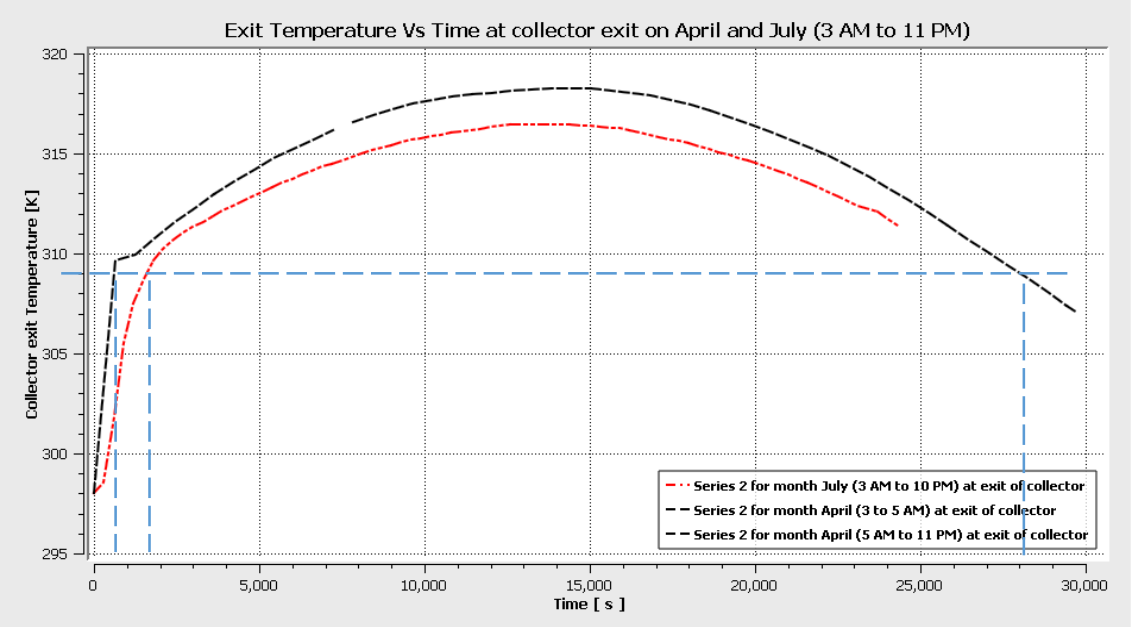

Figure 6.2: Collector Exit Temperature Vs Time for Month of April and July

indicator for almost all drying hours as described in [90].

Figure 6:3 shows temperature distribution through the dryer trays and it was noted that after 1 hour and 20 minute from the beginning till the end of drying period the temperature of all trays remains 5 K above the ambient temperature.

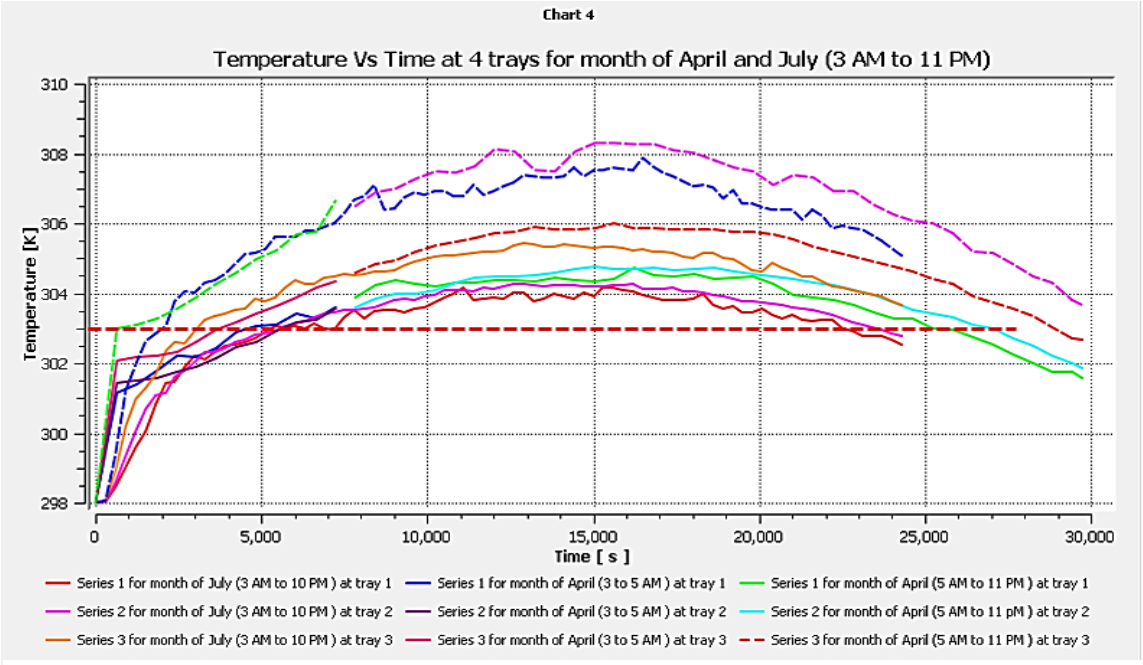

Figure 6.3:Temperature Distribution Through the Dryer Trays Vs Time

The average temperature of 303 K or 8 K above the ambient is observed in all trays for 2 hours after midday. The overall temperature distribution through the drying trays was shown in Figure 6.4 and it shows a uniform temperature distribution, which indicates the effectiveness of the vertical air distributer, which is a new future, used in this dryer. However the temperature distribution on tray 4 is slightly greater than the other tray and this increases in temperature is due to the solar radiation coming from the above transparent cover and this agrees with mixed mode dryer studies conducted by [63], [72] and this will help in facilitating the air flow through the drying chamber.

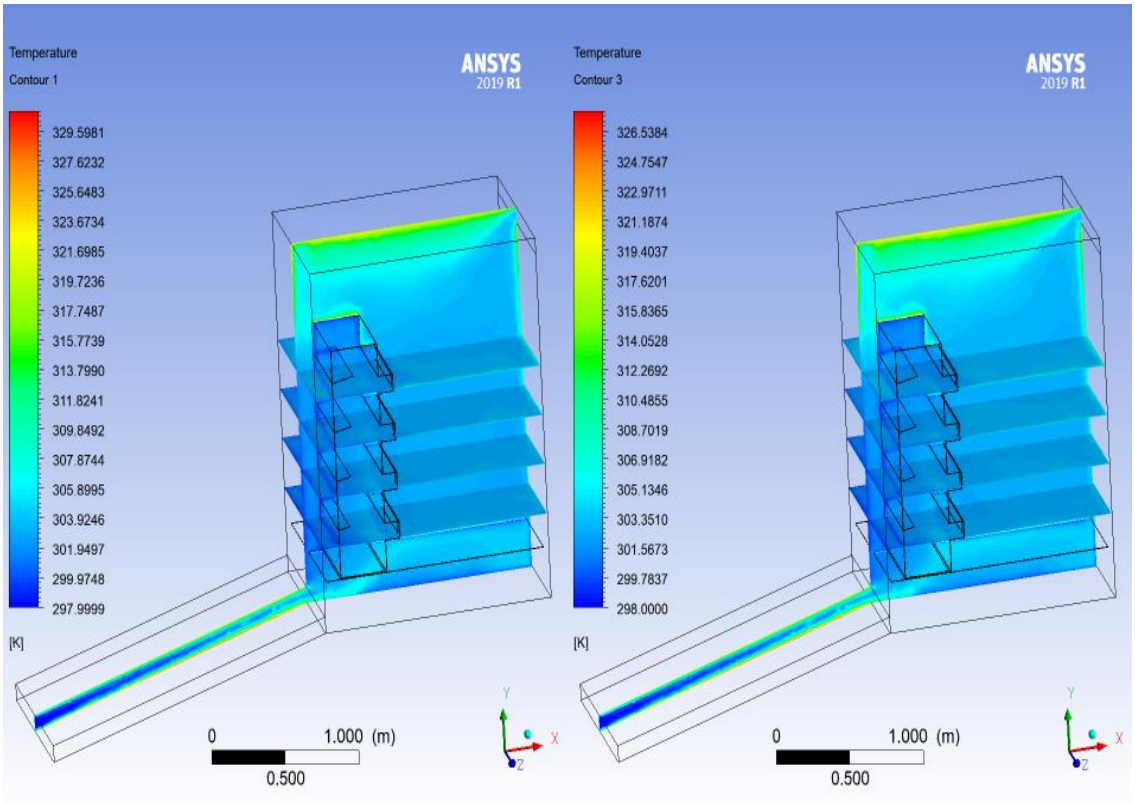

Figure 6.4: Temperature Distribution Contour on Dryer Trays Vs Time

The result in Figure 6:5 shows the average collector exit velocity and it indicates that the collector exit velocity remains above 0.48 m/s through the drying period. The velocity profile for month of April is slightly higher than July, this pattern was also appeared in the temperature profile, and we can conclude that the amount of temperature and velocity for month of April was higher when compared to July.

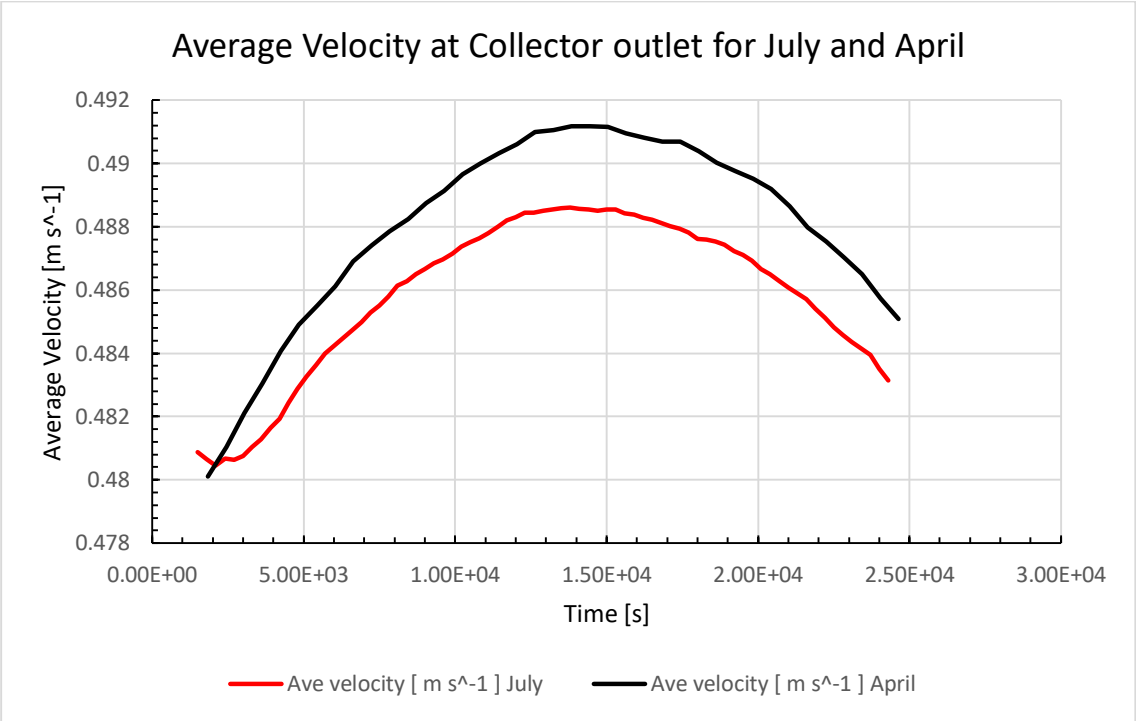

Figure 6.5: Average Collector Exit Velocity Vs Time for Month of April and July

Table 6.1 shows average velocity and pressure distribution through the drying trays, and it can be seen that the overall velocity inside the drier was fond to be uniform however there is small velocity variation between the trays due to the corresponding pressure variation as shown in Figure 6.6 which helps the air to flow through the drying chamber bottom tray to the upper trays. Unlike the temperature distribution, the velocity distribution in the upper tray is smaller than the lower trays. As indicated in temperature distribution the overall velocity distribution through the drying trays also shows a uniform distribution of velocity and this is due to the reason specified in temperature distribution before.

Table 6.1:Average Velocity and Pressure Distribution over Drying Trays

Location	**Velocity [m s^-1]**	**Pressure [Pa]**
Tray 1	1.290e-1	2.630e-1
Tray 2	1.26e-1	2.479e-1
Tray 3	1.123e-1	2.411e-1
Tray 4	1.037e-1	2.384e-1

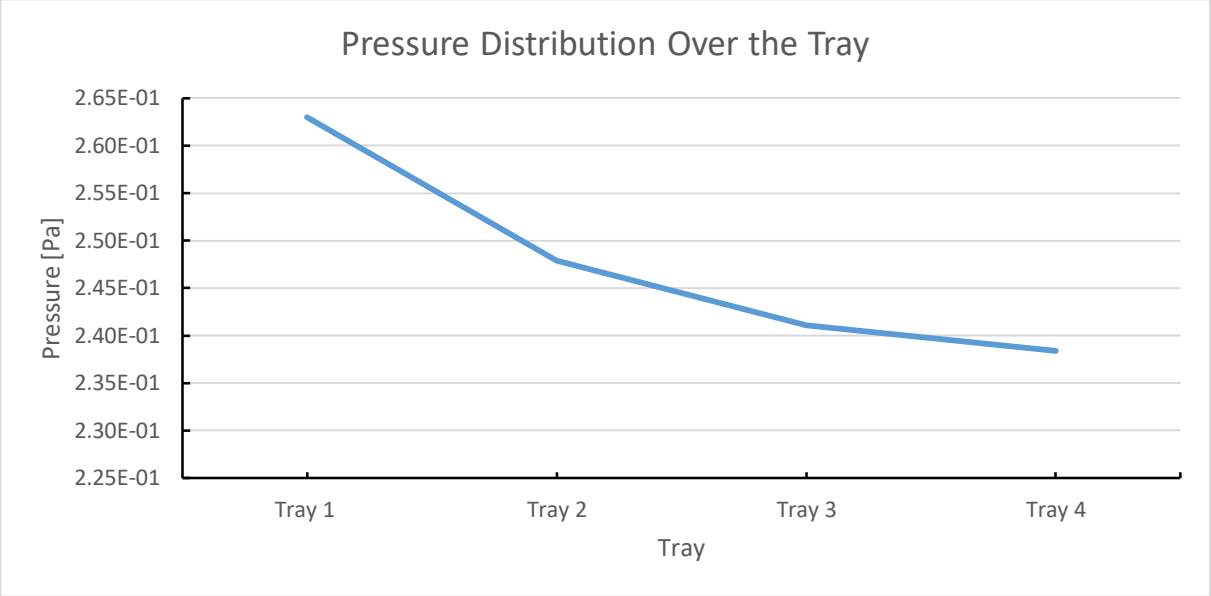

Figure 6.6:Pressure Over the Tray

Figure 6:7 shows average relative humidity distribution through the collector outlet and drying trays. Average relative humidity at collector outlet decreases rapidly and reaches below 50% RH for both months. However, for month of April it reaches this point in 1 hour and for month of July it reaches in 1 hour and 40 minute from the starting hour and after reaching this point it shows slight change and reaches its minimum value of 44% RH for April and 47% RH for July at 12:20 hours. It stays in this value until 13:30 hours, starts to rise slowly, and reaches above 50% RH at 15:00 hours for July and 15:50 hours for April month. At the end of the simulated hour 17:00 hours and 16:00 hours it reaches 57 % RH and 52% RH for month of April and July respectively.

Average relative humidity at all 4 trays decreases rapidly and reaches below 60% RH for both months in 1 hour and 40 minute from the starting hour and after reaching this point it shows slight change and reaches its minimum value of 55% RH for April and 57% RH for July at 13:10 hours. It stays in this value until 14:50 hours, starts to rise slowly, and it reaches 63 % RH and 60% RH for month of April and July at the end of the simulated hour, which are 17:00 hours and 16:00 hours respectively. The variation of the relative humidity over the simulated hours is due to the corresponding variation of solar radiation and similar pattern also reported in [72] work.

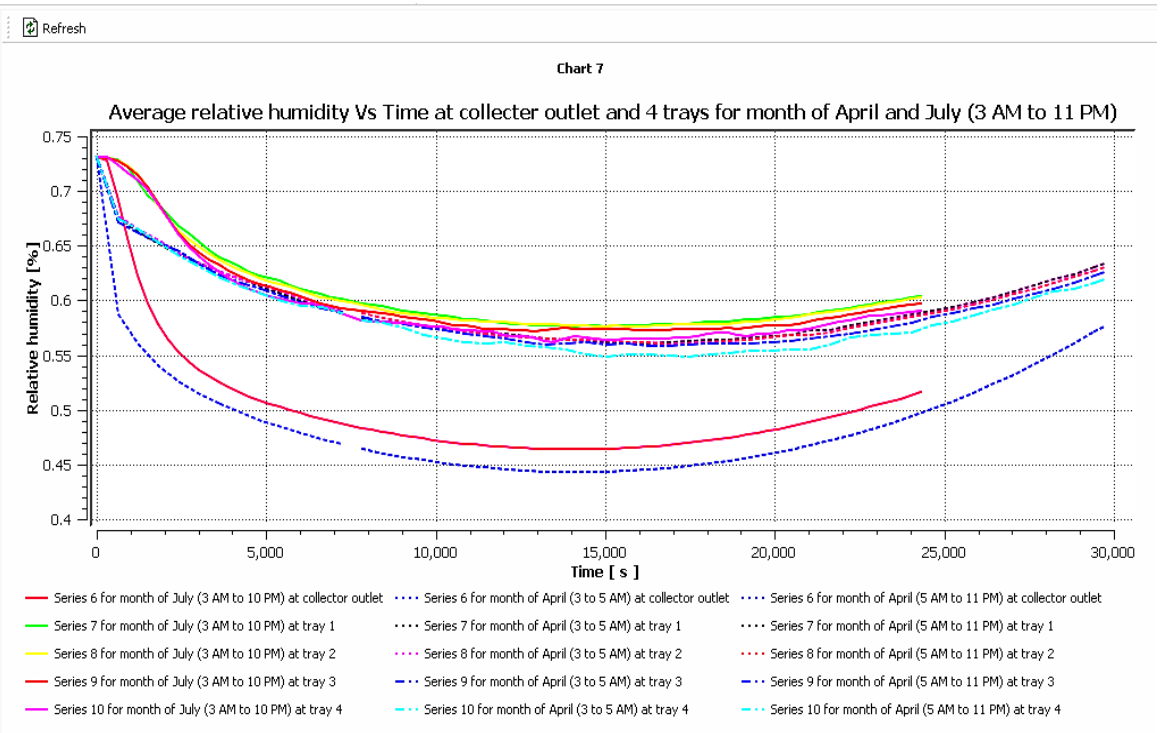

Figure 6.7: Average Relative Humidity at Collector Outlet and Drying Trays Vs Time

Figure 6:8 shows average pressure distribution through the drying trays. The average pressure at all trays increase's rapidly and reaches above 0.2 Pa for both months in 10 minute from the starting hour. Moreover, after reaching this point, the average pressure through all trays shows no significant change but it shows difference between each trays. Figure 6.9 shows the pressure distribution contour through the drier and the pressure in bottom tray is higher than the top tray and this difference allows the flow of air through the dryer in vertical direction.

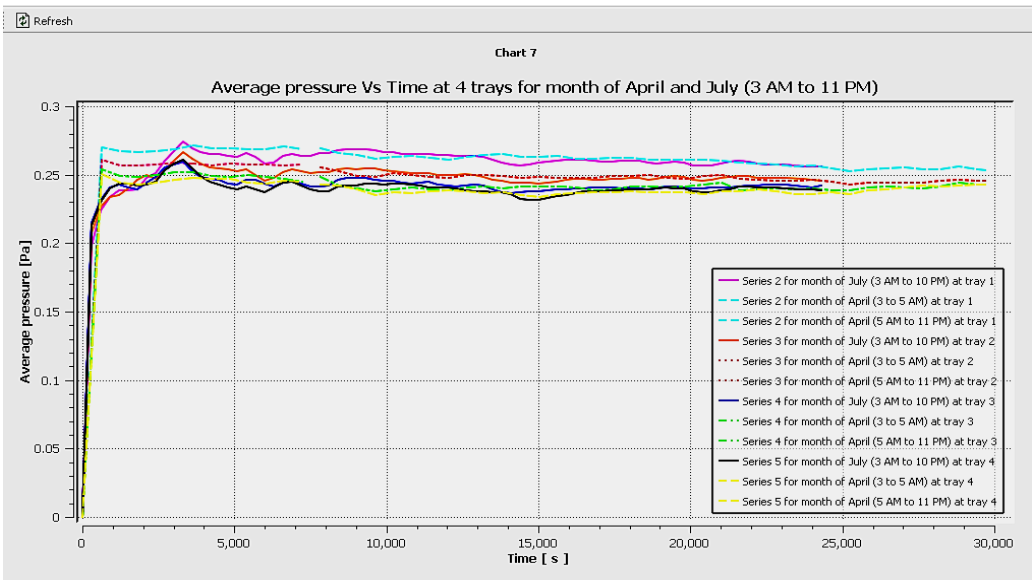

Figure 6.8:Average Pressure Distribution Through the Drying Trays Vs Time

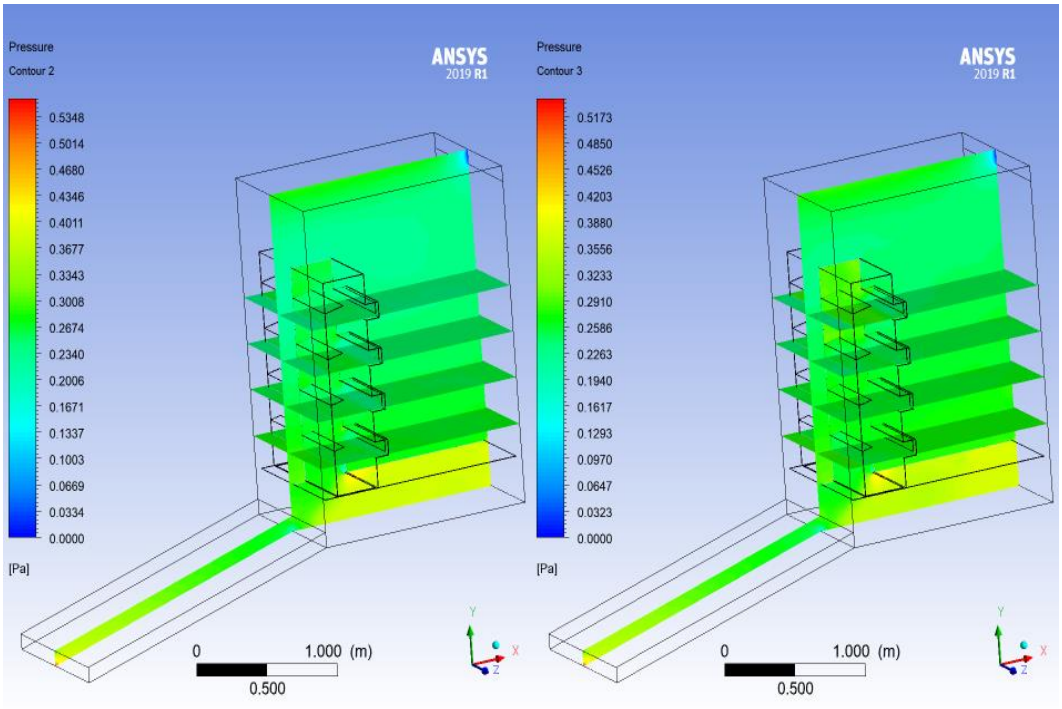

Figure 6.9: Pressure Distribution Contour Through the Drier

Figure 6:10 shows mass flow rate distribution through the drying trays and in the figure plane 2 to 5 represents dryer tray 1 to 4 which is plane 2 representing tray 1 and so forth. It can be seen that the mass flow rate through all 4 trays is almost uniform for both months and its value lie in the range 0.02 to 0.9 kg/s which is stated in [64] for mixed mode natural convection solar drier. The mass flow rate in all 4 trays increase's rapidly and reached above 0.06 kg/s for both months in 10 minute from the starting hour and after reaching this point the mass flow rate through all trays shows no significant change and remained uniform throughout the drying period.

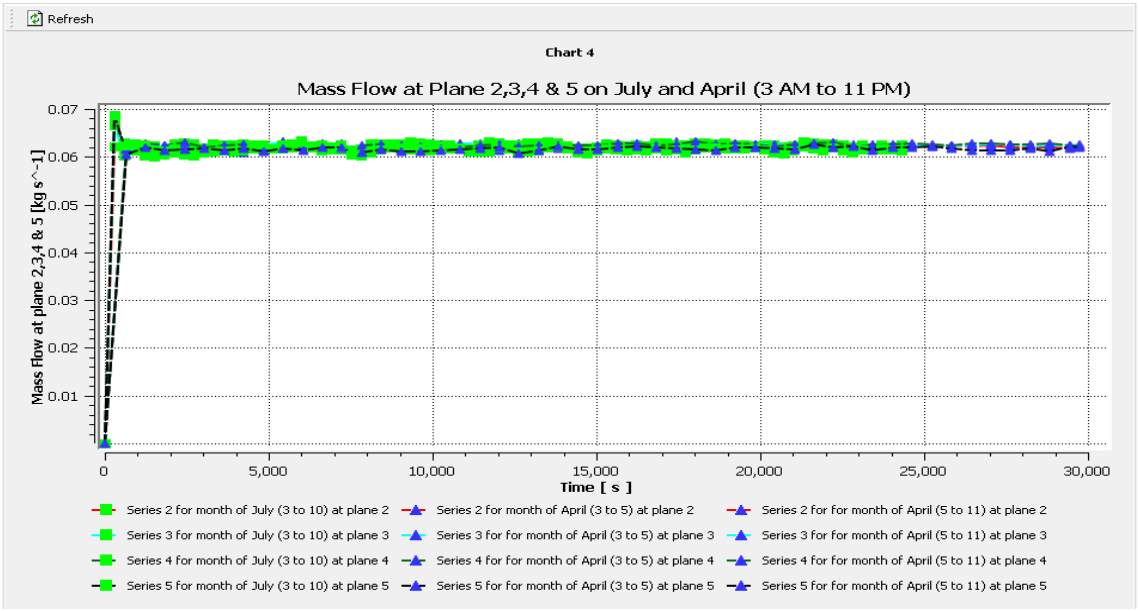

Figure 6.10: Mass Flow Rate Distribution Through the Drying Trays Vs Time

6.2 Expermental Results and Discussion

6.2.1 No load test

The no load test was performed during the month of August 2020 in the mechanical Engineering Workshop, Addis Ababa University, Addis Ababa Institute of Technology. The test was carried out in order to evaluate the performance of the drier without loading. Table 6.2 shows the temperature distribution through the drier. The collector outlet temperature was above 10ºC from the ambient in most of testing hour and the result shows an average collector efficiency of 30% and maximum collector outlet temperature of 35ºC.

Table 6.2:Tempreture Distribution on Unloaded tray

Time (hr)	T(ºC) at Tray 1	T(ºC) at Tray 2	T(ºC) at Tray 3	T(ºC) at Tray 4	T(ºC) at collector inlet	T(ºC) at collector outlet	Average dryer T (ºC)	T(ºC) at collector outlet – T(ºC) at collector inlet
10:30	24.18	23.78	29.82	32.08	21.99	28.64	27.47	6.66
11:00	28.52	26.18	32.34	32.54	22.27	33.09	29.89	10.82
11:30	28.52	25.34	32.69	33.65	22.51	33.44	30.05	10.93
12:00	28.14	25.43	30.99	32.11	22.99	33.34	29.17	10.33
12:30	27.69	24.86	31.92	32.93	23.31	33.31	29.35	10.00
13:00	27.75	25.75	31.21	31.29	23.37	33.47	29.00	10.10
13:30	28.12	25.87	32.85	34.09	23.52	35.23	30.23	11.70
14:00	28.22	25.77	32.82	34.32	23.08	35.42	30.28	12.37
Average value	27.65	25.38	31.83	32.88	22.88	33.24	29.43	10.36

The average temperature inside the dryer was found to be higher than the ambient temperature and it shows an increase at the start from 10:30 am to 11:00 am and remained approximately constant throughout the testing period. Even though the average temperature inside the dryer remains constant through the testing period, the temperature between trays shows difference and this is due to the solar radiation coming from the top cover of the dryer which increases the temperature of the top trays (Tray 3&4) compared to the bottom trays (Tray 1&2).

For verification purpose, the simulation was repeated following similar procedure for the month of august 25 and results of the experiment were compared. In doing so, the temperature

values were taken from the simulated geometry at similar sensor position, which were used in the experiment as shown in Figure 6.14.

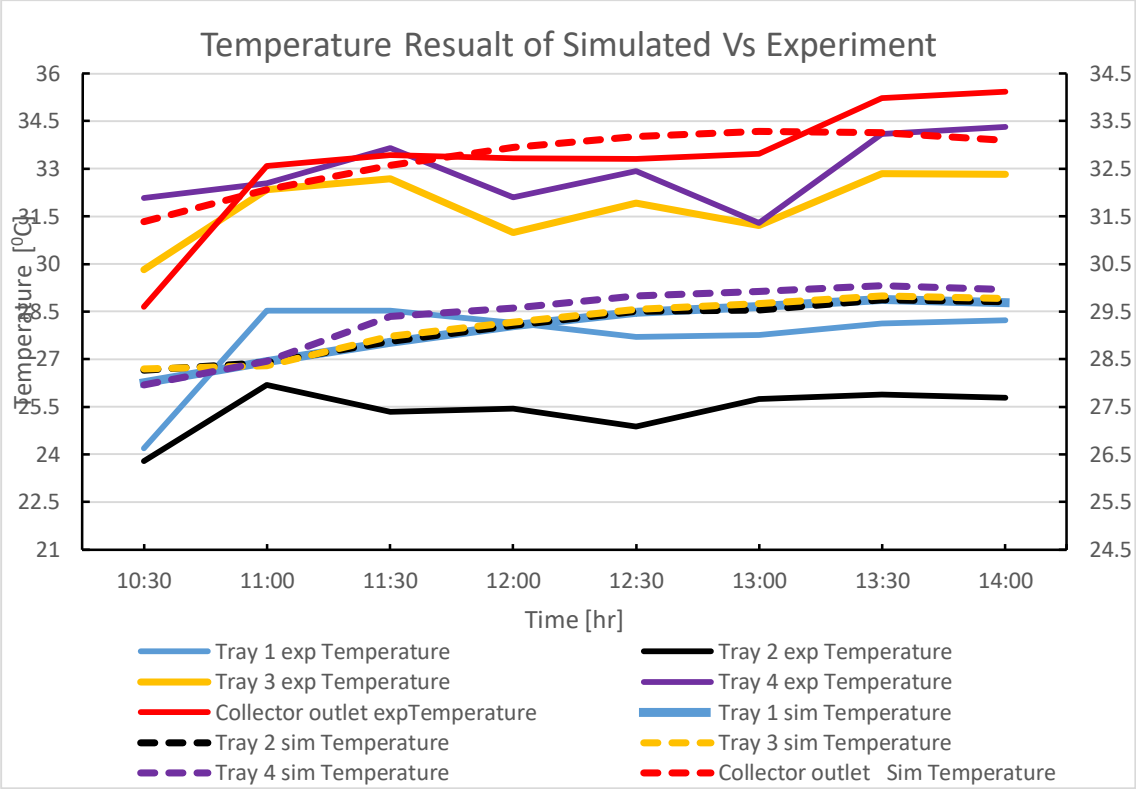

Figure 6.11:Simulated Resualt Vs Experiment for Temperature Inside the Drier

Figure 6.11 shows the simulation and the experimental result of temperature at the collector outlet and drying chamber tray. The temperature at tray 4 was higher than the bottom trays for both the simulation and experimental result however the variation of the temperature between tray 1,2 and 3 of the simulation were almost insignificant but for the experiment there was significant variation between these trays particularly between the bottom (Tray 1&2) and top trays (Tray 3&4). This might be in the experiment setup the wire mesh trays were inside the drying chamber whereas in the simulation, there were no trays in the drying chamber. Due to this the top trays absorb solar radiation coming from the top cover, which contributed to the increase in temperature at the top trays.

Table 6.3 shows the PBIAD result and it indicated the simulation overestimated the overall temperature distribution over the tray by -1.5% and underestimated the collector outlet by 1.6%. The result shows that the simulation overestimated the temperature at bottom tray 1&2 and this could be the consequence of heat loos from air infiltration through the gaps in the drying chamber corners. However, the result underestimated the temperature at top tray 3&4 and this is might be due to the top trays absorbs solar radiation coming from the top cover, which contributed to the increase in temperature and simultaneously compensated the heat loss effect, which was observed

in the bottom trays. However, at the collector outlet, the simulation result highly matches with the experimental result of the collector outlet temperature.

The other reason for this variation could also be that the ambient air temperature, wind speed and relative humidity were considered constant in the simulation but in the experiment, there was a variation on these variables through the testing hours and this could result the variation.

Table 6.3: Statistical validation of Temperature Distribution

	Percent Bias (PBIAD) (%)	
Tray 1	-5.4	overestimates
Tray 2	-14.9	overestimates
Tray 3	8.2	underestimates
Tray 4	10.6	underestimates
Collector outlet	1.6	underestimates

6.2.2 Load Experiments

Figures 6.15 shows the instrument setup for the modified mixed mode drier to measure the temperature at different locations on the drier. During testing hours, the maximum temperature of air at the collector outlet was found to be 35 °C with corresponding ambient temperature of 22 °C as shown in Table 6.4. The temperature distribution inside the drying chamber were almost uniform and this indicates the entire injera in the drier trays were equally exposed to warm air. Figure 6.12 shows the change in average drier temperature over drier trays and moisture content with the collecter inlet tempreture and as the drying air tempreture increses the moisture conten of injera drops and the rise in the ambient tempreture were obeserved to be low over the drying period.

The drying efficiency and normalized drying efficiency of the modified mixed mode drier was found to be 15.25 % and 0.134 %/kg respectively. The first day and overall drying rate of the direr was also found to be $3.2232*10^{-5}$ kg/s and $2.6345*10^{-5}$ kg/s respectively. The results obtained from the modified mixed mode drier shown a 19% higher performance when its normalized drying efficiency was compared with the result reported by [66], whom attempted to modify the mixed mode drier by improving the air distribution system.

Table 6.4:Temperature Distribution on Loaded Drier

Time (hr)	T(°C) at Tray 1	T(°C) at Tray 2	T (°C) at Tray 3	T(°C) at Tray 4	T(°C) at collector inlet	T(°C) at collector outlet	Average dryer T (°C)	T(°C) at collector outlet – T(°C) at collector inlet
10:30	22.88	23.73	24.06	25.23	21.12	34.41	23.98	13.29
11:00	23.73	24.54	25.46	26.59	22.27	35.08	25.08	12.81
11:30	24.81	25.67	26.81	27.50	21.51	33.44	26.19	11.93
12:00	23.31	23.94	24.84	25.53	21.66	32.83	24.40	11.17
12:30	22.49	23.38	24.32	25.16	21.45	33.72	23.84	12.28
13:00	26.15	25.51	26.42	28.28	20.33	32.34	26.59	12.01
13:30	28.01	27.74	28.63	29.18	21.98	35.89	28.39	13.92
14:00	28.23	29.15	29.89	28.64	21.39	33.99	28.98	12.59
Average value	24.95	25.46	26.30	27.02	21.46	33.96	25.93	12.49

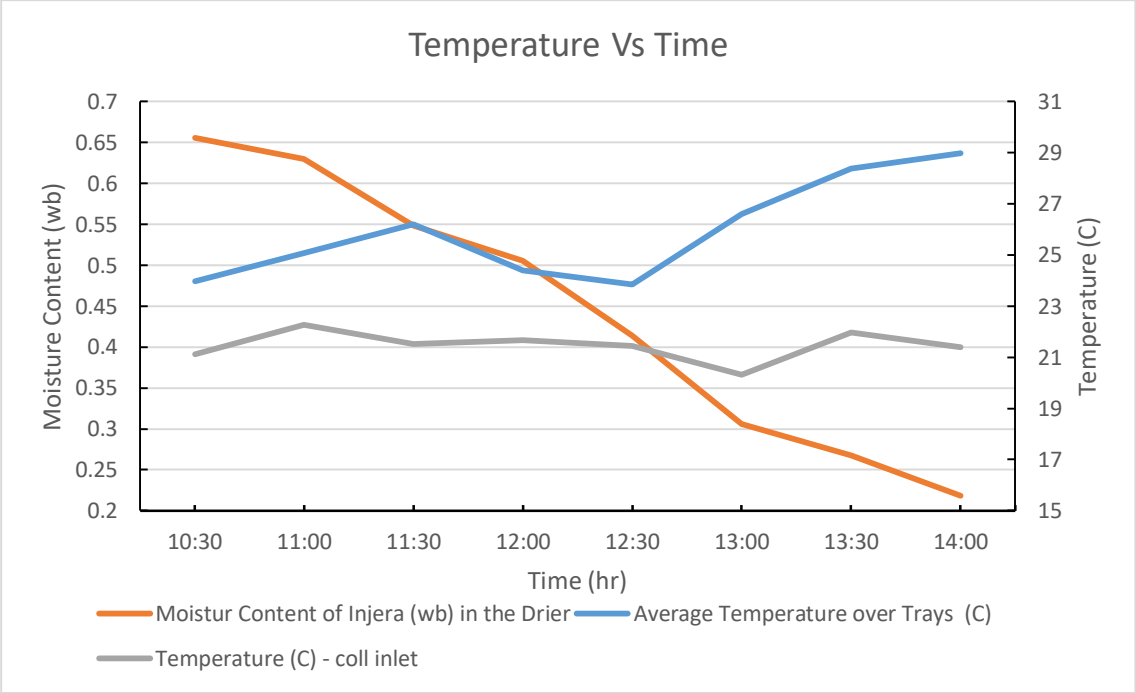

Figure 6.12: Temperature Vs Moisture Content

6.2.3 Drying test results

To measure the moisture content of injera samples were taken from six selected locations from each trays with approximate weight of 128g starting at 10:30 am with 30 min interval. To compare the performance of the modified mixed mode solar dryer with the traditional open sun

drying the same size samples were taken at the same time. Figures 6.13 shows the experimental setup for the modified mixed mode drier.

Figure 6.13: Experimental Setup for the Modified Mixed Mode Drier

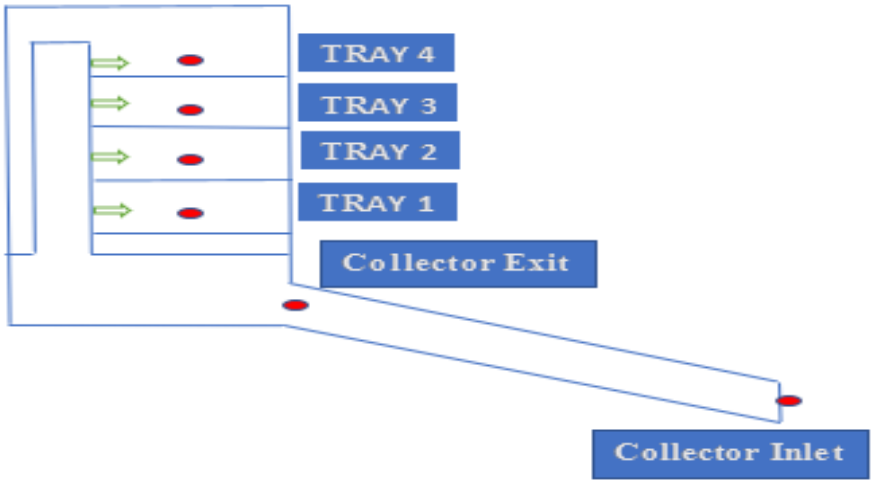

Figure 6.14:Experimental Test Points

Figure 6.15:Instrument Setup for the Modified Mixed Mode Drier

As shown in Figure 6.16, the moisture content of injera decreased rapidly at the initial stages of drying and it became slow as the drying proceeds. This is because at first, evaporation of free moisture from the outer surface takes place and then internal moisture migrates to the surface, which results in a gradual change towards the end of the drying process. The mass of injera had been reduced from 1.132kg to 435kg in 7 sunshine hours only.

From percentage moisture loss which is shown in Figure 6.17, we can notice that the moisture loss of injera in open sun drying was less than the mixed mode drier and also the drying rate of the mixed mode drier was found to be 5.03 $*10^{-5}$ kg/s and the open sun drying rate was $4.6*10^{-5}$kg/s which indicates that using mixed mode solar dryers will help to reduce the drying time of injera when compared to the traditional open sun drying.

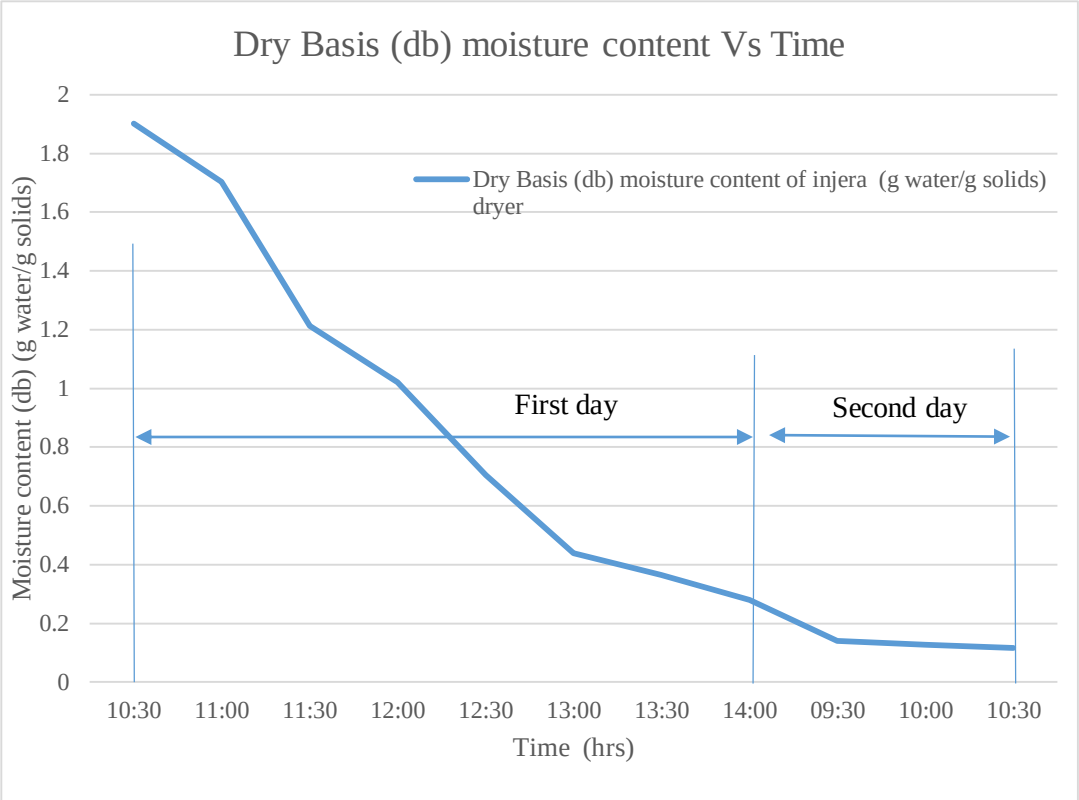

Figure 6.16: Drying Curves for Open Sun Drying and Mixed Mode Drying

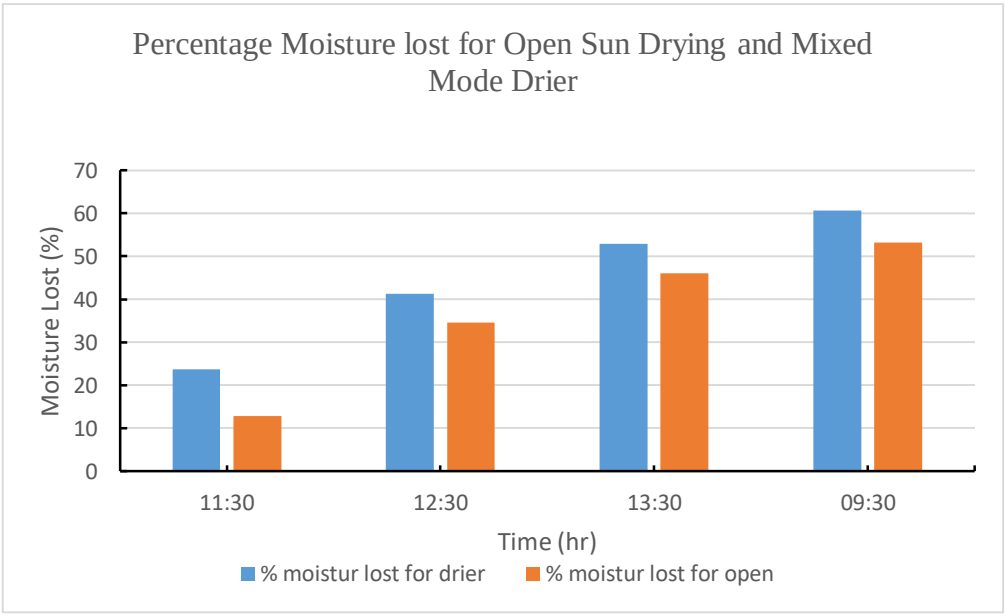

Figure 6.17:Percentage Moisture Lost for Open Sun Drying and Mixed Mode Drier

From the seven tested thin-layer drying models, Verma model was found to be the best model to describe the drying curve of injera with the highs R^2 value and the lowest X^2 and RMSE as shown in Table 6.5 below.[67], [82] also found this mode as a best-fit model for their product.

6.2.4 Performance of drier

From this result, we can say that the solar dryer can increase the drying air temperature above the ambient air temperature by 10 ^{o}C through the testing period and the drying efficiency and normalized drying efficiency of the modified mixed mode drier was found to be 15.25 % and 0.134 % per kg respectively. This normalized drying efficiency value was found to be better when compared with the result reported by [66] whom attempted to modify the mixed mode drier by improving the air distribution system.

In addition, the temperature distribution inside the solar drier trays were almost uniform which indicate the entire injera in the drier is equally exposed to the warm air from bottom to top and results homogenies moisture content of final dried injera.

Table 6.5: Thin layer drying modal resualt

S. no	Modal	Statistical parameters			Model constants		
1	Page Model	chi-square ($X^{\wedge 2}$)	RMSE	R^2	k	n	
		0.000689	0.023748	0.994588	0.001745	1.323229	
2	Modified Page-I Model	chi-square (X^2)	RMSE	R^2	k	n	
		0.003213	0.051275	0.974771	0.041087	0.205538	
3	Henderson and Pabis Model	chi-square (X^2)	RMSE	R^2	k	a	
		0.002333	0.04369	0.981683	0.009031	1.071481	
4	Lewis (Newton) model	chi-square (X^2)	RMSE	R^2	k		
		0.002892	0.051275	0.974771	0.008445		
5	Two-Term Exponential Model	chi-square (X^2)	RMSE	R^2	k	a	
		0.000602	0.022188	0.995276	0.012711	1.916618	
6	(Yagcioglu et al.) Logarithmic (Asymptotic) Model	chi-square (X^2)	RMSE	R^2	k	a	c
		0.001764	0.035822	0.987686	0.007169	1.159497	-0.11077
7	Verma et al. Model	chi-square (X^2)	RMSE	R^2	k	a	b
		0.000666	0.022004	0.995354	0.010311	1.226448	0.910688

This uniform temperature distribution in the drying chamber and the homogenies moisture content of final dried injera as shown in Figure 6.18 shows that the newly developed vertical air distributer which is integrated into the mixed mode drier, meets its objective.

The performances of the drier was tested in the rainy season and with the least solar insolation and short period of clear sky during daytime of the year in Addis Ababa, Ethiopia, and it could be concluded that the modified mixed mode drier with vertical air distributer performed better in terms of uniform drying air distribution within the drying chamber.

Quality of the dried product is mainly depending on the uniformity of the air distribution within the drying chamber. Uniform air distribution is a problem in the existing conventional passive mixed mode solar drier because in conventional drier, air enter from the bottom and moves upward losing its heat from the first tray to the next. This results in the final product a non-uniform moisture distribution that decreases the driers efficiency but in this modified mixed mode drier, this inherent problem was resolved.

Figure 6.18:Top Before Drying and Bottom After Drying

Chapter Seven : Conclusion and Recommendations

7.1 Conclusion

Open sun drying was used widely as food preservation mechanism for several thousand years by simply spreading the injera out on apparel mat and this technique suffer from many drawbacks such as, over drying, discoloration by ultraviolet radiation, attack of insects and fungi, consequently leading to contamination. It is also labour intensive and demands large area.

The modified mixed mode drier consists of three components; a drying chamber which houses four trays, vertical air distributer channel and a solar collector. The dimensions of the dryer were 2 m, 2 m^2, 1.4 m, 2.2 m, 1.5 m and 1 m for collector length, collector area, height of the vertical air distributer channel, the height of the drying chamber, length and width of the drying chamber respectively.

The simulation result indicated the collector outlet temperature was 10^0C above the ambient after 20 minutes only from the starting and continues throughout the drying period. The overall temperature and relative humidity distribution through the drying trays shows a uniform distribution. The average velocity and mass flow rate through the drying trays were found to be 0.1 m/s and 0.061 kg/s respectively and both were uniformly distributed through the drying trays. There was a pressure gradient through the drying tray, which helps to maintain the airflow through the dryer.

From the experimental result, it was clear that the modified mixed mode drier performance was higher than the open sun drying due to the temperatures of the air inside the drier was higher than the ambient temperatures for most of the drying time.

The collector and drying efficiency of the drier were found to be 30% and 15.25% respectively. The drying rate of the drier was $2.634*10^{-5}$ kg/s and the Verma et al. thin layer-drying model fits best for injera drying when its result compared with the other six selected models based on the chi-square (X^2), RMSE and R^2.

A uniform temperatures distribution was found through the drier, this is the result of the vertical air distributer channel, which was newly developed and integrated through the drying chamber, and

The experimental result was compared with the simulation result and it was observed that there was no significant difference between the two results. However, the simulated temperature result showed an overestimation on tray 1 and tray 2 and underestimation on tray 3, tray 4 and

collector outlet by -5.4 %, -14.9 %, 8.2 %, 10.6 % and 1.6 % respectively and this was due to the fact that the ambient condition which was assumed constant in the simulation was continuously changing in the testing hours.

Finally, it was observed that solar drying of injera could be a feasible method for preserving and maintaining the quality of dried injera with a minimum cost.

7.2 Recommendation

1) The performance of the drier should be measured throughout different season of the year.
2) The performance of the drier should also be measured with full loading.
3) The thin layer drying models should be tested in different drying condition with different temperature and mass flow rate.
4) The quality standard of injera should be researched including moisture sorption isotherms.
5) Improving the solar injera drier through integrating the backup heat source have to be analysed.
6) The society should be informed about solar injera drying through different researches and media to increase their awareness.
7) The economic and social benefits of solar injera drying have to be studied.

Reference

[1] K. Baye, 'Nutrient composition and health benefits', 2005, pp. 371–396.

[2] K. D. Adem and D. A. Ambie, 'A review of injera baking technologies in Ethiopia : Challenges and gaps', *Energy Sustain. Dev.*, vol. 41, pp. 69–80, 2017.

[3] A. Haileselassie, M. Bayray, and O. Jørgen, 'Solar powered heat storage for Injera baking in Ethiopia', *Energy Procedia*, vol. 57, pp. 1603–1612, 2014.

[4] Z. Ashagrie and D. Abate, 'IMPROVEMENT OF INJERA SHELF LIFE THROUGH THE USE OF CHEMICAL PRESERVATIVES', *African J. Fodd,Agriculture,Nutrition Dev.*, vol. 12, no. 5, 2012.

[5] M. Vasić1 and Z. Radojević, 'CALCULATION OF EFFECTIVE DIFFUSION COEFFICIENT', *Int. J. Mod. Manuf. Technol.*, vol. III, no. 1, pp. 93–98, 2011.

[6] V. Belessiotis and E. Delyannis, 'Solar drying', *Sol. Energy*, vol. 85, pp. 1665–1691, 2011.

[7] M. A. J. Al-Neama, 'Performance enhancement of solar air collectors applied for drying processes', Szent István University, Gödöllő, Hungary, 2018.

[8] R. F. Z. DAVILA, 'MATHEMATICAL MODELING OF DRYING PROCESS OF UNRIPE BANANA SLICES', Escola Politécnica of University of São Paulo, 2016.

[9] O. V Ekechukwu and B. Norton, 'Review of solar-energy drying systems II : an overview of solar drying technology', *Energy Convers. Manag.*, vol. 40, pp. 615–655, 1999.

[10] J. K. M. Kuwornu, I. S. Egyir, and A. K. Dankyi Anyinam, 'Design of Solar Drying Technology Equipment for Drying Food Consistent with Farmers ' Willingness to Pay : Evidence from Ghana', *Int. Inst. Sci. Technol. Educ.*, vol. 2, no. 6, pp. 13–39, 2011.

[11] J. A. Sadik, B. Demelash, and M. Gizaw, 'Hydration kinetics of teff grain', *Agric Eng Int CIGR*, vol. 15, no. 1, pp. 124–130, 2013.

[12] W. D. Attuquayefio, 'INFLUENCE OF PROCESSING PARAMETERS ON EYE SIZE AND ELASTICITY OF TEF-BASED INJERA', The Pennsylvania State University, 2014.

[13] Y. Mihrete and G. Bultosa, 'The Effect of Blending Ratio of Tef [Eragrostis Tef (Zucc) Trotter], Sorghum (Sorghum bicolor (L .) Moench) and Faba Bean (Vicia faba) and Fermentation Time on Chemical Composition of Injera', *J. Nutr. Food Sci.*, vol. 7, no. 2, pp. 1–7, 2017.

[14] B. Kebede, 'FOOD PEOPLE EAT : THE ENERGY ECONOMICS OF INJERA AND WOT', in *The Ethiopian Economy: Structure, Problems and Policy Issues BIBLIOGRAPHY*, 1991, pp. 211–219.

[15] S. F. Gamtessa, 'Household ' s Consumption Pattern and Demand for Energy in Urban Ethiopia', in *International Conference on African Development*, 2003, pp. 76–106.

[16] A. A. Hassen and D. A. Amibe, 'FINITE ELEMENT MODELING OF SOLAR POWERED INJERA'. pp. 1–8.

[17] R. Jones, J. C. Diehl, L. Simons, and M. Verwaal, 'The Development of an Energy Efficient Electric Mitad for Baking Injeras in Ethiopia', in *Domestic Use of Energy Conference: Towards Sustainable Energy Solutions for the Developing World (pp.*, 2017, pp. 75–82.

[18] G. Moges, 'Electric Injera Mitad Energy Efficiency Standards & Labeling , challenges and prospects', 2017.

[19] A. TEKLE, ‘EXPERIMENTAL INVESTIGATION ON PERFORMANCE CHARACTERISTICS AND EFFICIENCY OF ELECTRIC INJERA BAKING PANS („MITAD“)’, ADDIS ABABA UNIVERSITY, 2011.

[20] M. H. Hailu, M. B. Kahsay, and A. H. Tesfay, ‘Energy Consumption Performance Analysis of Electrical Mitad at Mekelle City’, *CNCS, Mekelle Univ.*, vol. 9, no. 1, pp. 43–65, 2017.

[21] A. A. Hassen, S. B. Kebede, and N. M. Wihib, ‘Design and manufacturing of thermal energy based Injera baking glass pan’, *Energy Procedia*, vol. 93, no. March, pp. 154–159, 2016.

[22] Awash Tekle, A. A. Hassen, and D. Alemu, ‘Experimental investigation on performance characteristics and efficiency of electric injera baking pans (Mitad)’, 2014.

[23] N. L. Panwar, S. C. Kaushik, and S. Kothari, ‘State of the art of solar cooking : An overview’, *Renew. Sustain. Energy Rev.*, vol. 16, no. 6, pp. 3776–3785, 2012.

[24] A. Gebresas, A. Tegegne, H. Berhe, and A. Kedir, ‘IMPROVING ENERGY CONSUMPTION AND DURABILITY OF THE CLAY BAKEWARE (MITAD)’, *Int. J. Softw. Hardw. Res. E ngineering*, vol. 1, no. 3, pp. 7–14, 2013.

[25] M. Gavhale, S. Kawale, and R. Nagpure, ‘Design And Development Of Solar Seed Dryer’, *IJISET*, vol. 2, no. 4, pp. 1005–1010, 2015.

[26] V. Shrivastava, A. Kumar, and P. Baredar, ‘Developments in Indirect Solar Dryer : A Review’, vol. 3, no. 4, pp. 67–74, 2014.

[27] W. F. P. E. Office and C. S. A. of Ethiopia, ‘Comprehensive Food Security and Vulnerability Analysis (CFSVA)’, 2019.

[28] P. M. Gupta, R. G. Pandav, R. V Singh, and S. K. Khuje, ‘Review of Solar Dryer for Drying Agricultural Products’, *IJSRD*, vol. 4, no. 11, pp. 524–528, 2017.

[29] A. Abebayehu, ‘THERMAL ANALYSIS OF SOLAR DRYERS’, *J. EAEA*, vol. 15, pp. 40–46, 1998.

[30] E. Quilligan, ‘Positioning Dirkosh Crunch for growth in international markets’, 2018.

[31] S. Abubakar, F. Anafi, and S. Umaru, ‘PERFORMANCE EVALUATION OF A NATURAL CONVECTION SOLAR CROP’, in *The Ahmadu Bello University Postgraduate Students’ Conference*, 2016, no. November, p. 6.

[32] R. J. Fuller, ‘SOLAR DRYING - A TECHNOLOGY FOR SUSTAINABLE AGRICULTURE AND FOOD PRODUCTION’, in *Solar Energy Conversion and Photoenergy Systems*, vol. III, Encyclopedia of Life Support Systems (EOLSS), 2002, p. 12.

[33] C. Ertekin and O. Yaldiz, ‘Drying of eggplant and selection of a suitable thin layer drying model’, *J. Food Eng.*, vol. 63, no. August, p. 11, 2004.

[34] C. L. Hii, S. V Jangam, S. P. Ong, and A. S. Mujumdar, *Solar Drying: Fundamentals,Applications and Innovations*. Transport Phenomena (TPR) Group, Singapore, 2012.

[35] A. Sharma, O. Chatta, and A. Gupta, ‘A Review of Solar Energy use in Drying’, *Int. J. Eng. Technol. Sci. Res.*, vol. 5, no. 3, pp. 351–358, 2018.

[36] S. J. SHARMA, V. K. SHARMA, R. JHA, and R. A. RAY, ‘EVALUATION OF THE PERFORMANCE OF A CABINET TYPE SOLAR DRYER’, *Energy Convers. Manag.*, vol. 30, no. 2, pp. 75–80, 1990.

[37] A. Maytham and F. István, ‘Utilization of Solar Air Collectors for Product ’ s Drying Processes’, *J. Sci. Eng. Res.*, vol. 5, no. 2, pp. 40–56, 2018.

[38] V. B. Chougule, A. A. Bhairappa, R. D. Hanchate, G. S. Kasegaonka, and P. V.V, ‘DESIGN AND FABRICATION OF A SOLAR DRYING SYSTEM FOR’, in *NATIONAL CONFERENCE ON INNOVATIVE TRENDS IN ENGINEERING & TECHNOLOGY*, 2016, no. March, pp. 1–10.

[39] N. Kumar and M. Piyush, ‘Review on Solar Energy Dryer for Drying the Agricultural Products’, vol. 5, no. 08, pp. 198–203, 2017.

[40] K. Amouzou, M. Gninginvi, and B. Kerim, ‘SOLAR DRYING PROBLEMS IN TOGO: Solar drying in Africa’, in *proceedings of a workshop held in Dakar*, 1986, pp. 252–271.

[41] M. Wakjira, ‘Solar drying of fruits and windows of opportunities in Ethiopia’, *African J. Food Sci.*, vol. 4, no. 13, pp. 790–802, 2010.

[42] S. N. S. M. MAQSOOD UL HAQUE, ‘A STUDY OF RADIATION AND NATURAL CONVECTION OF AIR ON DRYING OF COFFEE BEANS IN A HEAT RECOVERY SOLAR DRYER’, The University of New South Wales,Australia, 2013.

[43] A. L. Moyls, ‘EVALUATION OF A SOLAR FRUIT DRYER’, *Can. Agric. Eng.*, vol. 28, no. 627, pp. 137–144, 1986.

[44] M. W. Bassey, ‘DEVELOPMENT AND USE OF SOLAR DRYING TECHNOLOGIES’, *Int. Dev. Res. Cent.*, vol. 1989, 1989.

[45] E. Mathioulakis, V. T. Karathanos, and V. G. Belessiotis, ‘Simulation of Air Movement in a Dryer by Computational Fluid Dynamics : Application for the Drying of Fruits’, *J. Food Eng.*, vol. 36, no. 98, pp. 183–200, 1998.

[46] J. Olsson, ‘Modelling of a solar dryer for food preservation in developing countries’, Lund University, 2016.

[47] I. Othieno, ‘CIRCULATION OF AIR IN NATURAL-CONVECTION SOLAR DRYERS: Solar drying in Africa’, in *Proceedings of a Workshop held in Dakar*, 1986, pp. 47–59.

[48] H. Hallack, J. Hilal, F. Hilal, and R. Rahhal, ‘The staircase solar dryer: Design and characteristics’, *Renew. Energy*, vol. 7, no. 18, pp. 177–183, 1996.

[49] R. K. Goyal and G. N. Tiwari, ‘PARAMETRIC STUDY OF A REVERSE FLAT PLATE ABSORBER CABINET DRYER : A NEW CONCEPT’, *Sol. Energy*, vol. 60, no. I, pp. 41–48, 1997.

[50] D. Jain, ‘Modeling the performance of the reversed absorber with packed bed thermal storage natural convection solar crop dryer’, *J. Food Eng.*, vol. 78, pp. 637–647, 2007.

[51] Mursalim, Supratomo, and Y. S. Dewi, ‘DRAYING OF CASHEW NUT IN SHELL USING SOLAR DRYER’, *Sci. Technol.*, vol. 3, no. 2, pp. 25–34, 2002.

[52] P. Gbaha, H. Y. Andoh, J. K. Saraka, B. K. Koua, and S. Toure, ‘Experimental investigation of a solar dryer with natural convective heat flow’, *Renew. Energy*, vol. 32, pp. 1817–1829, 2007.

[53] R. V. S. Raju, R. M. Reddy, and E. S. Reddy, ‘Design and Fabrication of Efficient Solar Dryer’, *Int. J. Eng. Res. Appl.*, vol. 3, no. 6, pp. 1445–1458, 2013.

[54] T. B. Tibebu, ‘DESIGN , CONSTRUCTION AND EVALUATION OF PERFORMANCE OF SOLAR DRYER FOR DRYING FRUIT’, Kwame Nkrumah University of Science and

Technology, 2015.

[55] M. W. Bassey and E. Y. K. Malcolm J.C.C. Whitfield, 'PROBLEMS AND SOLUTIONS FOR NATURAL-CONVECTION SOLAR CROP DRYING: Solar drying in Africa', in *Proceedings of a Workshop held in Dakar*, 1986, pp. 208–233.

[56] A. A. El-sebaii and S. M. Shalaby, 'Solar drying of agricultural products : A review', *Renew. Sustain. Energy Rev.*, vol. 16, no. 1, pp. 37–43, 2012.

[57] V. K. Sharma, A. Colangelo, and G. Spagna, 'EXPERIMENTAL INVESTIGATION OF DIFFERENT SOLAR DRYERS SUITABLE FOR FRUIT AND VEGETABLE DRYING', *Renew. Energy*, vol. 6, no. 4, pp. 413–424, 1995.

[58] A. Madhlopa, S. A. Jones, and J. D. K. Saka, 'A solar air heater with composite – absorber systems for food dehydration', *Renew. Energy*, vol. 27, pp. 27–37, 2002.

[59] D. R. Pangavhane, R. L. Sawhney, and P. N. Sarsavadia, 'Design , development and performance testing of a new natural convection solar dryer', *energy*, vol. 27, pp. 579–590, 2002.

[60] BO.Bolaji, 'Development and performance evaluation of box-type absorber solar air collector for crop drying', *J. Food Technol.*, vol. 3, no. 4, pp. 595–600, 2005.

[61] A. Lingayat, V. P. Chandramohan, and V. R. K. Raju, 'Design,Development and Performance of Indirect Type Solar Dryer for Banana Drying', in *Energy Procedia*, 2017, vol. 109, no. November 2016, pp. 409–416.

[62] V. Belessiotis and E. Delyannis, 'Solar drying', *Sol. Energy*, vol. 85, no. 8, pp. 1665–1691, 2011.

[63] I. . . Simate, 'Optimization of mixed-mode and indirect-mode natural convection solar dryers', *Renew. Energy*, vol. 28, pp. 435–453, 2003.

[64] F. K. Forson, M. A. A. Nazha, F. O. Akuffo, and H. Rajakaruna, 'Design of mixed-mode natural convection solar crop dryers : Application of principles and rules of thumb', *Renew. Energy*, vol. 32, pp. 2306–2319, 2007.

[65] B. O. Bolaji and A. P. Olalusi, 'Performance Evaluation of a Mixed-Mode Solar Dryer', *AU J. Technol.*, vol. 11, no. 4, pp. 225–231, 2008.

[66] Abubakar.S, Umaru.S, K. M.U, U. U.A., B. Ashok, and K. Nanthagopal, 'Development and performance comparison of mixed-mode solar crop dryers with and without thermal storage', *Renew. Energy*, vol. 128, no. 2018, pp. 285–298, 2017.

[67] B. O. OSODO, 'SIMULATION AND OPTIMISATION OF A DRYING MODEL FOR A FORCED CONVECTION GRAIN DRYER', Kenyatta University, 2018.

[68] C. B. Maia, A. G. Ferreira, L. Cabezas-Gómez, and S. de M. Hanriot, 'Simulation of the airflow inside a hybrid dryer', *IJRRAS*, vol. 10, no. March, pp. 382–389, 2012.

[69] A. Alqadhi, S. Misha, M. A. M. Rosli, and M. Z. Akop, 'Design and Simulation of an Optimized Mixed Mode Solar Dryer Integrated With Desiccant Material', *Int. J. Mech. Mechatronics Eng.*, vol. 17, no. 06, pp. 65–73, 2017.

[70] V. . Romero, E. Cerezo, M. . Garcia, and M. . Sanchez, 'Simulation and validation of vanilla drying process in an indirect solar dryer prototype using CFD Fluent program', *Energy Procedia*, vol. 57, pp. 1651–1658, 2014.

[71] A. A. Adeniyi, A. Mohammed, and K. Aladeniyi, 'Analysis of a Solar Dryer Box with Ray

Tracing CFD Technique', *Int. J. Sci. Eng. Res.*, vol. 3, no. 10, pp. 1–5, 2012.

[72] A. Sanghi, R. P. K. Ambrose, and D. Maier, 'CFD simulation of corn drying in a natural convection solar dryer', *Dry. Technol. An Int. J.*, vol. 3937, no. August, pp. 1–40, 2017.

[73] M. A. Teja, K. Ayyappa, S. Katam, and P. Anusha, 'Analysis of Exhaust Manifold using Computational Fluid Dynamics', *Fluid Mech. Open Access*, vol. 3, no. 1, pp. 1–16, 2016.

[74] S. S. Onimisi, V. Adekunleadetoro, N. C. Nosike, and I. D. Chibuzor, 'Optimization of Developed Multipurpose food dryer using ANSYS', *J. Sci. Eng. Res.*, vol. 3, no. 5, pp. 72–76, 2016.

[75] A. Maytham and F. István, 'Utilization of Solar Air Collectors for Product ' s Drying Processes', *J. Sci. Eng. Res.*, vol. 5, no. 2, pp. 40–56, 2018.

[76] Z. Erbay and F. Icier, 'A Review of Thin Layer Drying of Foods :Theory , Modeling ,and Experimental Results', *Crit. Rev. Food Sci. Nutr.*, vol. 50, no. 2009, pp. 441–464.

[77] S. Poonia, A. K. Singh, and D. Jain, 'Design development and performance evaluation of photovoltaic/thermal (PV/T) hybrid solar dryer for drying of ber (Zizyphus mauritiana) fruit', *Cogent Eng.*, vol. 5, no. 1, pp. 1–18, 2018.

[78] A. Midilli, H. Kucuk, and Z. Yapar, 'A NEW MODEL FOR SINGLE-LAYER DRYING', *Dry. Technol. An Int. J.*, vol. 20, no. April 2002, pp. 1503–1513, 2002.

[79] J. Crank, *THE MATHEMATICS OF DIFFUSION*, Second edi. BRISTOL, ENGLAND: CLARENDON PRESS, 1975.

[80] A. Touil, S. Chemkhi, and F. Zagrouba, 'Moisture Diffusivity and Shrinkage of Fruit and Cladode of Opuntia ficus-indica during Infrared Drying', *J. Food Process.*, vol. 2014, no. 2014, p. 10, 2014.

[81] J. Srikiatden and J. S.Roberts, 'MOISTURE TRANSFER IN SOLID FOOD MATERIALS : A REVIEW OF MECHANISMS , MODELS , AND MEASUREMENTS', *Int. J. Food Prop.*, vol. 10, no. December 2006, pp. 739–777, 2007.

[82] D. V. N. Lakshmi, P. Muthukumar, J. P. Ekka, P. K. Nayak, and A. Layek, 'Performance comparison of mixed mode and indirect mode parallel flow forced convection solar driers for drying Curcuma zedoaria', *Food Process Eng.*, no. February, pp. 1–12, 2019.

[83] L. B. Cano, 'Modelling and experimental investigation on the processes involved in the indirect solar drying of Granny Smith apples', Universidad Carlos ||| de Madrid, 2016.

[84] K. Rayaguru and W. Routray, 'Mathematical modeling of thin layer drying kinetics of stone apple slices', *Int. Food Res. J.*, vol. 19, no. 4, pp. 1503–1510, 2012.

[85] T. O. Olurin, A. O. Adelekan, and W. A. Olosunde, 'Mathematical modelling of drying characteristics of blanched field pumpkin (Cucurbita pepo L) slices', *Agric Eng Int CIGR J.*, vol. 14, no. 2012, pp. 246–254, 2012.

[86] M. Hemis, A. Bettahar, C. B. Singh, D. Bruneau, and D. S. Jayas, 'Experimental Study of Wheat Drying in Thin Layer and Mathematical Simulation of a Fixed-Bed Convective Dryer', *Dry. Technol. An Int. J.*, vol. 27, pp. 1142–1151, 2009.

[87] C. George, R. McGruder, and K. Torgerson, 'Determination of Optimal Surface Area to Volume Ratio for Thin-Layer Drying of Breadfruit (Artocarpus altilis)', *Int. J. Serv. Learn. Eng.*, vol. 2, no. 2, pp. 76–88, 2007.

[88] D. G. Mercer, 'An Introduction to the Dehydration and Drying of Fruits and Vegetables',

Ontario, Canada, 2014.

[89] S. S. Mohapatra, 'DEVELOPMENT AND PERFORMANCE EVALUATION OF A NATURAL CONVECTION GRAIN DRYER', ndian Institute of Technology Guwahati, 2012.

[90] M. A. Leon, S. Kumar, and S. C. Bhattacharya, 'A comprehensive procedure for performance evaluation of solar food dryers', *Renew. Sustain. Energy Rev.*, vol. 6, no. 2002, pp. 367–393, 2001.

[91] W. Weiss and J. Buchinger, 'Solar Drying. Austrian Development Cooperation: Institute for Sustainable Technologies', IN ZIMBABWE, 2002.

[92] D. P. Margaris and A. Ghiaus, 'Dried product quality improvement by air flow manipulation in tray dryers', *J. Food Eng.*, vol. 75, pp. 542–550, 2006.

[93] M. S. Sodha and R. Chandra, 'SOLAR DRYING SYSTEMS AND THEIR TESTING PROCEDURES: A REVIEW', *Energy Convers. Manag.*, vol. 35, no. 3, pp. 219–267, 1994.

[94] D. A. Amibe and A. Tiruneh, 'CFD ANALYSIS OF HEAT TRANSFER AND FLUID FLOW IN FLAT', Addis Ababa, Ethiopia, 2011.

[95] H. Tkubet, 'SIMULATION OF SOLAR CEREAL DRYER USING TRNSYS', Addis Ababa University, 2007.

[96] L. C. Osondu, C. C. Chikelu, E. C. Ugwuoke, S. T. Ukwuani, and N. N. Eze, 'Grain (Maize) Solar Dryer', *Int. J. Adv. Eng. Res. Sci.*, vol. 2, no. 7, pp. 7–10, 2015.

[97] G. Getenet, 'HEAT TRANSFER ANALYSIS DURING THE PROCESS OF INJERA BAKING BY FINITE ELEMENT METHOD', 2011.

[98] E.-A. O. M. AKOY, 'MATHEMATICAL MODELLING OF SOLAR DRYING OF MANGO SLICES', University of Khartoum, 2007.

[99] Ansys Fluent, *Ansys fluent Theory Guide*, no. April. 2009.

[100] G. Iordanou, 'Flat-Plate Solar Collectors for Water Heating with Improved Heat Transfer for Application in Climatic Conditions of the Mediterranean Region', University of Durham, 2009.

[101] Y. Ji, 'CFD Modelling of Natural Convection in Air Cavities', *ISSR*, vol. 6, no. 2013, pp. 15–31, 2014.

[102] A. Bohoj, 'NUMERICAL MODELLING OF HUMID AIR FLOW AROUND A POROUS BODY', *acta Mech. Autom.*, vol. 9, no. 3, pp. 161–166, 2015.

[103] S. Wong, W. Zhou, and J. Hua, 'CFD modeling of an industrial continuous bread-baking process involving U-movement', *J. Food Eng.*, vol. 78, no. 2005, pp. 888–896, 2007.

[104] M. A. Moghimi, K. J. Craig, and J. P. Meyer, 'A novel computational approach to combine the optical and thermal modelling of Linear Fresnel Collectors using the finite volume method', *Sol. Energy*, p. 60, 2015.

[105] J. G. Pieters and J. M. R. Deltour, 'Performances of Greenhouses with the Presence of Condensation on Cladding Materials', *Silsoe Res. Institute,J. agric. Engng Res*, vol. 68, no. September 1996, pp. 125–137, 1997.

[106] Ethio Resource Group with Partners, 'Final Report : Solar and Wind Energy Utilization and Project Development Scenarios', 2007.

[107] R. A. Saeed, V. Popov, and A. N. Galybin, ‘Advances in Fluid Mechanics IX’, in *NINETH INTERNATIONAL CONFERENCE ON ADVANCES IN FLUID MECHANICS*, 2012, p. 609.

[108] F. ANSYS, *ANSYS Fluent Meshing User Guide*, vol. 15317, no. November. 2013.

[109] M. Ozen, ‘INTRODUCTION TO ANSYS MESHING’, 2014.

[110] ASHRAE., *Fundamentals Handbook.American Society of Heating, Refrigerating and Air-Conditioning Engineers*. Atlanta, GA, 1999.

[111] M. W. Bassey and J. Sarr, ‘IMPROVING THE PERFORMANCE OF INDIRECT NATURAL CONVECTION SOLAR DRYERS’, 1991.

[112] H. P. Garg, R. B. Mahajan, V. K. Sharma, and H. S. Acharya, ‘DESIGN AND DEVELOPMENT OF A SIMPLE SOLAR DEHYDRATOR FOR CROP DRYING’, *Energy Convers. Manag.*, vol. 24, no. 1983, pp. 229–235, 1984.

Appendix A: Design Concept and Evaluation

a) Design concept A (DC-A)

This direct and passive solar dryer is a cabinet style as shown in the Figure and contains at the back a support which helps the dryer to tilt back to face the sun and utilize direct sunlight as the source of heat for the product to be dried through the front and top transparent cover. Passive airflow is created by convection, through the bottom holes, and small outlets at the top to allow the hot air to rise and then escape.

This design is very simple, having multiple tray or racks where the injera is held. It is a cheap method for drying not only simple to construct, but also very simple to operate, and easy to see when the contents are dried. Direct heating can be efficient and provides fast drying since the sun is able to quickly heat the injera. This type of design, however, does not promote abundant airflow, immediately cools down when the sun sets, and cannot perform well in conditions with cloud coverage. The direct sunlight can also cause depletion of nutrients in the injera, along with discoloration that is not desirable. It is also limited in size, and therefore cannot generate a large

b) Design concept B (DC-B)

A mixed solar dryer seen in the Figure uses direct sun and a heat collector attached to dry the injera. This method utilizes the energy from the sun more efficiently by collecting it on more surfaces, one of the surfaces being the injera directly. Using the heat collector can help create more air flow through natural convection moving from the heat collector and through the heating chamber. This design adds little complexity comparing to the previously discussed passive direct solar dryer while adding more efficiency. With a greater absorption of solar rays the drying time can be greatly decreased. There would be limitations placed on the amount of tray or racks put in the drying chamber because racks below would not be getting direct sunlight and would dry much slower. Direct sunlight to the fruit can once again cause the depletion of some essential nutrients from the injera.

c) Design concept C (DC-C)

A mixed solar dryer seen in the Figure uses direct sun and have 3 heat collector attached to the drying chamber to dry the injera. This method utilizes the energy from the sun more efficiently by collecting it on more surfaces, one of the surfaces being the injera directly also Using 3 heat collector which can help to create more air flow through natural convection moving from the heat collector and through the heating chamber with relatively higher temperature compared to single collector. This design adds little complication comparing to the previously discussed two

type of solar dryer while adding more efficiency. With a greater Absorption of solar rays the drying time can be greatly decreased. In the second type of dryer there was limitations placed on the amount of tray or racks put in the drying chamber because racks below would not be getting direct sunlight and would dry much slower but in this type of dryer it can overcame this constraint due to the multiple collector place at the bottom of the drying chamber. Direct sunlight to the fruit can once again cause the depletion of some essential nutrients from the injera. Also there is additional cost due to additional components.

d) Design concept D (DC-D)

A mixed solar dryer seen in the Figure uses direct sun and have a single heat collector which is separated from the drying chamber and this collector have a hose which is used to supply the heated air to the drying chamber. also the flat plate can be contend in the surface of the drying chamber if we need to transport it to some other place and this future will add a flexibility to the solar dryer. Other futures of this dryer is similar to that of design concept 2.

e) Design concept E (DC-E)

The absorber plate is horizontal and downward facing. A fraction of polygonal shape reflector is placed under the flat plate absorber to introduce solar radiation from below. The radius (of polygon) of opening of reflector is same as that of the absorber plate. A drying setup is placed above the absorber plate-I at the gap of 0.04 m for entering ambient air and also at the top there is a chimney set up to remove the hot air from the chamber and it helps to increase the air flow in the drying chamber and helps to have relatively good quality output product. The complexity of the design and absence of reference material on the arrangement makes its performance in question. Cost of the design is relatively higher.

Appendix B: Design Selection Parameter

Table B1: Design selection parameter

	Design Parameters	Rank	Description
1	Function/Performance	3	The function of the dryer will be to dry injera to a certain level of moisture in a given amount of time. The goal is between 2 days.
2	Product Cost	3	The cost of the dryer will include all material and labour costs used to construct the prototype, as well as any maintenance required. It is essential that the cost of the dryer be cheap and the construction utilize only locally accessible materials.
3	Safety	3	Keeping the operator safe is important and the dryer will be designed with no sharp edges and with stable structure.
4	Quality	3	A key aspect of the quality of a dryer is to eliminate the growth of mould and increase shelf life. Also there are bugs that will try to contaminate the injera, as well as dust in the air that could enter the drying chamber so the device will need to be as air tight as possible, and slightly elevated to combat these issues.
5	Aesthetics	1	Even if this will not affect the function of the device it is important to aim for the best aesthetics and provide an appealing structural appearance.
6	Personnel	3	The personnel operating the dryer have to be take into account in any design parameter that will affect them.
7	Service Life	2	The aim is to design a dryer that will last as long as possible without a need to replace a part. The goal is a service life of longer than 5 years.
8	Operating Instructions	3	It is essential to have clear instructions on how to operate the dryer and how to build the dryer that is designed so it can be reproduced.
9	Energy Consumption	3	While in some cases it might be useful to use electric energy to aid the dryer, but It's better to rely on the free and abundant energy of the sun to power the dryer.
10	Reliability	3	The dryer must be reliable in order to function properly. Human interaction should be kept minimal.
11	Maintenance	3	It should not be needed to worry about doing regular maintenance on the dryer and

			maintenance duration should be kept minimal.
12	Mechanical Loading	1	There will be no significant loading that can occur but structural stability have to be ensured even if there is a moving parts and making sure the weight of the product can be supported.
13	Size/Weight	3	The dryer can be stationary or movable, so limiting the weight is crucial, but it must be an appropriate size to be fully accessible and able to dry the amount of injera desired.
14	Health Issues	3	Materials chosen must be safe for direct food contact.
15	Operating Costs	2	Depending on the final design, the operating costs should be almost zero.
16	Environmental Conditions	3	The conditions in Addis Ababa like weather data and other variables related to environmental condition should be referred since these conditions play a large role in selection and design of dryer.

Appendix C: Decision Matrix

Table C1: Decision Matrix

			Conceptual Design										
			Rating (1-5)					Rating x Weighting Factor					Ideal
No.	Evaluation Criteria	Weight Factor	DC A	DC B	DC C	DC D	DC E	DC A	DC B	DC C	DC D	DC E	
1	Function	3	3	4	5	4	3	9	12	15	12	9	15
2	Cost	3	5	4	2	4	3	15	12	6	12	9	15
3	Environment	3	2	4	5	3	2	6	12	15	9	6	15
4	Safety	3	5	5	5	5	5	15	15	15	15	15	15
5	Size	3	5	5	4	5	4	15	15	12	15	12	15
6	Personnel	3	5	5	4	3	4	15	15	12	9	12	15
7	Reliability	3	4	5	5	3	4	12	15	15	9	12	15
8	Maintenance	3	5	4	3	4	4	15	12	9	12	12	15
9	Energy	3	5	5	5	5	5	15	15	15	15	15	15
10	Quality	3	2	5	4	3	2	6	15	12	9	6	15
11	Health Issues	3	5	5	5	5	5	15	15	15	15	15	15
12	Operating Instructions	3	5	5	5	5	5	15	15	15	15	15	15
13	Service life	2	5	5	5	5	5	10	10	10	10	10	10
14	Operating Costs	2	5	4	3	4	4	10	8	6	8	8	10
15	Aesthetics	1	5	5	3	4	4	5	5	3	4	4	5
16	Mechanical Loading	1	5	5	4	5	4	5	5	4	5	4	5
	Totals							183	196	179	174	164	210

Appendix D: Data collection spreadsheet format

Table D1: Data collection spreadsheet format 1

Time (min)	Wt. of injera (g)	Wt. of injera in open sun drying (g)	Wt.of moisture or Wt. Loss (g)	Wt.of solid (g)	Wet basis Moisture Content (%)	Dry basis Moisture Content (g water/g solid)
0						
30						
60						
90						
120						
150						
180						
210						
240						
270						
300						
330						
360						

Table D2: Data collection spreadsheet format 2

Time (min)	Solar Collector			Drying Chamber Temperature, ^{0}C			
	T_{in} (^{o}C)	T_{out} (^{o}C)	ΔT (^{o}C)	Tray 1 (Bottom)	Tray 2	Tray 3	Tray 4 (Top)
0							
30							
60							
90							
120							
150							
180							
210							
240							
270							
300							
330							
360							

Appendix E: Assembly and Part Drawing of Solar Injera Drier

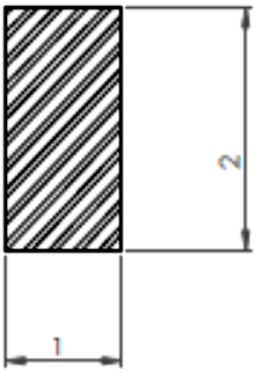

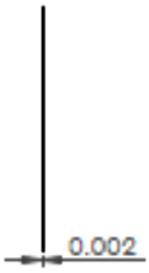

UNLESS OTHERWISE SPECIFIED: DIMENSIONS ARE IN MM TOLERANCES: LINEAR: ANGULAR:	FINISH:				DO NOT SCALE DRAWING	REVISION
					Addis Ababa University Addis Ababa Institute of Technology School of Mechanical and Industrial Engineering	
	NAME	SIGNATURE	DATE		TITLE:	
DRAWN	Senay.T		4/10/19		Collector absorber plate	
CHK'D						
APP'VD						
MFG						
Q.A	1			MATERIAL: Black G.Steel	DWG NO. 9	A4
				WEIGHT:	SCALE: NS	SHEET 1 OF 1

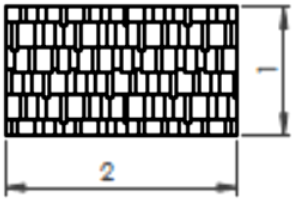

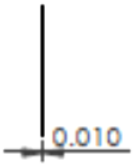

UNLESS OTHERWISE SPECIFIED: DIMENSIONS ARE IN METRES SURFACE FINISH: TOLERANCES: ±3mm LINEAR: ANGULAR:		FINISH:			DEBUR AND BREAK SHARP EDGES		DO NOT SCALE DRAWING	REVISION
							Addis Ababa University Addis Ababa Institute of Technology School of Mechanical and Industrial Engineering	
	NAME	SIGNATURE	DATE				TITLE: collect bottom side	
DRAWN	Senay.T		4/10/19					
CHK'D								
APP'VD								
MFG								
Q.A	1			MATERIAL: Wood			DWG NO. 7	A4
				WEIGHT:			SCALE: 1:10	SHEET 1 OF 1

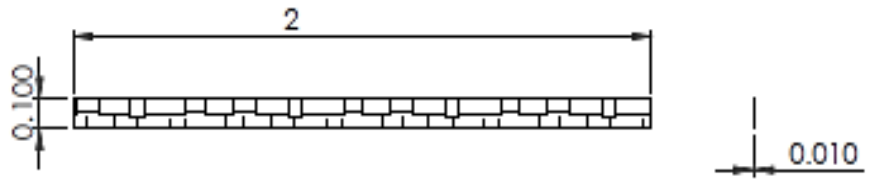

UNLESS OTHERWISE SPECIFIED: DIMENSIONS ARE IN METRES SURFACE FINISH: TOLERANCES: ±2mm LINEAR: ANGULAR:		FINISH:				DEBUR AND BREAK SHARP EDGES:	DO NOT SCALE DRAWING
							Addis Ababa University Addis Ababa Institute of Technology School of Mechanical and Industrial Engineering
	NAME	SIGNATURE	DATE				TITLE: Collector right & left side
DRAWN	Senay.T		4/10/19				
CHK'D							
APPV'D							
MFG							
Q.A	2			MATERIAL: Wood			DWG NO. 8 & 13
							A4
				WEIGHT:			SCALE:1:20 SHEET 1 OF 1

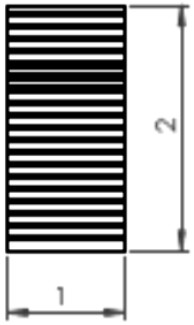

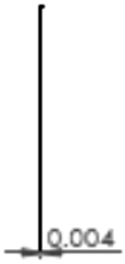

UNLESS OTHERWISE SPECIFIED: DIMENSIONS ARE IN METRES SURFACE FINISH TOLERANCES: ±3mm LINEAR: ANGULAR:			FINISH:			DRAW AND BREAK SHARP EDGES	DO NOT SCALE DRAWING	REVISION
							Addis Ababa University Addis Ababa Institute of Technology School of Mechanical and Industrial Engineering	
	NAME	SIGNATURE	DATE				TITLE:	
DRAWN	Senay.T		4/10/19				Collector glass cover	
CHK'D								
APP'VD								
MFG								
Q.A	1			MATERIAL:			DWG NO.	A4
				Window Glass			10	
				WEIGHT:			SCALE:1:50	SHEET 1 OF 1

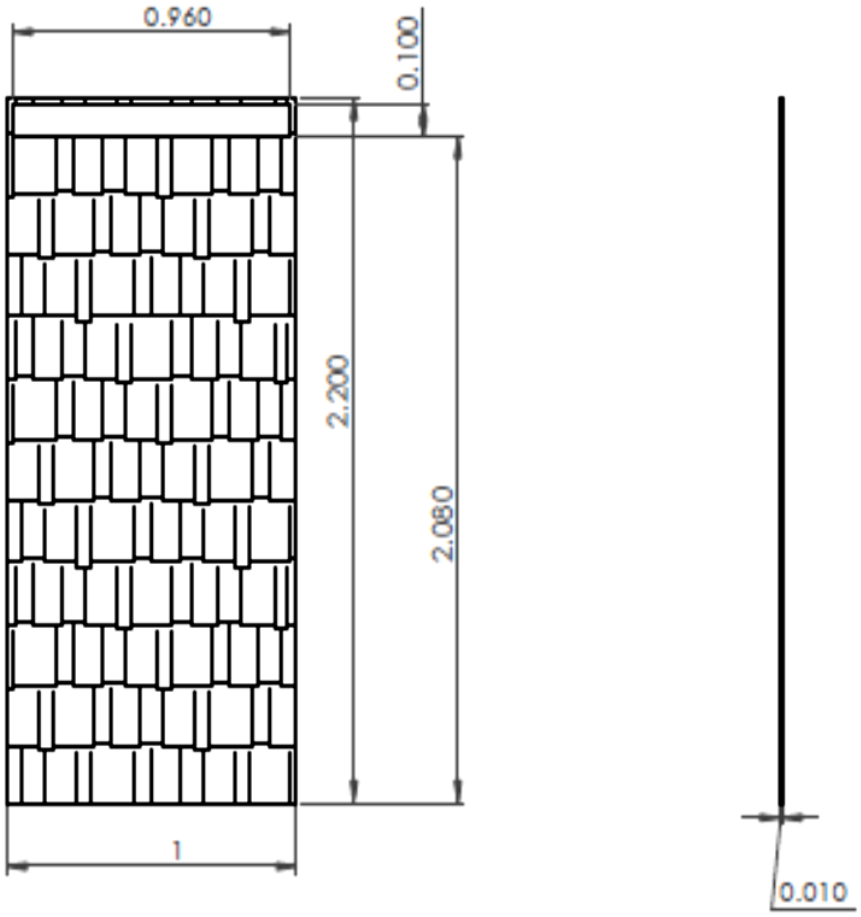

UNLESS OTHERWISE SPECIFIED: DIMENSIONS ARE IN METRES SURFACE FINISH: TOLERANCES: ±3mm LINEAR: ANGULAR:		FINISH:				DEBUR AND BREAK SHARP EDGES	DO NOT SCALE DRAWING
							REVISION
Addis Ababa University Addis Ababa Institute of Technology School of Mechanical and Industrial Engineering							
	NAME	SIGNATURE	DATE				TITLE:
DRAWN	Senay.T		4/10/19				Dryer back part
CHK'D							
APP'VD							
MFG							
Q.A	1			MATERIAL:			DWG NO.
				Wood			6
							A4
				WEIGHT:			SCALE:1:20 SHEET 1 OF 1

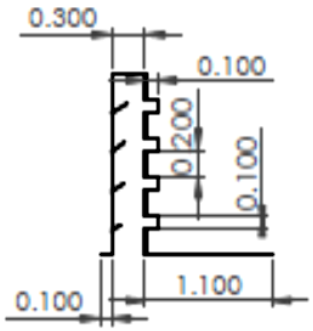

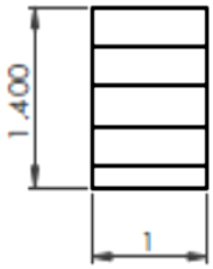

UNLESS OTHERWISE SPECIFIED: DIMENSIONS ARE IN METRES SURFACE FINISH: TOLERANCES: ±5mm LINEAR: ANGULAR:	FINISH:			DEBUR AND BREAK SHARP EDGES	DO NOT SCALE DRAWING	REVISION	
					Addis Ababa University Addis Ababa Institute of Technology School of Mechanical and Industrial Engineering		
	NAME	SIGNATURE	DATE		TITLE:		
DRAWN	Senay.T		4/10/19		Vertical air distributer		
CHK'D							
APP'VD							
MFG							
Q.A	1			MATERIAL:	DWG NO.		A4
				G.Steel	16		
				WEIGHT:	SCALE:1:50	SHEET 1 OF 1	

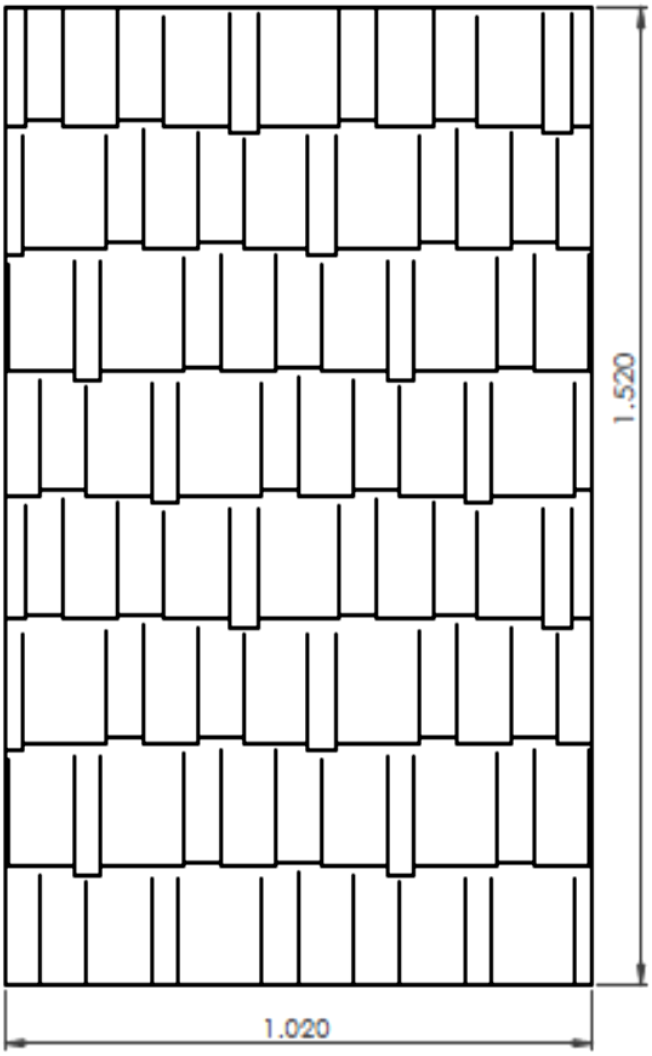

UNLESS OTHERWISE SPECIFIED: DIMENSIONS ARE IN METRES SURFACE FINISH: TOLERANCES: LINEAR: ANGULAR:		FINISH:		DEBUR AND BREAK SHARP EDGES	DO NOT SCALE DRAWING		REVISION:
					Addis Ababa University Addis Ababa Institute of Technology School of Mechanical and Industrial Engineering		
	NAME	SIGNATURE	DATE		TITLE:		
DRAWN	Senay.T		04/10/19		Dryer top and bottom part		
CHK'D							
APP'VD							
MFG							
Q.A	2			MATERIAL: Wood	DWG NO.	2&4	A4
				WEIGHT:	SCALE:1:10	SHEET 1 OF 1	

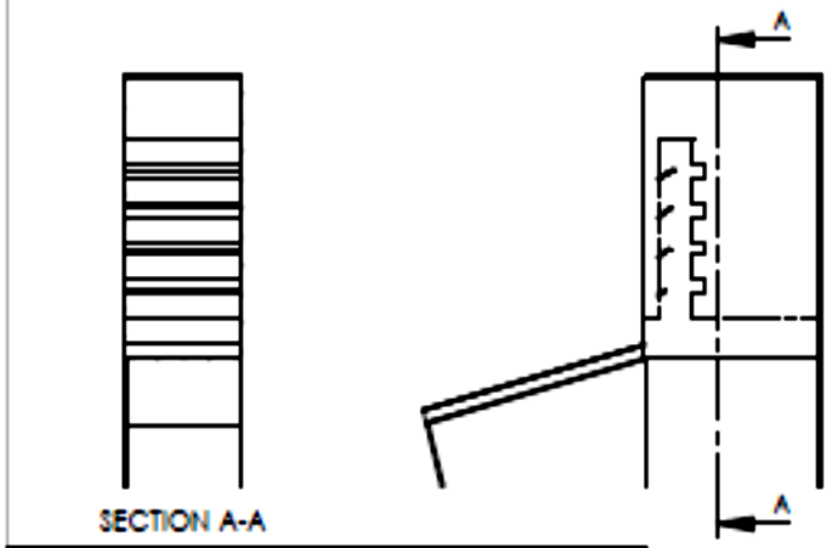

SECTION A-A

ITEM NO.	PART NUMBER	DESCRIPTION	QTY.
1	Dryer left side Part	Wood	1
2	Dryer top Part	Wood	1
3	Dryer right side Part	Wood	1
4	Dryer bottom Part	Wood	1
5	Dryer front Part	Wood	1
6	Dryer back Part	Wood	1
7	Collect bottom side	Wood	1
8	Collector lft side wall	Wood	1
9	Collector absorber plate	Black G.Steel	1
10	Collector glass cover	Window Glass	1
11	Collector support	Wood	1
12	Collecter support	Wood	1
13	Collector right side wall	Wood	1
14	Dryer support	Wood	2
15	Dryer support	Wood	2
16	vertical air distributer	G.Steel	1

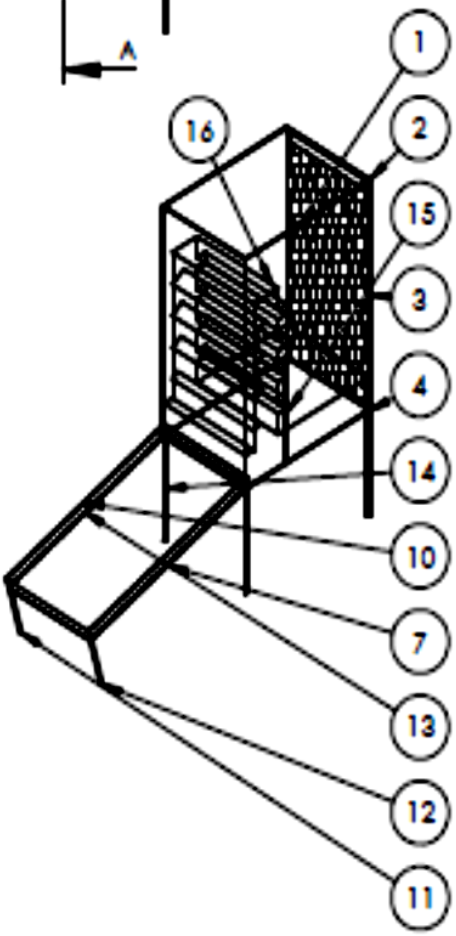

	NAME	SIGNATURE	DATE				
DRAWN	SENAY TESHOME		4/10/19				
CHK'D							
APP'D							
MFG							
Q.A	1						

Addis Ababa University
Addis Ababa Institute of Technology
School of Mechanical and Industrial Engineering

SOLAR INJERA DRYER

1

A4